2015-11-12

RNA Exosome & Chromatin: The Yin & Yang of Transcription: A Dissertation

Mayuri Rege
University of Massachusetts Medical School

RNA EXOSOME & CHROMATIN: THE YIN & YANG OF TRANSCRIPTION

A Dissertation Presented

By

MAYURI REGE

Submitted to the Faculty of the
University of Massachusetts Graduate School of Biomedical Sciences, Worcester
In partial fulfillment of the requirements for the degree of

DOCTOR OF PHILOSOPHY

November 12th, 2015

Interdisciplinary Graduate Program

RNA EXOSOME & CHROMATIN: THE YIN & YANG OF TRANSCRIPTION

A Dissertation Presented
By

Mayuri Rege

The signatures of the Dissertation Defense Committee signify completion and approval as to style and content of the Dissertation

_____
Craig Peterson, Ph. D., Thesis Advisor

_____
Allan Jacobson, Ph. D., Member of Committee

_____
Oliver Rando, Ph. D., Member of Committee

_____
Anthony Imbalzano, Ph. D., Member of Committee

_____
Steve Buratowski, Ph. D., Member of Committee

The signature of the Chair of the Committee signifies that the written dissertation meets the requirements of the Dissertation Committee

_____
Paul Kaufman, Ph. D., Chair of Committee

The signature of the Dean of the Graduate School of Biomedical Sciences signifies that the student has met all graduation requirements of the school.

_____
Anthony Carruthers, Ph.D., Dean of the Graduate School of Biomedical Sciences

Interdisciplinary Graduate Program
November 12th, 2015

DEDICATION

To my teachers, and the culture of excellence at Umass

ACKNOWLEDGEMENTS

I've had the honor of working with some of the smartest people as a member of the Peterson lab, and Craig epitomizes this ideal. His open-minded approach to experiments that 'disprove the model' and eternal optimism while maintaining a perspective are qualities I aspire to live up to. The unique mix of independence, open dialogue and camaraderie that he has cultivated in the lab has transformed me into the scientist I am today.

I benefitted greatly from Ben's insights into my science and laughed hard at his puns. I admire Sarah's impeccable taste and streak of individuality. A fellow late-night lab inhabitant, Nick taught me a few neat science tricks with a generous dose of American pop-culture. I miss our scientific discussions over coffee and beer. Chris, thank you, for putting up with my eccentricities as I troubleshot scripts and, for all the baked goods. I am in awe of Shinya's biochemistry prowess and beautiful gels. Kim's calm and cool attitude when responding to a lab crisis is truly remarkable. Thanks to the talented new recruits: Sal, Jess, Nate, Raushan and Welles, for the goofy jokes and fun times.

My TRAC committee members Allan Jacobson, Ollie Rando, Paul Kaufman and Tony Imbalzano have gone out of their way to support me. Their brilliant suggestions and incisive questions have challenged me to always be at the top of my game. Special thanks to my eternal examiner, Steve Buratowski,

for taking the time to examine my thesis. Alper Kucukural, thank you for your patience and time in answering my naïve data-analysis questions. Ollie's lab has been a second-home thanks to all the technical advice that Amanda Hughes and Marta Radman-Livaja willingly shared with me. I am grateful to Dave Weaver, Joel Richter and Ken Knight for advice regarding my career path. Darla, Marty, Gene, Mike and Cheryl, thank you for your contributions in running the IGP program and the Biotech II enterprise seamlessly.

On a personal front, I want to thank Basu for his mentorship, constructive criticism and emotional support during this time. I could not have done this without you. I am grateful to my family for their unconditional love, and for the strong work ethic they instilled in me. Ginny, Kishore kaka and Jojo made me feel at home whenever I needed it.

I've been lucky my roommates turned out to be the best of friends: Ankita with her "bhapo" powers, and Sri, being a wonderful role model. Thanks to Karthik, Sandhya, Naveen, Rehan, Sneha, Sam, Seemin, Vahbiz, Swapnil, Arvind, Siva, Sreya, Divya, Sonal, Mihir, Adu, Pallo, Pallavi, Ankit, Hari and Sattu for all the memories in Woostah!

Finally, Phadke Sir and Dada Ajoba, my teachers in Bombay, instilled the joy of learning in me, and to them I will be eternally grateful. Someday, I hope I can pay it forward.

ABSTRACT

Eukaryotic genomes can produce two types of transcripts: protein-coding and non-coding RNAs (ncRNAs). Cryptic ncRNA transcripts are bona fide RNA Pol II products that originate from bidirectional promoters, yet they are degraded by the RNA exosome. Such pervasive transcription is prevalent across eukaryotes, yet its regulation and function is poorly understood.

We hypothesized that chromatin architecture at cryptic promoters may regulate ncRNA transcription. Nucleosomes that flank promoters are highly enriched in two histone marks: H3-K56Ac and the variant H2A.Z, which make nucleosomes highly dynamic. These histone modifications are present at a majority of promoters and their stereotypic pattern is conserved from yeast to mammals, suggesting their evolutionary importance. Although required for inducing a handful of genes, their contribution to steady-state transcription has remained elusive. In this work, we set out to understand if dynamic nucleosomes regulate cryptic transcription and how this is coordinated with the RNA exosome.

Remarkably, we find that H3-K56Ac promotes RNA polymerase II occupancy at a large number of protein coding and noncoding loci, yet neither histone mark has a significant impact on steady state mRNA levels in budding yeast. Instead, broad effects of H3-K56Ac or H2A.Z on levels of both coding and ncRNAs are only revealed in the absence of the nuclear RNA exosome. We show that H2A.Z functions with H3-K56Ac in chromosome folding, facilitating

formation of Chromosomal Interaction Domains (CIDs). Our study suggests that H2A.Z and H3-K56Ac work in concert with the RNA exosome to control mRNA and ncRNA levels, perhaps in part by regulating higher order chromatin structures. Together, these chromatin factors achieve a balance of RNA exosome activity (yin; negative) and Pol II (yang; positive) to maintain transcriptional homeostasis.

Table of Contents

Title Page ii
Signature Page iii
Dedication iv
Acknowledgements v
Abstract vii
Table of Contents ix
List of Tables xi
List of Figures xii
List of Third Party Copyrighted Material xiv
List of Abbreviations and Notations xv
List of External Datasets xviii
Preface xix

Chapter I. **Introduction**
I-A. Changing paradigms in transcription 1
i. Transcription: Initiation, elongation, termination 1
ii. Promoter architecture 8
iii. Eukaryotic promoters are bidirectional 9

I-B. RNA surveillance machinery: gatekeepers of the transcriptome 10
i. RNA exosome and Rrp6 10
ii. Exosome associated cofactors: TRAMP and NNS 12
iii. Discovery of cryptic transcripts 13
iv. Types of cryptic transcripts in yeast and their functions 17

I-C. Transcription occurs in the context of chromatin 21
i. Chromatin: Definition and need 21
ii. Histone modifications modulate chromatin 22
iii. Histone variants punctuate chromatin 28
iv. Chromatin remodeling enzymes actively mobilize chromatin 30
v. Folding and 3D genome interactions 34

I-D. Chromatin factors that regulate cryptic transcription 38
i. Histone chaperones and variants 38
ii. Histone modifications 39
iii. Chromatin remodeling enzymes 40
iv. Chromatin factors that promote cryptic transcription 41

Chapter II. ***RTT109* regulates ncRNAs and ORFs in concert with *RRP6***
II-A. Summary 43
II-B. Introduction 44
II-C. Results 47
II-D. Discussion 64
II-E. Materials and Methods 70

Chapter III. ***SWR1* regulates ncRNAs in concert with *RRP6***
III-A. Summary 79
III-B. Introduction 80
III-C. Results 83
III-D. Discussion 99
III-E. Materials and Methods 108

Chapter IV. **Conclusions and outlook**
IV-A. Transcription: Then and Now 110
IV-B. In this work 113
IV-C. Outstanding questions 121

Appendix 1: Table S1 and Table S2 124
Appendix 2: SWI/SNF antagonizes Sir3 to activate transcription of genes at G2/M phase of the cell cycle. 128
Appendix 3: List of strains 164

Bibliography 166

LIST OF TABLES

Table 1.1: Classification of cryptic transcripts described in yeast and their characteristics (Chapter I)

Table S1: Limma summary (Appendix A1)

Table S2: Primer sequences for qPCR analysis (Appendix A1)

LIST OF FIGURES AND TABLES

Fig 1.1: Genomic location of factors associated with transcription

Fig 1.2: H3-K56Ac residue on the nucleosome and its biophysical implication

Fig 2.1: Steady state RNA levels are largely unaffected by *rtt109Δ*, although RNAP II recruitment is reduced dramatically

Fig 2.2: *rrp6Δ* does not affect Pol II occupancy but RNA abundance is increased

Fig 2.3: Defects in transcriptional termination do not account for upregulated ORFs in the *rrp6Δ*

Fig 2.4: H3-K56Ac positively regulates transcription in the absence of the nuclear exosome

Fig 2.5: qRT-PCR confirmation of yeast tiling array data

Fig 2.6: Rrp6 regulates ORFs that are highly transcribed and have high Pol II density

Fig 3.1: H2A.Z does not affect RNA levels alone, but positively regulates transcription in the absence of the nuclear exosome

Fig 3.2: H2A.Z interacts with *SSU72* and inhibits two classes of transcripts associated with NFR-regions

Fig 3.3: Tiling array screenshots of different types of transcripts observed

Fig 3.4: SWR-C promotes formation of Chromosome Interaction Domains (CIDs)

Fig 3.5: Micro-C analysis of different genomic regions, and transcripts of interest

Fig 4.1: Model of how chromatin factors may coordinate with the RNA exosome to maintain transcriptional homeostasis

LIST OF THIRD PARTY COPYRIGHTED MATERIAL

Fig 1.2: H3-K56Ac residue on the nucleosome and its biophysical implication

A) Originally made by J. Feldman. Explicit permission to use was obtained in writing. License number not applicable.

B) Originally made for Jason Chin's lab website. Explicit permission to use was obtained in writing. License number not applicable.

LIST OF ABBREVIATIONS AND NOTATIONS

ORFs	Open Reading Frames
CTD	carboxyl terminal domain
GTFs	general transcription factors
PIC	pre-initiation complex
TSS	Transcription Start Site
TBP	TATA box binding protein
TAFs	TBP-associated factors
CPF/CF	Cleavage and Polyadenylation/Cleavage factor
NNS	Nrd1/Nab3/Sen1
NFR	nucleosome free regions
RNA	Ribo-nucleic acid
mRNA	messenger RNA
ncRNA	non-coding RNA
TRAMP	Trf4/Air2/Mtr4
snRNAs	small nuclear RNAs
snoRNAs	small nucleolar RNAs
ENCODE	Encyclopedia of DNA Elements Consortium
CUTs	Cryptic Unstable Transcripts
SUTs	Stable Unannotated Transcripts
XUTs	Xrn1-sensitive Unstable non-coding Transcripts

NUTs	Nrd1-Unterminated Transcripts
SRTs	Ssu72 Restricted Transcripts
SSU72	Suppressor of SUa7, gene 2
CRRATs	Chromatin Remodeling-Repressed Antisense Transcripts
H3-K56Ac	acetylation of lysine 56 of histone H3
H3K4me3	trimethylated lysine 4 of histone H3
H3K4me2	dimethylated lysine 4 of histone H3
HAT	histone acetyltransferases
HDAC	histone deacetylase
FRET	fluorescence resonance energy transfer
SWI/SNF	Mating type SWItching defective/ Sucrose Non-Fermenting
ISWI	Imitation SWItch
INO80	INOsitol requiring
3C	Chromosome conformation capture (assay)
4C	Circularized Chromosome Conformation Capture
5C	Carbon-Copy Chromosome Conformation Capture
Hi-C	High throughput sequencing variant of 3C
Micro-C	Micrococal nuclease digested method based on Hi-C
TADs	Topologically Associated Domains
CTCF	CCCTC-binding factor
CIDs	Chromosomal Interaction Domains

Yeast nomenclature notations used in published literature

Gene names are capitalized and italicized.

Eg: The gene *SWR1*

Recessive alleles are lower case and italicized.

Eg: The null mutant *swr1*Δ.

Proteins are title case, sometimes written with the ‘p’ suffix.

Eg: The protein Swr1

Multi-subunit complexes are capitalized and not italized.

Eg: The complex SWR-C

LIST OF EXTERNAL DATASETS

The following data are deposited in online databases to allow easy access:

Accession number GSE73145: Raw and processed tiling microarray data and Pol II ChIP-seq data

Accession number GSE72845 and GSE68016: Micro-C data for WT and *swr1*Δ

Supplementary tables below are part of the online submission and incompatible to directly include in this work:

Rege et al., Cell Reports (2015), http://dx.doi.org/10.1016/j.celrep.2015.10.030

Table S3: SWR-repressed transcripts annotations

Table S4: Heatmap groups and order; GO terms of Group A ORFs

PREFACE

Chapter II and III of this work is *in press* at *Cell Reports* as:

Mayuri Rege, Vidya Subramanian, Chenchen Zhu, Tsung-Han S. Hsieh, Assaf Weiner, Nir Friedman, Sandra Clauder-Münster, Lars M. Steinmetz, Oliver J. Rando, Laurie A. Boyer and Craig L. Peterson. Chromatin dynamics and the RNA exosome function in concert to regulate transcriptional homeostasis. Cell Reports (2015), http://dx.doi.org/10.1016/j.celrep.2015.10.030

Author contributions:

M.R and C.L.P conceptualized the study and designed the experiments. M.R performed the yeast experiments and Pol II data analysis. M.R. and C.Z. analyzed the tiling array data. S.C.M helped with sample preparation for tiling arrays. V.S. performed the mouse experiments (not included in this work) and analyzed the data together with L.A.B. TH-S.H made the Micro-C libraries and O.J.R, A.W and N.F analyzed Micro-C data. C.L.P. wrote the manuscript with help from M.R with comments from all authors.

Appendix I of this work is a manuscript under preparation:

Mayuri Rege and Craig L. Peterson. SWI/SNF antagonizes Sir3 to activate transcription of genes expressed at G2/M phase of the cell cycle.

Not included in thesis:

Lijian Yu*, Mayuri Rege*, Craig L. Peterson and Michael R. Volkert. RNA polymerase II depletion promotes transcription of specific mRNA species with alternative poly(A) tails. *Manuscript under preparation*

*equal contribution.

INTRODUCTION

I-A. CHANGING PARADIGMS IN TRANSCRIPTION

I-A.i. Transcription: Initiation, elongation, termination

Transcription can be defined as the process of creating a nascent RNA strand from a DNA template in a directional manner. In eukaryotes, the three RNA polymerases Pol I, Pol II and Pol III transcribe the genome. These enzymes share some subunits, although there are distinctions in their structure and genomic targets (Cramer et al., 2008). Pol I transcribes the rRNA precursor (35S), which is then processed into the mature 18S, 5.8S and 25S rRNAs while Pol III transcribes the tRNAs and the 5S rRNA. Together, rRNAs and tRNAs are technically the first non-coding RNAs discovered, as their function does not involve translation into proteins. RNA Polymerase II (Pol II) transcribes the entire repertoire of protein coding genes into mRNAs. In the budding yeast, *Saccharomyces cerevisiae*, ~6000 protein coding genes (also referred to as Open Reading Frames; ORFs), constitute > 90% of all genes in the genome, are dependent on Pol II for transcription. As proteins participate in a variety of essential cellular processes like DNA replication, DNA repair and establishment of cell identity, historically, the study of Pol II has focused on how ORFs are transcribed into mRNAs.

Pol II is composed of 12 subunits and the crystal structure of the core enzyme has been resolved (Armache et al., 2005; Cramer, 2002; Meyer et al., 2009). Most of the genes encoding these subunits are essential, underscoring their importance. Nonetheless, key insights into the contributions of individual subunits were elucidated using a variety of conditional mutants (Braberg et al., 2013). In addition to structural and genetic studies, biochemical purification/ *in vitro* reconstitution of these proteins has led to an understanding of specific functions of each part (Christie et al., 1994; Edwards et al., 1991). *RPO21* (also called *RPB1*) is the largest subunit of RNA Pol II with a characteristic carboxyl terminal domain (CTD). The CTD contains many copies of the consensus YSPTSPS heptapeptide sequence, which is evolutionarily conserved. The exact number of copies of this sequence varies depending on the species; budding yeast have 26 repeats. The CTD is a major nexus of many regulatory steps as described below (Buratowski, 2009; Phatnani and Greenleaf, 2006).

The process of transcription involves three steps: initiation, elongation and termination. For initiation, Pol II associates with a group of proteins called the general transcription factors (GTFs) upstream of the ORF. Collectively, this complex is called the pre-initiation complex (PIC) and this opens the DNA to initiate transcription at the Transcription Start Site (TSS). Robust biochemistry and ingenious genetic experiments have revealed the order in which these

factors assemble to form the PIC (Buratowski et al., 1989; Conaway and Conaway, 1993; Grünberg and Hahn, 2013; Kornberg, 1998; Roeder, 1996).

As the name suggests, GTFs are components of the basal transcription machinery that function at most genes where they create a platform to load Pol II at the TSS and, ultimately, release it. TFIID, one of the GTFs, contains the TATA box binding protein (TBP) as well as other TBP-associated factors (TAFs). TBP is required by all three RNA polymerases to initiate transcription, while the TAFs function in a more gene specific manner (Cormack and Struhl, 1992; Fan et al., 2005; Hampsey, 1998). After PIC assembly, the Kin28 kinase rapidly phosphorylates Ser5 in the YSPTSPS repeat of the CTD, which is thought to promote exit of Pol II from the promoter into the coding region (Figure 1.1) (Søgaard and Svejstrup, 2007). This is accompanied by recruitment of mRNA capping/ splicing factors and other histone modifying enzymes associated with active transcription, like Set1 (Drouin et al., 2010; Govind et al., 2010; Kim and Buratowski, 2009; Ng et al., 2003; Perales and Bentley, 2009).

The transition from initiation to elongation is facilitated by a reduction in Ser5-P and an increase in Ser2-P of the CTD, mediated by the Ctk1/ Bur1 kinases (Bartkowiak et al., 2010; Keogh et al., 2003; Komarnitsky et al., 2000). These changes in serine phosphorylation recruit Set2 (methylates histone H3 lysine 36) and activate Rpd3S (histone deacetylase), that suppress cryptic initiation from within coding regions (Carrozza et al., 2005; Keogh et al., 2005).

Figure 1.1: Genomic location of factors associated with transcription

A typical eukaryotic gene, with its upstream nucleosome free region, is shown. Panels include the phosphorylation states of the CTD of Pol II, histone modifications present throughout the gene, transcription termination factors and histone variants. Color densities indicate abundance of the mark averaged over the entire genome. The enzymes that catalyze each mark are listed on the right, if applicable. H3-K56Ac and H2A.Z, which are of special interest to this work, are emphasized.

Figure 1.1

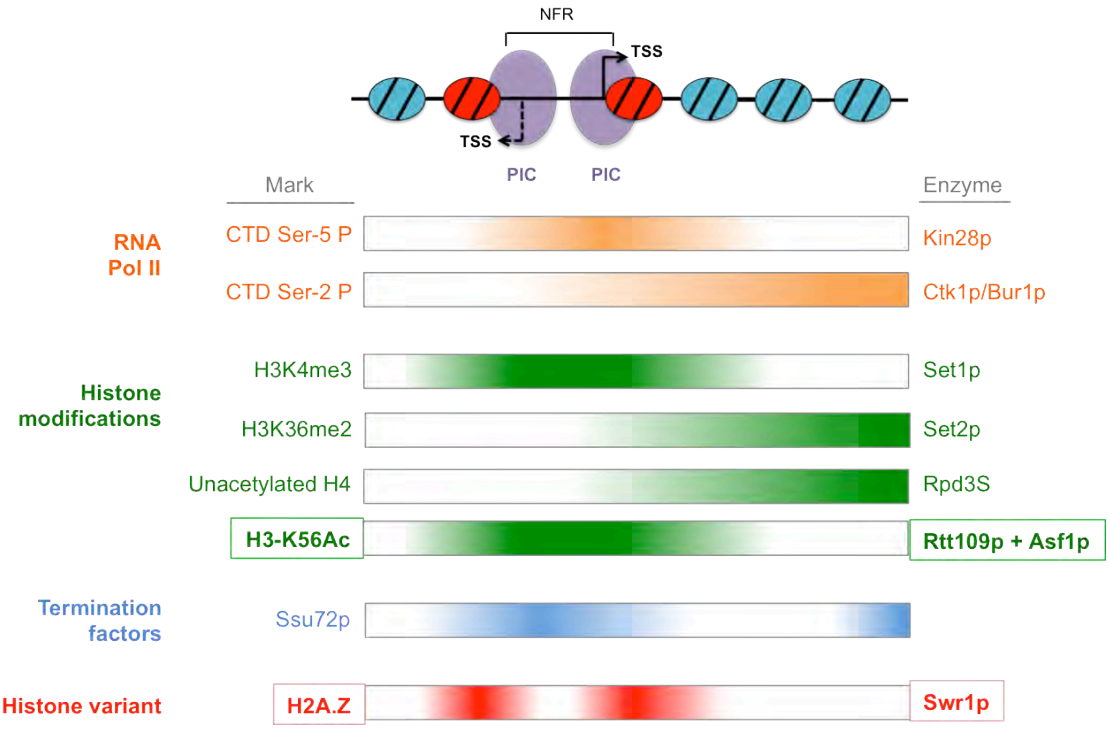
NFR
TSS
TSS
PIC
PIC
Mark
Enzyme
RNA Pol II
CTD Ser-5 P
Kin28p
CTD Ser-2 P
Ctk1p/Bur1p
Histone modifications
H3K4me3
Set1p
H3K36me2
Set2p
Unacetylated H4
Rpd3S
H3-K56Ac
Rtt109p + Asf1p
Termination factors
Ssu72p
Histone variant
H2A.Z
Swr1p

In yeast, there are two main mechanisms of transcriptional termination (Mischo and Proudfoot, 2013; Tudek et al., 2015). For protein-coding mRNAs, the Cleavage and Polyadenylation/Cleavage factor (CPF/CF) binds to an AU-rich sequence in the nascent RNA, and cleaves it to release the mRNA from the polymerase. The elongating polymerase, which now has a free 5' end, is chased by the 5' exonuclease Rat1 in yeast and dislodged, thereby causing termination. This is referred to as the 'Torpedo' mechanism, and it reduces readthrough into an adjacent locus (Kim et al., 2004; West et al., 2008). In addition to mRNAs, a few ncRNA transcripts in yeast also appear to use the CPF/CF pathway for termination (Marquardt et al., 2011).

In yeast, termination of short non-coding transcripts primarily occurs via the Nrd1/Nab3/Sen1 (NNS) complex and includes snRNAs, snoRNAs and certain classes of cryptic transcripts (Arigo et al., 2006; Kim et al., 2006; Steinmetz et al., 2001; Thiebaut et al., 2006). Nrd1 and Nab3 trigger termination by binding to recognition motifs in the RNA and recruiting the Sen1 helicase, which removes the RNA from the transcription bubble and collapsing it. Nrd1 also has a CTD interaction domain that binds preferentially to the Ser-5 phosphorylated form enriched at 5' ends of genes, enforcing an additional level of regulation (Vasiljeva et al., 2008). By intercepting both the nascent RNA and the status of the phospho-CTD as a docking site, transcripts longer than 450 bp are no longer susceptible to termination by NNS, specifying a 'window of termination'

(Hazelbaker et al., 2013; Kim et al., 2010). The RNA is now a substrate for the exosome, Rrp6, TRAMP machinery, and is either trimmed (in case of snRNAs and snoRNAs) or degraded (in case of cryptic transcripts). The distinction between the stable and unstable transcripts is likely conferred by the Sm complex bound near the 3' end of the stable RNAs that limits exosome activity and leads to formation of mature sn- and sno-RNAs (Coy et al., 2013; Vasiljeva and Buratowski, 2006). There is also evidence that TRAMP may recruit Nrd1 to the termination complex, that NNS components can bind CPF/CF targets and vice versa, suggesting interdependence and redundancy in termination pathways (Grzechnik and Kufel, 2008; Schneider et al., 2008; Vasiljeva and Buratowski, 2006).

Other alternative termination mechanisms have been described, but are out of the scope of this work (Ghazal et al., 2009; Rondón et al., 2009). During or following termination, the CTD is dephosphorylated and the polymerase can be recycled for another round of transcription (Cho et al., 2001). This final dephosphorylation step is thought to be catalyzed by two phosphatases, Ssu72 and Fcp1 (Cho et al., 2001; Krishnamurthy et al., 2004). The dual role of Ssu72 in initiation and termination is described in detail in Section I-B-iv.

Taken together, the phosphorylation state of the CTD seems to be a major player coordinating various steps of transcription. How might phosphorylation of the CTD differentially regulate the various steps? One possibility suggested by

Cramer and colleagues is that the length of CTD may change depending on the phosphorylation status (Meinhart et al., 2005). An unphosphorylated CTD may form a compact structure compared to the extended tail formed by a phosphorylated CTD, concomitantly changing the interaction partners.

Thus, transcription is an extremely complex process that involves the interplay of a large number of proteins for the initiation, elongation and finally, termination of every RNA molecule. The tremendous regulatory potential of non-coding RNAs produced by Pol II has only recently been appreciated. Thus, the study of transcriptional regulation: both coding and non-coding, is fundamental to the understanding of gene regulation.

I-A.ii. Promoter architecture

Promoter regions are regulatory sequences upstream of a protein-coding gene that can affect the transcription of that gene. These regions are typically devoid of nucleosomes, and thus are ‘nucleosome free regions’, or NFRs. A typical yeast promoter is consists of an NFR bound on either side by strongly-positioned nucleosomes. The promoter is where the PIC is formed before transcription can be initiated.

Work from multiple labs has investigated the mechanisms that establish NFR regions across the genome. Both *cis* and *trans* factors seem to play a role. *Cis* factors include characteristic sequences: polyA:T tracts in yeast and CpG

DNA regions in mammals, which are unfavorable to wrap around a histone octamer. *Trans* factors that affect nucleosome positioning are chromatin remodeling enzymes, transcription factors and the general transcriptional machinery. Trans factors seem to play a dominant role in positioning nucleosomes *in vivo*. Nucleosome occupancy is a key factor that regulates access of the transcriptional machinery to DNA.

I-A.iii. Eukaryotic promoters are bidirectional

Promoter NFRs are permissive to PIC formation. In addition to this, eukaryotic promoters are also ‘bidirectional’: they allow formation of two individual PICs. Genome-wide mapping has revealed that PIC formation for protein-coding genes, and ncRNA occurs at their respective promoters using the same shared NFR. These ncRNAs are not necessarily co-regulated with the neighboring ORF and efficiently degraded in wild type (Rhee and Pugh, 2012). This has changed the paradigm of the transcription field from asking ‘what recruits Pol II to particular loci?’ to ‘which “indiscriminately” transcribed loci may be functional in certain experimental conditions?’

I-B. RNA SURVEILLANCE MACHINERY: GATEKEEPERS OF THE TRANSCRIPTOME

RNA production by the polymerase must be balanced by its degradation; the quintessential yin to the yang. This is important not just to recycle nucleotides, but also to prevent accumulation of regulatory RNAs (siRNAs, miRNAs) or cryptic ncRNAs described in the previous section. RNA Pol I, II and III produce very different types of transcripts as described previously, yet the RNA surveillance machinery can apparently identify them all. The yeast degradation system is therefore, universal, and all three RNA types can be targets for degradation by the exosome/TRAMP or by the 5' exonuclease Rat1 in the nucleus. No obvious physical features distinguish which of these diverse substrates are targets of either degradation pathway. Thus, the specificity of identifying and degrading aberrant RNAs is usually conferred by cofactors described below, which associate with the core exosome.

I-B.i. RNA exosome and Rrp6

The RNA exosome is a highly conserved decay complex that is the primary RNA degradation machinery. The core exosome components are structurally similar to the bacterial PNPase, although the eukaryotic version has lost its catalytic ability (Liu et al., 2006; Lorentzen et al., 2005; Symmons et al., 2002). Instead the eukaryotic RNA exosome can associate with endonucleases and exonucleases

that enhance and diversify its function. Here, we first discuss the exosome, followed by the relevant exosome associated co-factors, and finally the types of RNAs that the degradation machinery encounters. Together, this helps us understand how the cell distinguishes functional RNAs from aberrant ones.

As mentioned above, the core eukaryotic exosome has no nuclease activity. In contrast, the related bacterial PNPase and the archeal exosome both have three active sites. The endo- and exonuclease activities of the eukaryotic exosome are conferred by the cofactors Rrp44p (also called Dis3p) and Rrp6, respectively (Lebreton et al., 2008; Schaeffer et al., 2009; Schneider et al., 2007). A clue as to why the eukaryotic exosome has lost the ancient exonuclease activities may come from the laws of thermodynamics (Dziembowski et al., 2007). The prokaryotic/ archeal exonucleases carry out a phosphorolysis reaction, which is energetically neutral. Conversely, the eukaryotic analogs perform an energetically favored hydrolysis reaction, possibly making them more efficient (Houseley and Tollervey, 2009).

Rrp44p/Dis3p has both endo and 3’ exonuclease activities, while Rrp6 is a 3’ exonuclease (Lebreton et al., 2008; Schaeffer et al., 2009; Schneider et al., 2008). The former constitutively associates with the core exosome, while Rrp6 is only part of the nuclear exosome. Like most of the core exosome subunits, Rrp44 null mutants are inviable. This makes it challenging to study the function of the core exosome. In contrast, although part of the nuclear exosome, *rrp6Δ* mutants

are viable and defective in RNA processing, making them a valuable tool to investigate exosome biology. Transcriptome analysis of *rrp6Δ* in yeast have revealed that it targets ncRNAs and unspliced pre-mRNAs for degradation (Schneider et al., 2012), facilitates processing of sn/snoRNAs (Gudipati et al., 2012a), promotes oligoA tail addition, and may play a more general surveillance role that governs nuclear mRNA levels (Schmid et al., 2012).

A key feature of the RNA degradation machinery is the multiplicity of function. For example, in yeast, the 3' exonucleases of the exosome degrade RNAs transcribed by all three RNA polymerases. In addition to this, they also participate in generating mature ends of stable ncRNA molecules. Thus, these highly conserved proteins have established house-keeping roles, and may have evolved to target many ncRNAs as well.

I-B-ii. Exosome associated cofactors: TRAMP and NNS

A key core exosome-associated co-factor present in all organisms is an enzyme that can add poly A tails to RNA. Exonucleases are unable to initiate degradation near the stable stem structure unless provided with an extension that can serve as a 'landing pad' (Deutscher, 2006 and references therein). In eukaryotes, the TRAMP polyadenylation complex tags defective RNAs with a short polyA tail to make it an ideal substrate for the exosome (Houseley et al., 2006; West et al., 2006). This combination is a potent mechanism responsible for RNA surveillance

inside the cell. A second major exosome-associated co-factor is the Nrd1-Nab3 complex. Nrd1- and Nab3- binding sites are preferentially present in cryptic ncRNA and these factors are recruited co-transcriptionally. Nrd1-Nab3 can associate with nascent transcripts, pretargeting these RNAs for degradation as soon as their synthesis is complete (Carroll et al., 2007; Vasiljeva et al., 2008).

In budding yeast, RNA Pol II produces messenger RNAs (mRNAs) and a host of other ncRNAs. Of the latter, the classically studied, stable ncRNAs include some small nuclear RNAs (snRNAs) that function in splicing, and small nucleolar RNAs (snoRNAs) involved in ribosome biogenesis. In addition to this, recent analyses have identified that almost all organisms transcribe a majority of their genome, producing a huge number of hidden, or cryptic, ncRNAs as described in the following section (Amaral et al., 2008; Core et al., 2008; He et al., 2008; Neil et al., 2009; Preker et al., 2008; Seila et al., 2008; Xu et al., 2009).

I-B.iii. Discovery of cryptic non-coding transcripts

The landmark human ENCODE project first reported the existence of a large number of non-coding RNAs transcribed in human genomes and thus coined the word ‘pervasive transcription’ (Birney et al., 2007; Carninci et al., 2005; Kapranov et al., 2007; Katayama et al., 2005). They reported that although 75% of the genome was transcribed in the 15 human cell lines analyzed, only 25% of this belonged to protein-coding genes (Djebali et al., 2012). Following this, the advent

of next generation sequencing technology revealed this as a common feature of most eukaryotes.

Remarkably, cryptic ncRNAs are not degradation by-products: many of them are 5’ capped, oligoadenylated and thus, transcribed by RNA Pol II (Xu et al., 2009). They can be divided into two broad categories depending on the genomic locus they are antisense to: NFR regions or gene bodies. Cryptic transcripts that are short span about 3 nucleosomes in length (200- 600bp in yeast) and overlap with bidirectional promoter NFRs, upstream of protein-coding genes. Most long cryptic transcripts (> 600 bp in yeast) are antisense to protein-coding genes and often originate from the 3’ end of a gene. Both short and long cryptic ncRNAs are targets for the degradation machinery. The unstable nature of these cryptic transcripts probably explains why they were only detected recently, using high-throughput technologies (Neil et al., 2009; Xu et al., 2009). Numerous studies have now characterized the enormous variety of these cryptic transcripts by inactivating different components of the degradation machinery. Each stabilizes a particular set of ncRNA as listed in Table 1.1, although there are some overlaps between these classes.

Table 1.1: Classification of cryptic transcripts described in yeast and their characteristics

CUTs (Cryptic Unstable Transcripts), SUTs (Stable Unannotated Transcripts), XUTs (Xrn1-sensitive Unstable non-coding Transcripts), NUTs (Nrd1-Unterminated Transcripts), SRTs (Ssu72 Restricted Transcripts) and CRRATs (Chromatin Remodeling-Repressed Antisense Transcripts) and their characteristic features are listed.

Chromatin factors that inhibit these classes of ncRNAs are colored red and those that promote their production are colored green. See main text for references.

Table 1.1

Name; number	Orientation wrt ORF	Median length (bp)	RNA termination pathway	RNA degradation factors	Chromatin factors
CUTs; 925	Antisense divergent; some tandem	440	NNS	TRAMP, Rrp6, exosome	Isw2, CAF1, Rtt109*, Swr1* and possibly SWI/SNF
SUTs; 847	Antisense divergent; some tandem	761	CPF/CF, NNS	Rrp6, exosome, Xrn1	Rtt109*, Swr1*
XUTs; 1658	Antisense overlapping	~ 850	CPF/CF	Xrn1	-
NUTs; 1526	Antisense divergent; Antisense overlapping	~ 1500	NNS	Rrp6, Xrn1	-
SRTs; 605	Tandem 3' extensions; 135 antisense divergent	-	CPF/CF, NNS (inferred)	Rrp6, exosome	Ssu72, Swr1* (only a subset)
CRRATs; 814	Antisense overlapping	~ 450-800	unknown	Rrp6, Xrn1 (only a subset)	Ino80, Rsc, Iswi2

* Reported in this work

I-B.iv. Types and functions of cryptic transcripts in yeast

Cryptic non-coding transcripts were first observed in *S. cerevisiae* by the Winston lab when they mutated factors involved in transcriptional elongation. The elongation factors, Spt6p and Spt16p reassemble nucleosomes behind the RNA polymerase, and prevent spurious intragenic transcription from cryptic promoters within gene bodies (Kaplan et al., 2003). Alongside this, RNA analysis of *RRP6/ TRF4* null mutants first detected what we now call Cryptic Unstable Transcripts (**CUTs**). CUTs are normally not allowed to accumulate to detectable levels in wild-type cells and represent the founding class of cryptic non-coding RNAs in yeast (Davis and Ares, 2006; Wyers et al., 2005). Subsequently, use of arrays that tile the genome, instead of ones that probe for known regions, characterized the complete set of 925 yeast CUTs (Neil et al., 2009; Xu et al., 2009). These cryptic transcripts are 200-600 nucleotides long and are associated with promoter regions on either strand. With respect to an adjacent ORF, a CUT is typically transcribed in a divergent and antisense orientation, although some can also be in an upstream tandem orientation. The NNS machinery binds to CUTs and recruits the exosome and TRAMP machinery to degrade this class of transcripts.

Another class of transcripts that are somewhat less sensitive to the exosome in yeast are Stable Unannotated Transcripts (**SUTs**, n= 847) (Xu et al., 2009). They can be detected even in the presence of a functional exosome, although some SUTs increase in abundance in *rrp6Δ* strains, similar to CUTs. At

a median length of ~ 750 bp SUTs tend to be slightly longer than CUTs. The distinction between CUTs and SUTs is not definite, because some CUTs can be stabilized in wild type cells contingent on certain environmental conditionals or growth media. SUTs are believed to escape degradation by the NNS machinery because they may recruit the CPF/CF factor used to terminate protein-coding mRNAs.

Similarly, Xrn1-sensitive Unstable non-coding Transcripts (**XUTs**, n= ~1600), identified by the Morillon lab, are stabilized in the absence of the cytoplasmic exonuclease Xrn1 (van Dijk et al., 2011a). They overlap considerably with SUTs and 66% are antisense to ORFs. Interestingly, XUTs were also upregulated in wild type cells exposed to lithium, suggesting that they may be involved in the response to lithium toxicity and possibly, other environmental responses.

Depletion of NRD1, an essential protein involved in termination, stabilizes Nrd1-Unterminated Transcripts (**NUTs**, n= ~1500) (Schulz et al., 2013). NUTs can be divergently transcribed from bidirectional promoter regions, or from regions antisense to ORFs. Promoter associated NUTs appear to overlap with a majority of previously annotated CUTs, and are enriched for NRD1 binding sites. This was the first clue in yeast that preferential CUT degradation is likely determined by sequence specific motifs; similar to previous work in mouse ESCs (Almada et al., 2013).

The final class of transcripts, characterized by the Proudfoot lab, are SRTs (Ssu72 Restricted Transcripts, n=605), which accumulate when the *SSU72* gene is inactivated (Tan-Wong et al., 2012). Initially discovered as a Suppressor of SUa7 (TFIIB in yeast; required for transcriptional initiation), *SSU72* is an essential gene, and the *ssu72-2* ts allele was used to profile changes in transcription. Work from the Hampsey lab has shown that Ssu72 has a dual function: as a CTD Ser-5 phosphatase during initiation, and as a termination factor (Krishnamurthy et al., 2004). Due to its role in termination, most SRTs tend to be 3' read-through extensions of ORFs, while a subset of them (n=136) are promoter-associated, owing to its function during initiation. Although SRTs are detectable in the *ssu72-2* single mutant, their abundance synergistically increases in the *ssu72-2 rrp6Δ* double mutant, suggesting that they are also partially inhibited by the exosome. As a protein enriched and functional at both 5' and 3' ends of a gene, it has been suggested that Ssu72 acts as a gene looping factor (Tan-Wong et al., 2012) that promotes 'directionality' of transcription.

Given the enormous variety of cryptic transcripts described above, it is a wonder that the degradation machinery is able to distinguish them from other short stable RNAs. A crucial regulatory step that helps degradation factors to distinguish functional RNAs from non-functional ones is transcriptional termination. As described in section I-A, instead of the CPF/CF pathway used for mRNAs, short transcripts are bound co-transcriptionally by Nrd1- Nab3 proteins

to direct their processing. The fate of a nascent transcript bound by the Nrd1/ Nab3 proteins is likely determined by whether other protective proteins also associate with it, as is the case with sn- and sno- RNAs.

Although cryptic transcripts in yeast are apparently ubiquitous, their general function remains a mystery. A few studies have suggested that transcribing a cryptic ncRNA overlapping with an ORF typically inhibits ORF transcription, and is called ‘transcriptional interference’ (Camblong et al., 2007; Castelnuovo et al., 2014). Either the RNA or the act of transcription itself appears to be antagonistic to expression of the protein-coding gene.

In summary, RNA degradation and transcriptional termination pathways are crucial for functioning of the cell and show some redundancy with respect to their targets. It is clear that the redundant mechanisms ensure a fail-safe to eliminate cryptic, potentially deleterious transcripts. Also, these systems are coupled to the transcriptional machinery, likely to achieve transcriptional homeostasis. Thus, understanding how RNA degradation pathways modulate their activities temporally, or under specific environmental conditions, may reveal novel mechanisms of transcriptional regulation.

I-C. TRANSCRIPTION OCCURS IN THE CONTEXT OF CHROMATIN

I-C.i. Chromatin: Definition and need

Contrary to the classical textbook representation, transcription does not occur on a naked DNA template inside the cell. In the eukaryotic nucleus, transcription occurs in the presence of chromatin. Walther Fleming is believed to have coined this word to describe cytological samples of protease resistant nuclei as '"...in view of its refractile nature, its reactions, and above all its affinity to dyes, is a substance which I have named chromatin" (Flemming, 1882).

The basic unit of chromatin is the nucleosome and it consists of 147 base pairs of DNA wrapped 1.47 times around an octamer of positively charged proteins called histones. Each octamer contains two copies each of histones H2A, H2B, H3 and H4. These canonical histone proteins are highly conserved and are essential for life in all eukaryotes. While these basic proteins help to neutralize the negatively charged DNA to facilitate packaging, they also block access to DNA during critical cellular processes like transcription, replication and DNA repair. In fact, in the early years of chromatin biology, this nucleoprotein complex was thought to be required for packaging of DNA alone, a structure that was static and, as a consequence, uninteresting. However, this concept has been strongly revised over the last two decades. It is clear that chromatin is highly dynamic, and that changes in chromatin correlate strongly with transcription, replication, DNA repair and in development. To maintain chromatin

in a dynamic state, access to the underlying DNA is controlled using three strategies in all eukaryotes: i) Histone modifications ii) Histone variants and iii) Chromatin remodeling enzymes.

I-C.ii. Histone modifications modulate chromatin

Histone modifications are chemical moieties added post-translationally to histone proteins. Acetylation, phosphorylation, methylation, ubiquitinylation are examples of chemical groups that can characteristically alter the properties of nucleosomes *in vitro*, and they are found on specific residues of histones *in vivo*. The highest frequency of histone modifications occur on the unstructured N-terminal histone tails, although examples of modifications in the globular domain of the histones, like H3-K56Ac have been reported (Hyland et al., 2005; Ozdemir et al., 2005). The finding that specific histone modifications are conserved and correlate with transcriptional activation or repression lead to the histone code hypothesis, which proposed that the combinatorial presence of specific histone modifications dictates the binding of effector proteins (Strahl and Allis, 2000). However, data from multiple labs are inconsistent with this hypothesis, suggesting that histone modifications likely act at a target set of genes in a context specific manner and/or allosterically modify chromatin remodeling enzymes at those genes (Lenstra et al., 2011; Rando, 2012; Weiner et al., 2012, 2015). Rather than a

comprehensive account, we focus on histone modifications strongly associated with transcription in many model organisms and relevant to this work.

A typical eukaryotic gene is associated with a characteristic pattern of histone modifications as described in Figure 1.1. At the TSS of a gene, the Pol II CTD phospho-Ser5 recruits Set1, which methylates lysine 4 of histone H3 (H3K4me) (Ng et al., 2003, Kirmizis et al., 2007). H3K4me3 is known to recruit various histone acetyltransferases (HATs) such as SAGA and Nua4 and correlates strongly with active transcription (Shi et al., 2006; Taverna et al., 2006). The dimethylated H3K4 (H3K4me2) is more predominant around the TSS, and work from the Buratowski lab has demonstrated that the histone deacetylase (HDAC) Set3C binds to this mark to mediate deacetylation of histones at 5' ends of genes (Kim and Buratowski, 2009). Near the middle and 3' ends of genes, Set 2 methylates lysine 36 of histone H3 (H3K36me) (Kizer et al., 2005; Krogan et al., 2003; Li et al., 2002). This mark is associated with the elongating polymerase and activates the Rpd3 small complex (Rpd3S), a histone H4 deacetylase, to prevent *de novo* initiation from within genes (Carrozza et al., 2005; Keogh et al., 2005). In summary, these conserved methylation patterns modulate histone acetylation at different stages during the process of transcription.

Histone acetylation has largely been associated with transcriptional activation. In contrast to tail residues, acetylation of lysine 56 in the globular domain of histone H3 (H3-K56Ac) occurs prior to its incorporation into chromatin

(Masumoto et al., 2005; Tsubota et al., 2007). The Rtt109 HAT, in association with Asf1 chaperone, catalyzes this acetylation reaction, and promotes histone incorporation. Consequently, H3-K56Ac marks newly incorporated nucleosomes during replication-coupled and replication-independent assembly (Li et al., 2008). In line with this role, mutants in this assembly pathway are sensitive to various genotoxic agents, suggesting that H3-K56Ac functions in the DNA damage response and is required for genome stability (Avvakumov et al., 2011; Chen et al., 2008; Collins et al., 2007; Driscoll et al., 2007; Han et al., 2007; Li et al., 2008; Masumoto et al., 2005).

Located near the DNA entry- exit point, the K56 acetylation disrupts a water-mediated contact with the DNA phosphate backbone (Figure 1.2 A) (Luger et al., 1997). Biophysical experiments including FRET have shown that H3-K56Ac generally makes DNA accessible, possibly by increasing the frequency of DNA breathing on a nucleosome (Figure 1.2 B) (Masumoto et al., 2005; Neumann et al., 2009; Ozdemir et al., 2005). Greater accessibility could impact the remodeling of this nucleosome, and as a matter of fact, the sliding activity of SWI/SNF and RSC is modestly increased in the presence of H3-K56Ac (Neumann et al., 2009).

In non-replicative cells, H3-K56Ac is most enriched in promoter-proximal nucleosomes near the TSSs of genes, similar to the variant H2A.Z. These nucleosomes have high turnover rates and undergo multiple rounds of

assembly/disassembly in apparent futility. Importantly, this turnover is independent of both DNA replication and transcription (Kaplan et al., 2008; Rufiange et al., 2007). Replication independent histone turnover has been implicated in transcriptional activation and repression at the *PHO5* gene, and as a boundary to prevent the spread of heterochromatin marks into euchromatin (Adkins et al., 2004; Dion et al., 2007; Korber et al., 2006; Williams et al., 2008). Although Rtt109, Asf1 and H3-K56Ac also promote histone turnover, genome-wide RNA profiling of *rtt109Δ* and *asf1Δ* has revealed few changes (Lenstra et al., 2011; Williams et al., 2008; Xu et al., 2005a). Thus, unlike its function during replication and DNA repair, the role of H3-K56Ac in transcription remains unclear.

This histone mark was previously thought to be restricted to the fungal species, but recent studies have now identified a role for H3-K56Ac in mammals (Tan et al., 2013; Xie et al., 2009). In higher organisms, H3-K56Ac is present at active genes and appears to promote pluripotency (Tan et al., 2013; Xie et al., 2009). This particular histone mark is not as abundant in these systems as in yeast, likely why its existence in mammals was debated for some time. Thus, lessons learnt from yeast may now have functional implications for H3-K56Ac in mammalian biology.

Figure 1.2: H3-K56Ac residue on the nucleosome and its biophysical implication

A) Crystal structure of the nucleosome (PDB#1AOI, (Luger et al., 1997)) highlighting the H3-K56Ac residue (red box) located at the DNA entry-exit point on the nucleosomal surface. Reproduced with permission from J. Feldman.

B) Illustration of increased DNA accessibility using FRET, after modification of H3-K56. The donor and acceptor fluorophore sites are shown in red and green and the histone proteins in grey. The site of H3K56 acetylation is shown in blue. Reproduced with permission from the Chin lab website.

Figure 1.2

A)

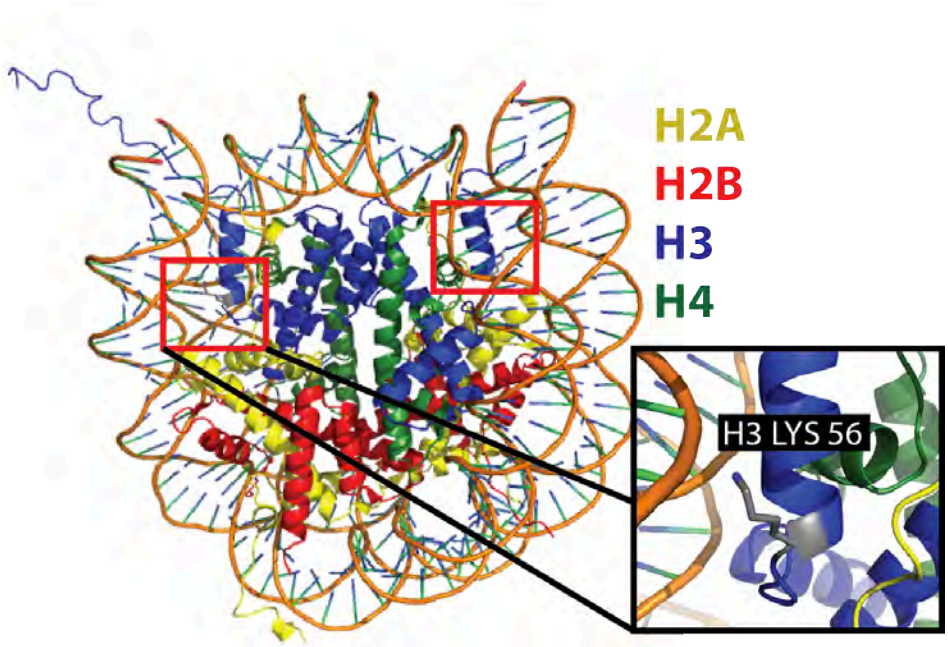

B)

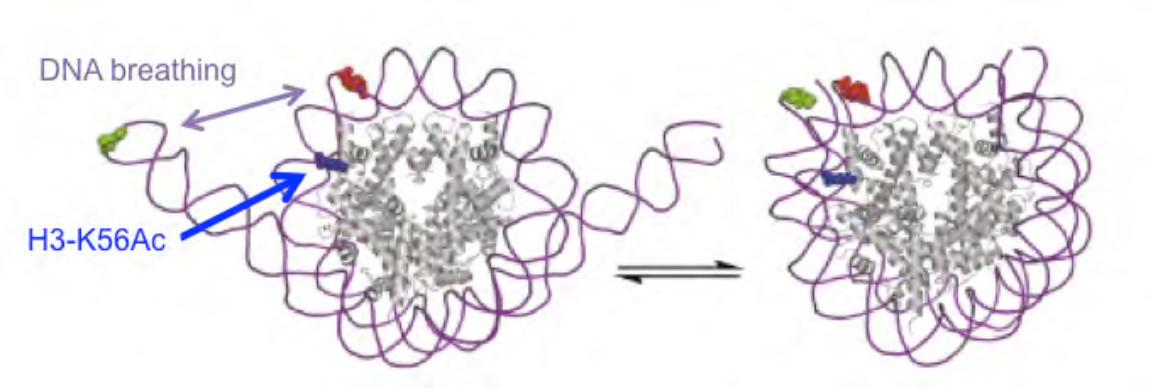

I-C.iii. Histone variants punctuate chromatin

Histone variants are derivatives of canonical histones with changes in the amino acid sequence. Unlike canonical histones, these variants are expressed throughout the cell cycle and many are restricted to specific chromatin domains. H2AZ is an H2A histone variant that is highly conserved across eukaryotes; it is essential in metazoans (Clarkson et al., 1999; van Daal and Elgin, 1992; Faast et al., 2001; Iouzalen et al., 1996; Liu et al., 1996; Ridgway et al., 2004). H2A.Z mutants are viable in yeast, and thus amenable to mechanistic study in these model systems.

Although H2A.Z is only 60% identical to H2A at the sequence level, there are comparatively subtle changes in the properties of an H2A.Z nucleosome (Weber and Henikoff, 2014; Zlatanova and Thakar, 2008). Crystal structure of an H2A.Z nucleosome reveals two primary differences: first, H2A.Z has an extended acidic patch on the nucleosome surface that is expected to alter inter-nucleosomal interactions with the H4 tail of an adjacent nucleosome (Suto et al., 2000). Consistent with this, analytical ultracentrifugation analyses of H2A.Z nucleosomal arrays reveal that they are more folded than H2A arrays (Suto et al., 2000). Secondly, the L1 loop within the core domain that docks with H3/H4, has a glutamine-to- glycine substitution in H2A.Z that compromises three hydrogen bonds (Suto et al., 2000). Although this is expected to weaken the interaction with H3/H4, biophysical data have revealed conflicting results of the effect of the

L1 loop on the stability of the H2A.Z nucleosome (Weber and Henikoff, 2014). While these differences may arise from different DNA templates used, it is clear that *in vivo*, H2A.Z nucleosomes are generally unstable compared to the H2A counterpart, and associated with open chromatin (Bönisch and Hake, 2012).

A unique feature of H2A.Z nucleosomes is that they are stereotypically enriched at promoter proximal nucleosomes adjacent to the TSS in all eukaryotes (Albert et al., 2007; Guillemette et al., 2005; Li et al., 2005; Mavrich et al., 2008; Millar et al., 2006; Raisner et al., 2005; Zhang et al., 2005). A majority of studies have implicated H2A.Z in gene activation, such that H2A.Z is lost on transcriptional activation (Adam et al., 2001; Farris et al., 2005; Larochelle and Gaudreau, 2003; Santisteban et al., 2000). Thus, H2A.Z is thought to mark transcriptionally poised genes (Zhang et al., 2005). In contrast to this, H2A.Z can also act as a transcriptional repressor by facilitating binding of the Polycomb heterochromatin proteins (Creyghton et al., 2008). Thus, H2A.Z is probably used as a punctuation mark to bookmark gene ends, and its effect on transcription is dependent on the effector proteins that are conditionally recruited (Weber and Henikoff, 2014). Importantly, the transcriptional roles described above have been observed primarily in single locus studies and there are few changes in RNA abundance in *htz1Δ*, or *swr1Δ*, the enzyme that incorporates this variant into chromatin (Lenstra et al., 2011; Mizuguchi et al., 2004; Morillo-Huesca et al.,

2010). Thus, despite the widespread and conserved chromatin localization, the exact mechanistic role of H2A.Z remains elusive.

I-C.iv. Chromatin remodeling enzymes actively mobilize chromatin

Chromatin remodeling enzymes are protein complexes that utilize ATP to remodel nucleosomes and regulate access to DNA. They catalyze various reactions such as “sliding” the histone octamer in cis, eviction of histone dimers or removal of the entire octamer (Clapier and Cairns, 2009). Thus, they enable various sequence dependent activators and basal transcription factors to bind to the exposed DNA.

Historically, SWI/SNF was the first enzyme discovered that could remodel chromatin. Two genetic screens for transcriptional activators using yeast were performed in parallel in the Herskowitz and Carlson labs. The Herskowitz lab focused on mutants that failed to induce the *HO* endonuclease so they could not switch (*swi* $^{-}$) mating types (Stern et al., 1984). Conceptually, mating type is a cell fate choice in yeast and wild type haploids chose either ‘a’ or ‘alpha’ mating type, with the ability to switch from one to the other. The Carlson lab studied mutants defective in the induction of the invertase gene, SUC2, required for fermentation of sucrose (*snf* $^{-}$, sucrose non fermenting) (Neigeborn and Carlson, 1984). Surprisingly, it was later discovered that *SWI2* and *SNF2* were, in fact, the same gene, and also affected transcriptional activation of other target genes (Peterson

and Herskowitz, 1992). This key finding set the stage for functional studies of how SWI/SNF helps the transcriptional process. Over the years, work in all model organisms strongly implicates SWI/SNF as a transcriptional activator. This is a textbook example of how genetic screens in model organisms such as yeast have accelerated identification of analogous proteins in 'higher' organisms.

Following the discovery of SWI/SNF, a number of labs identified enzymes related to *SWI2* based on sequence similarity. Currently, there are four families of chromatin remodeling enzymes: SWI/SNF, ISWI, CHD and INO80 family and each consists of several multi-subunit complexes (Bao and Shen, 2011; Corona and Tamkun, 2004; Marfella and Imbalzano, 2007; Mohrmann and Verrijzer, 2005). All chromatin remodeling enzymes contains a catalytic ATPase subunit that belongs to the Swi2/Snf2 subfamily and disrupt histone/DNA contacts to mobilize the nucleosome. In spite of the similarities, the individual families have unique subunits and specialization in cellular function. Particular characteristics of the families relevant to this work are mentioned below, with an emphasis on how they affect transcription.

SWI/SNF family consists of two highly related remodelers that share many subunits, SWI/SNF and RSC (Cairns et al., 1998). SWI/SNF and RSC both effectively slide and eject nucleosomes, but cannot assemble them, and have biochemical similarities. However, their genomic targets and functions appear to be largely non-overlapping. SWI/SNF is intimately linked to HATs like SAGA,

interacts with co-activators and is generally positively associated with transcriptional initiation and elongation (Armstrong et al., 2002; Cosma et al., 1999; Holstege et al., 1998; Schwabish and Struhl, 2007; Wilson et al., 1996; Yudkovsky et al., 1999). Although *swi2Δ* null mutants (encodes for the SWI/SNF catalytic subunit) show severe growth defects, only a small fraction of the genome changes significantly in these mutants, arguing that this enzyme has specific targets during steady-state transcription (Holstege et al., 1998; Sudarsanam et al., 1999). Peterson and colleagues has described a unique role for SWI/SNF (and not RSC) in eviction of the heterochromatin protein Sir3 (Manning and Peterson, 2014; Sinha et al., 2009). Given the low abundance of SWI/SNF (~200 protein molecules/ cell), this property may have been excluded from the abundant RSC complex to avoid unwanted and widespread disruption of heterochromatin (Ghaemmaghami et al., 2013). In contrast to this, RSC is the only essential remodeling enzyme in yeast (*STH1* encodes the RSC catalytic subunit) and *STH1* conditional alleles affect Pol III and Pol II genes (Parnell et al., 2008). Recent work has implicated SWI/SNF and RSC in activating and inhibiting cryptic transcription, respectively (Alcid and Tsukiyama, 2014; Marquardt et al., 2014).

The **ISWI family** remodeling enzymes can be thought of as counteracting the actions of the SWI/SNF family because they promote nucleosome assembly. ISWI enzymes such as ACF, CHRAC were first purified from fly embryo extracts

by the Wu, Becker and Kadonaga labs (Ito et al., 1997; Tsukiyama et al., 1995; Varga-Weisz et al., 1997). These ATPases were similar in sequence to the *Drosophila SWI2/SNF2* homolog (Brahma) and were therefore named Imitation SWItch (Elfring et al., 1994). This family of enzymes is also involved in optimizing nucleosome spacing, which changes access to linker DNA regions. In yeast, there are two homologs of this family: Isw1p and Isw2p (Tsukiyama et al., 1999). The specialization into two enzymes might be explained by a difference in their activities: *ISWI1* can activate or repress transcriptional initiation by assembling into distinct complexes while *ISWI2* represses many ORFs, including meiotic genes that are Ume6 targets (Fazzio et al., 2001; Goldmark et al., 2000). ISWI2 also suppresses antisense transcription from intergenic regions, as described in a later section (Whitehouse et al., 2007).

The **INO80 family** consists of two classes of multi-subunit enzymes: INO80 and SWR1, and were first purified in yeast by the Wu lab (Shen et al., 2000). Similar to other chromatin remodelers, the INO80 enzyme can mobilize nucleosomes in *cis*. INO80 also functions in transcriptional activation, DNA repair and to inhibit cryptic transcription (van Attikum et al., 2004; Jónsson et al., 2004; Mizuguchi et al., 2004; Papamichos-Chronakis and Peterson, 2008; Papamichos-Chronakis et al., 2011; Shimada et al., 2008). In spite of the similarity between the INO80 and SWR1 enzymes, the latter has very weak nucleosome sliding activity (Mizuguchi et al., 2004). However, both INO80 and SWR1 have the

unique ability to carry out an ATP-dependent histone dimer exchange reaction. In the forward reaction (catalyzed by SWR-C), the H2A/H2B dimer in a canonical nucleosome is replaced with a H2A.Z/H2B dimer, while the reverse reaction (catalyzed by INO80) restores the nucleosome to its original state; by replacement of a H2A.Z/H2B dimer with one containing H2A/H2B (Mizuguchi et al., 2004, Papamichos-Chronakis and Peterson, 2008).

SWR-C is likely the sole H2A.Z deposition mechanism in yeast because no chromatin incorporation of H2A.Z is observed in the null mutant (*swr1Δ*). Targeting of SWR1 through its bromodomain to acetylated promoter regions was thought to restrict this H2A.Z incorporation activity to promoter proximal nucleosomes (Ranjan et al., 2013; Yen et al., 2013). However, data from the Robert lab showing that histone chaperones FACT/Spt6 actively eliminate H2A.Z from within coding regions suggests that the pattern of H2A.Z enrichment arises from a combination of targeting at promoters and eviction from gene bodies (Jeronimo et al., 2015).

I-C.v. Chromatin folding and 3D genome interactions

Chromatin factors help package the genome inside the nucleus, so instead of a linear molecule, it is more realistic to think of chromatin in terms of the interactions it makes in 3D space inside the nucleus. Although a lot of work in the chromatin field has focused on assembly of nucleosomes *in vitro*, techniques to

ask how genomes are packaged *in vivo* were only established about a decade ago. Chromosome conformation capture (3C) assays, pioneered by Dekker and co-workers, first facilitated the analysis of how frequently certain regions of the genomes 'touch' each other (Dekker et al., 2002). Initial studies were performed using a handful of long genes in the yeast genome, such as *FMP27* and *BLM10*, because they were easy to assay using PCR (O'Sullivan et al., 2004; Singh and Hampsey, 2007). 3C assays led to the observation that the 5' and 3' ends of genes interact most frequently compared to the other regions within the same gene, and coined the term 'gene looping' (reviewed in Hampsey et al., 2011). The CTD phosphatase/ termination factor Ssu72, was one such factor required to form a 'gene loop' (Krishnamurthy et al., 2004; Tan-Wong et al., 2009).

Improvements to the original 3C concept were possible with progress in detection technologies: 'bait' fragments used in 4C, multiplex PCR in 5C, and deep-sequencing used in Hi-C (Dekker et al., 2013). These techniques have lead to the identification and characterization of Topologically Associated Domains (TADs), which are regions of the genome that tend to cluster together and interact preferentially (Dixon et al., 2012). TAD formation is mediated by several DNA binding proteins with zinc-finger domains (Gómez-Díaz and Corces, 2014). Remarkably, most TADs are conserved across different cell types, and the differences appear to correlate with cell-type specific behavior (Dixon et al., 2012; Nora et al., 2012; Pope et al., 2014).

Are TADs functional, such that they dynamically rearrange inside the nucleus? There is now accumulating evidence that TAD organization is meaningful and sometimes, instructive; changing the orientation of a CTCF binding site is sufficient to change the corresponding TAD and mediate transcriptional changes (Guo et al., 2015). Likewise, the Blobel lab has shown that artificially tethering an active enhancer to a functional hemoglobin allele can not only restore the cell with a functional protein, but also relieve some of the phenotypes associated with the naturally-expressed non-functional allele (Deng et al., 2014). Thus, TADs appear to be functional entities that may serve to partition the genome into compartments to better coordinate transcriptional activity (Ulianov et al., 2015).

While Hi-C captures a snapshot of higher-order chromosome structures (aka TADs), it does not tell us how these higher-order domains are assembled from an array of nucleosomes. In other words, restriction enzymes used to cut the crosslinked samples limit the resolution of Hi-C to a few kilobases, due to the number of sites present in the genome. While useful for larger genomes, Hi-C is limiting for organisms with small genomes, such as budding yeast. To overcome this drawback, Rando and colleagues recently improved the resolution of the Hi-C technique by using MNase, an enzyme that cuts linker DNA, to digest samples to mononucleosome length (~ 150 bp) (Hsieh et al., 2015). This method, called

Micro-C, theoretically allows us to determine the interaction frequency of every nucleosome with every other nucleosome in the genome.

Micro-C analyses of the budding yeast genome showed that in comparison to mammalian TADs, equivalent structures in yeast appear to scale down to the size of the genome. Such interaction regions are called Chromosomal Interaction Domains (CIDs) and CIDs are made up of about 1-5 genes (Hsieh et al., 2015). Surprisingly, Micro-C analyses showed no evidence of 'gene looping' described previously from 3C assays. Instead, CIDs are similar to a gene crumple, with all nucleosomes within one gene interacting more frequently with each other than a nucleosome from a neighboring gene, even if the latter is 'nearby' in linear genomic distance. Thus, Micro-C appears to interrogate higher order chromosome structure in a way that complements the observations from other established assays. The functional implication of CIDs in genome organization remains to be fully elucidated.

I-D. Chromatin factors that regulate cryptic transcription

Chromatin regulation clearly affects the transcriptome of a eukaryotic cell. The identification of cryptic ncRNAs in yeast spurred a number of studies to investigate whether chromatin factors might also affect these unstable transcripts. Although early lines of inquiry targeted a handful of candidates, genetic screens using fluorescent reporter constructs as well as strains where RNAi+ was artificially reconstituted have now systematically addressed this question (Alcid and Tsukiyama, 2014; Cheung et al., 2008; Marquardt et al., 2014). Most known chromatin factors appear to affect cryptic transcription, expanding their regulatory role in the cell.

I-D.i. Histone chaperones and variants

Histone chaperones that incorporate histones during replication, as well as after a round of transcription, inhibit ncRNA expression. Buratowski and colleagues found that inactivation of the nucleosome assembly factor, CAF1, leads to increased expression of ncRNAs at many divergent yeast promoters (Marquardt et al., 2014). They suggested that assembly and/or stability of nucleosomes that occupy ncRNA promoters plays a key role in restricting their expression and reinforcing expression of the adjacent mRNA gene. Analogous to this, FACT and Spt6 are Pol II elongation-associated histone chaperones that restore nucleosomes in the wake of the polymerase. These chaperones prevent initiation

of ncRNAs within coding regions of ORFs (Kaplan et al., 2003). Work from Winston lab in both budding and fission yeast has revealed that Spt6 mutants show elevated antisense transcripts at > 70% of all protein-coding genes (DeGennaro et al., 2013). Recent *in vitro* and *in vivo* data from the Robert lab emphasized the remarkable specificity of Spt6/FACT to selectively incorporate H2A (and exclude the variant H2A.Z) within transcribed regions. In the absence of FACT/ Spt6, accumulation of H2A.Z in gene bodies promotes initiation from cryptic promoters located in gene bodies (Jeronimo et al., 2015). This positive role for H2A.Z is consistent with the previous observation by Grewal and co-workers, that this histone variant also assists transcriptional termination at convergent genes and prevents readthrough (Zofall et al., 2009).

I-D.i. Histone modifications

In addition to histone chaperones and variants, acetylation/ methylation of specific histone residues associated with transcription of ORFs also affects non-coding RNA expression (Smolle and Workman, 2013). H3K36me3, catalyzed by the Set2 methyltransferase, is enriched over the body of the gene and appears to serve a dual purpose: to recruit the HDAC Rpd3S and to prevent histone turnover within coding regions. H3K36me3 activates Rpd3S to deacetylate histones behind the polymerase and prevent initiation from intragenic cryptic promoters (Carrozza et al., 2005; Joshi and Struhl, 2005; Keogh et al., 2005). The

H3K36me3 histone mark also blocks the interaction of the chaperone Asf1 with histones in the coding region, thereby reducing histone exchange over gene bodies (Venkatesh et al., 2012). The H3K4me2 mark located upstream of H3K36me3 is also involved in repressing transcription from internal cryptic promoters within ORFs. The Set3C complex binds to H3K4me2 and represses internal cryptic promoters at distinct regions from the Set2/Rpd3S pathway described above (Kim et al., 2012).

I-D.iii. Chromatin remodeling enzymes

Chromatin remodeling enzymes that mobilize nucleosomes to change the accessibility of the underlying DNA can also affect ncRNA initiation. Tsukiyama and colleagues have reported that the remodelers ISW2, RSC and INO80-C, directly inhibit expression of distinct sets of ncRNAs in yeast, together called chromatin remodeling-repressed antisense transcripts (CRRATS) (Table 1.1) (Alcid and Tsukiyama, 2014). CRRATs initiate from NFRs and, are antisense to 3' regions of ORFs such that some can interfere with ORF expression. Work from the Carey lab also reported that INO80-C blocks ncRNA transcription within intragenic regions (Xue et al., 2015). Fazzio and colleagues reported that esBAF, the mammalian SWI/SNF homolog, represses expression of a large set of ncRNAs in mouse ESCs by positioning nucleosomes over ncRNA promoters

(Hainer et al., 2015). Thus, a considerable amount of resources in the cell prevent ncRNA expression using multiple parallel mechanisms.

I-D.iv. Chromatin factors that promote cryptic transcription

Evolutionary conservation argues for a positive role for cryptic transcription, however, we know very little about the factors that promote ncRNA production. Certainly, a fraction of promoter-associated transcription is likely to be reflective of the inherent noise in the transcriptional machinery finding a cognate promoter (Struhl, 2007). The only report we are aware of that has tested this is work from Buratowski and co-workers; they showed that the yeast SWI/SNF chromatin remodeling enzyme can promote divergent non-coding transcription from a couple of gene loci (Marquardt et al., 2014). As SWI/SNF is a low abundance enzyme, it may target only a subset of the enormous number of ncRNA produced in budding yeast. Whether any other mechanisms promote cryptic promoter-associated transcripts remains to be determined.

In summary, transcriptional regulation involves coordination between multiple players: the RNA Pol II CTD tail, histone modifications, variants, chromatin remodeling enzymes and the RNA degradation machinery. The discovery of a large number of cryptic, non-coding transcripts suggests a hidden layer of regulation. Although considerable progress has been made in

determining what inhibits cryptic RNAs, more efforts are needed to understand what mechanisms and conditions might promote cryptic transcripts. This work attempts to bridge this knowledge gap.

Chapter II: *RTT109* regulates ncRNAs and ORFs in concert with *RRP6*

II-A. SUMMARY

Eukaryotic genomes are packaged into a nucleo-protein complex called chromatin. Chromatin is made up of nucleosomes, which consist of 147bp of DNA wrapped around a histone octamer. Nucleosomes that carry lysine 56-acetylated histone H3 (H3-K56Ac) are particularly enriched at the 5' ends of most genes. This histone modification has been shown to increase accessibility to DNA. Given its genome-wide presence, it is unclear whether H3-K56Ac globally affects transcription of genes. Here, we find that H3-K56Ac promotes RNA polymerase II occupancy at most protein coding and noncoding loci, yet this histone mark does not significantly impact steady state mRNA levels in yeast. Instead, broad effects of H3-K56Ac on RNA levels are only revealed in the absence of the nuclear RNA exosome. Amongst protein-coding genes, highly transcribed loci are negatively regulated by the exosome and depend on H3-K56Ac to counter this effect. Our study suggests that H3-K56Ac works in concert with the RNA exosome to control mRNA and ncRNA expression, perhaps in part by regulating higher order chromatin structures.

II-B. INTRODUCTION

Eukaryotic genomes are packaged into the nucleus using chromatin. The fundamental building block of chromatin is a nucleosome, composed of an octamer of histone proteins assembled on 147 base pairs of DNA. The octamer typically contains two copies of each core histone: H2A, H2B, H3 and H4, which are highly conserved across eukaryotes. While histones help DNA folding, they also make the sequence inaccessible. Thus, access to DNA must be regulated to mediate cellular processes such as transcription and replication. Histone modifications are chemical moieties added post-translationally to histone tails or core regions, which can regulate access to chromatin.

An example is the lysine 56 residue of histone H3 (H3-K56) that is present in the globular domain. In the presence of a histone chaperone Asf1, the HAT Rtt109 acetylates this histone residue prior to incorporation into chromatin (Tsubota et al., 2007). Thus, H3-K56Ac marks newly incorporated nucleosomes and plays an important role in histone assembly. Replication and transcription are widespread genomic processes that require proper histone assembly; while the former occurs during the S-phase, transcription takes place throughout the cell cycle. To determine the rate of histone replacement (or turnover) outside of S phase, Rando and colleagues compared chromatin bound levels of a constitutively expressed histone H3 to an inducible, FLAG-tagged version of the

H3 gene (Dion et al., 2007). Surprisingly, histone turnover was highest at nucleosomes that flank promoters of genes, and independent of active gene transcription. H3-K56Ac was enriched in these nucleosomes, and histone turnover dramatically slowed in the absence of either Rtt109 or Asf1, suggesting that H3-K56Ac directly promotes histone turnover, independent of replication. Histone turnover likely makes DNA more accessible by increasing the frequency of DNA breathing. The dynamic nature of these nucleosomes has contributed to the prevailing view that H3-K56Ac may generally promote transcription. However, previous studies have failed to reveal extensive transcription roles for this mark, and thus its contribution to steady-state transcription remains unclear (Lenstra et al., 2011).

In addition to harboring dynamic nucleosomes, eukaryotic promoter regions are commonly bidirectional in nature, with divergent noncoding RNAs (ncRNAs) and mRNAs expressed from different promoters that share a common nucleosome free region (NFR) (Neil et al., 2009; Xu et al., 2009). In yeast, many divergently transcribed ncRNAs like CUTs are 5' capped and oligoadenylated (< 10 adenines), with a median length of 400 nucleotides. Normally, CUTs are rapidly degraded because they contain binding motifs for the NNS termination machinery, which, in turn, promote recruitment of the RNA exosome (Arigo et al., 2006; Schulz et al., 2013; Thiebaut et al., 2006). Consequently, inactivation of the nuclear exosome subunit, Rrp6, is necessary to monitor changes in CUT

transcription. Rrp6 is a 3'-5' exonuclease that also targets ncRNAs and unspliced pre-mRNAs for degradation (Schneider et al., 2012), facilitates processing of sn/snoRNAs (Gudipati et al., 2012), and may play a more general surveillance role that governs nuclear mRNA levels (Schmid et al., 2012). Whether H3-K56Ac regulates expression of ncRNAs has not been thoroughly addressed.

In this study, we present evidence that H3-K56Ac is a global, positive regulator of ncRNA expression in yeast. We also show that H3-K56Ac has a dramatic effect on RNAPII occupancy at many protein-coding genes, but corresponding changes in mRNA levels are masked by a functional nuclear exosome. We suggest that H3-K56Ac works in concert with the RNA exosome to control mRNA and ncRNA expression genome-wide.

II-C. RESULTS

Absence of H3-K56Ac has little apparent impact on steady state RNA abundance

In order to monitor the effect of H3-K56Ac on both coding and noncoding RNA expression, we isolated total RNA from isogenic wild type and mutant budding yeast strains, and prepared samples for hybridization to strand-specific, DNA tiling arrays. These arrays provide high-density coverage of the yeast transcriptome (Castelnuovo et al., 2014; David et al., 2006; Huber et al., 2006). Our initial analysis included strains with gene deletions inactivating Rtt109p, which catalyzes acetylation of H3-K56 (*rtt109*Δ). We observed that inactivation of Rtt109p had a minor overall effect on the transcriptome, as only 72 transcripts were decreased 1.5-fold or more compared to wild type (WT) at an FDR < 0.1 (Fig. 2.1A, B and Table S1, in Appendix 1) (Lenstra et al., 2011). The two most strongly decreased genes other than *RTT109* are, *PRY3*, which encodes a cell wall-associated protein involved in sterol secretion, and a small nuclear RNA, *SNR39B*. It is not obvious how defects in expression of these two genes might affect our results. We were surprised to find a minor overall effect of H3-K56Ac on RNA levels, given that the enhanced nucleosome dynamics promoted by this histone mark are expected to generally promote transcription.

Figure 2.1: Steady state RNA levels are largely unaffected by *rtt109Δ*, although RNAP II recruitment is reduced dramatically

A) RNA abundance measured by strand-specific tiling microarrays in *rtt109Δ* strains. Density scatterplots (top panels) show median signal intensity values in comparison to wild type arrays (WT). The black diagonal line indicates x=y (no change) and the horizontal and vertical lines indicate the noise threshold cut-off.

B) Volcano plots show the transcripts that change significantly in the mutant compared to the wild type (WT) highlighted in blue (p_{adj} = FDR < 0.1 and Log_2 Fold Change > ±0.59). The Y-axis shows the p_{adj}-value (after FDR correction). See also Table S1 in Appendix 1.

C) Representative genome browser view of Pol II ChIP-seq data for the wild type (black) and *rtt109Δ* (red), normalized to the respective total library read count.

D) Density scatterplots of Pol II IP/input values in the *rtt109Δ* compared to wild type at 5171 ORFs (top) and 925 CUTs (bottom). The black line indicates x=y (no change).

Figure 2.1

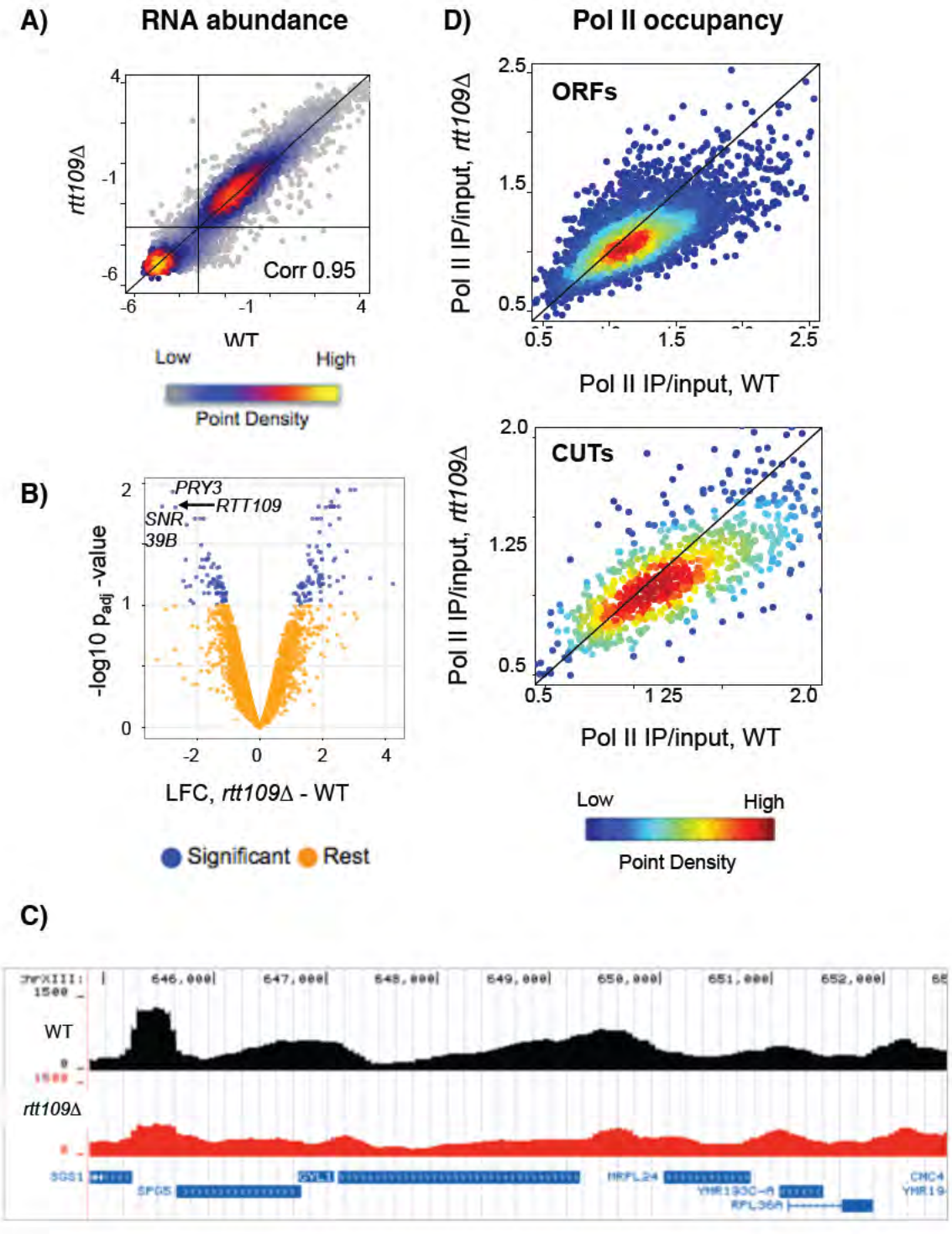
A)
RNA abundance
rtt109Δ
WT
Corr 0.95
Low
High
Point Density
B)
PRY3
RTT109
SNR39B
-log10 padj -value
LFC, rtt109Δ - WT
Significant
Rest
D)
Pol II occupancy
ORFs
Pol II IP/input, rtt109Δ
Pol II IP/input, WT
CUTs
Low
High
Point Density
C)
WT
rtt109Δ

RNAP II occupancy is reduced in the absence of Rtt109p

As RNA abundance reflects both synthesis and decay of RNA molecules, we sought to probe the transcription process more directly by monitoring genome-wide RNAPII occupancy in isogenic WT and *rtt109*Δ strains by ChIP-seq. We performed ChIP-seq and prepared samples as described previously (Watanabe et al., 2013). Two different biological samples were sequenced for each genotype. We used the anti-CTD antibody (8WG18, Covance) for IPs, as it is known to capture total RNA Pol II in genome-wide data (Bataille et al., 2012; Wong et al., 2014).

We analyzed the ChIP-seq data using multiple different pipelines to ensure rigor, as described in detail in the Materials and Methods. Briefly, Model-based Analysis of ChIP-Seq (MACS2) (Zhang et al., 2008) was used to identify differential peaks in mutant compared to wild type, and displayed in genome browser view (Figure 2.1C). We complemented this analysis by adopting a well-defined approach described by the Rine group that required us to write our own scripts (Teytelman et al., 2013). The second method has the advantage that it omits all black-box model-fitting steps done in MACS, which can distort results if certain assumptions are violated by the data. This approach also makes it easy to compare IP/input values at defined regions across multiple strains, while peak coordinates typically vary depending on the the dataset being used. Nonetheless, our findings are robust, as they have been verified by both analyses methods.

In contrast to the minor defects observed for mRNA abundance (Figure 2.1A), the absence of H3-K56Ac led to widespread decreases in RNAPII levels at 567 open reading frames (ORFs) and 184 CUTs (>1.3 fold) (Figure 2.1C, D). We reasoned that the discordance between changes in RNAPII and steady state RNA levels suggested that compensatory actions on transcript stability/degradation may obscure changes in gene expression (Haimovich et al., 2013; Sun et al., 2013).

Rrp6 negatively regulates not only CUTs but also some specific ORFs

The major RNA degradation machinery in the nucleus is the exosome and Rrp6, is a 3' exonuclease that is associated with it. To assay effects of H3-K56Ac on transcription in the absence of confounding effects of exosome-mediated RNA degradation, we isolated total RNA from isogenic WT, *rrp6Δ* and *rtt109Δ rrp6Δ* strains, and hybridized samples to strand-specific DNA tiling arrays. Rrp6 is known to regulate the stability of RNAPII transcripts, including pre-mRNAs and ncRNAs (Schmid et al., 2012).

While analyzing data from additional replicates, we serendipitously discovered that our first set of two *rrp6*Δ replicates had muted signal intensities ('low signal'), including for CUTs. Therefore, we systematically analyzed and compared all of our *rrp6Δ* replicate data with two previously published datasets (Castelnuovo et al., 2014a; Tan-Wong et al., 2012). Pearson correlation plots

clearly revealed that our ‘low signal’ arrays were somewhat of an outlier compared to the rest of the samples, prompting us to omit that data from analysis. Additionally, we also performed PCA (Principle component analysis), which tries to capture the cause of variation across datasets. The majority of the variance in the data (PC1) came from a small number of genes that are affected by transcriptional interference (see below), which varied, to some extent, depending on whether RNA samples were collected from strains that had been stored at -80°C. In fact, this variability was also obvious when we compared these interference genes amongst published *rrp6Δ* tiling array datasets, thus validating our sample preparation methods (Castelnuovo et al., 2014a; Gudipati et al., 2012b; Tan-Wong et al., 2012). We concluded that *rrp6Δ* likely have unstable genomes and recommend that future studies should control for the ‘age’ and possible epigenetic changes occurring from storage in -80°C, similar to empirical observations in other strains (Rando, OJ, personal communication).

Nonetheless, given our limited understanding of this phenomenon, we used freshly dissected haploids that presumably have no other background mutations, and repeated the experiments. We performed a total of 11 replicates, of which 7 correlated well with each other and published data (R^2 = 0.9- 0.98). As expected, in this rigorously tested dataset, inactivation of the nuclear exosome caused a dramatic accumulation of CUTs, as well as increased expression of other ncRNAs such as SUTs (Figure 2.2A, B) (Neil et al., 2009; Xu et al., 2009).

In addition, 985 ORFs were consistently increased in the *rrp6Δ* mutant 1.5-fold or more compared to the wild type (WT) strain (FDR <0.1) (Figure 2.2A, B and Table S1D in Appendix 1). Notably, the increased expression of ORF transcripts in the *rrp6Δ* mutant is not due to defects in transcription termination from upstream loci (Figure 2.3A, B), as the upstream expression level (defined as -100 to TSS) from these ORFs correlates poorly with the downstream expression levels (defined as TSS to +100). Although Rrp6 was shown to promote proper termination at a handful of ORFs and CUTs (n= 7) (Fox et al., 2015), our analyses suggest that this may not be a widespread phenomenon, at least when the Nrd1 termination factor is functional (Schulz et al., 2013). Furthermore, the set of exosome-inhibited ORFs are not enriched for spliced transcripts (90 out of 985 have introns), indicating that the increases we observe are not generally due to splicing defects.

Loss of *RRP6* also led to a decrease in expression of a similar number of ORFs (n=851), and they include the set of ~100 transcripts that were previously shown to be repressed by transcriptional interference from adjacent ncRNAs (Camblong et al., 2007; Castelnuovo et al., 2014). Notably, RNAPII ChIP-seq analysis in the *rrp6Δ* strain did not reveal significant effects of exosome loss on genome-wide Pol II occupancy, indicating that the observed changes in RNA abundance in the *rrp6Δ* are due to defects in RNA turnover (Figure 2.2C, D) (Fox et al., 2015).

Figure 2.2: *rrp6Δ* does not affect Pol II occupancy but RNA abundance is increased

A) RNA abundance measurements as in Figure 1A represented as density scatterplot.

B) Volcano plots show the transcripts that change significantly in the mutant compared to the wild type highlighted in blue (p_{Adj} <0.1 and Log_2 Fold Change≥ ±0.59).

C) Representative genome browser view of ChIP-seq analysis of Pol II for the wild type (black), *rrp6Δ* (green) and *rtt109Δ* (red) normalized to the total library read count. The peaks marked as “Affected” and “Unchanged” were derived from analysis with MACS2.

D) Density scatterplots of Pol II IP/input values at coding regions of all ORFs (left) and CUTs (right) in the *rrp6Δ* compared to wild type. The black line indicates x=y (no change).

Figure 2.2

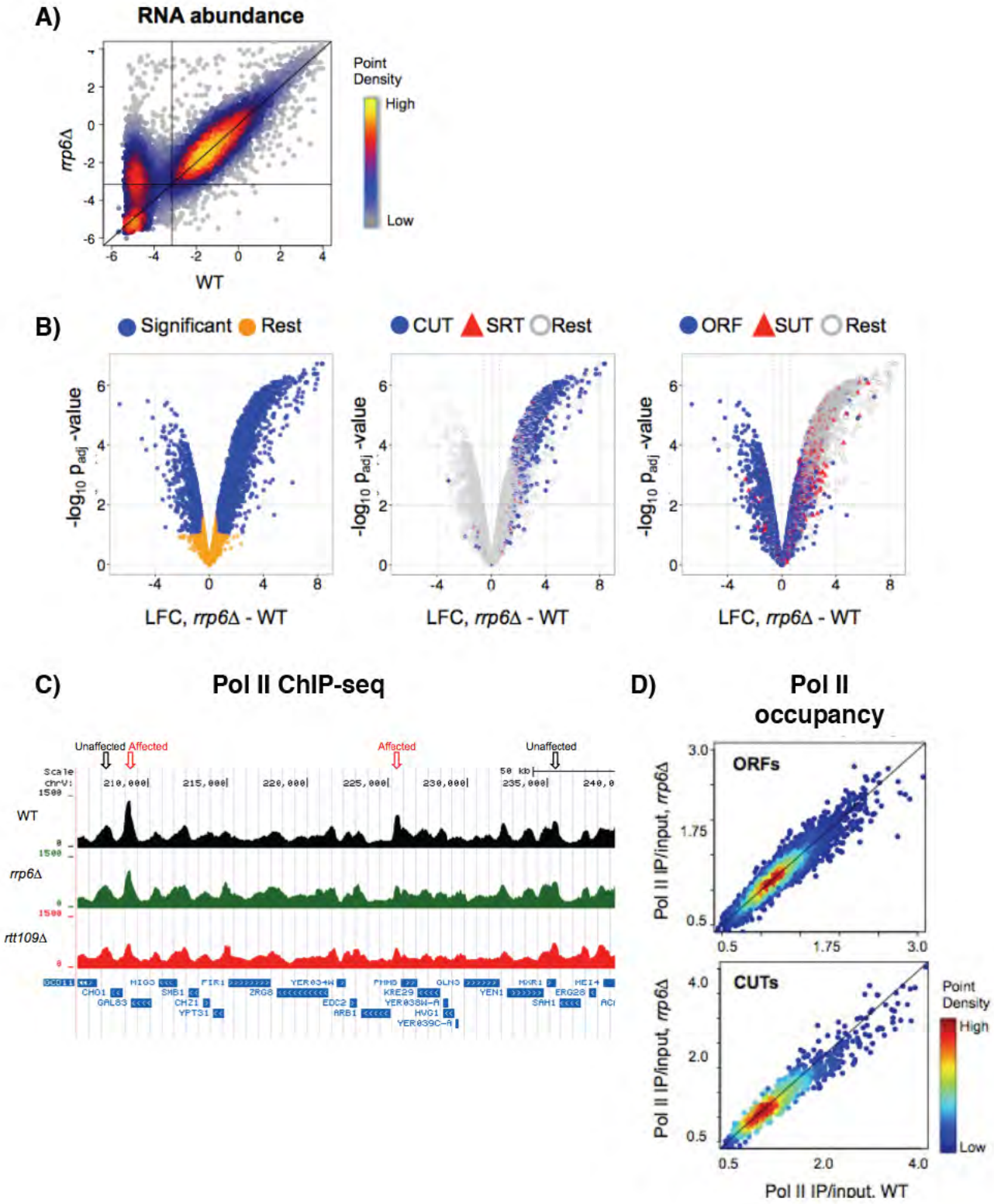
A)
RNA abundance
rrp6Δ
WT
Point Density
High
Low
B)
Significant
Rest
CUT
SRT
Rest
ORF
SUT
Rest
-log10 padj -value
LFC, rrp6Δ - WT
C)
Pol II ChIP-seq
Unaffected
Affected
Affected
Unaffected
WT
rrp6Δ
rtt109Δ
D)
Pol II occupancy
ORFs
CUTs
Pol II IP/input, rrp6Δ
Pol II IP/input, WT
Point Density
High
Low

Figure 2.3: Defects in transcriptional termination do not account for upregulated ORFs in the *rrp6*Δ

A) Schematic illustrating the upstream (“Up”) and downstream (“Down”) coordinates relative to the TSS of ORFs from which the signal intensity was extracted. The set of 985 ORFs upregulated in *rrp6*Δ was used for the analysis.

B) Boxplot for the two genotypes of the median signal over replicates is shown. Mann-Whitney-Wilcoxon Test was performed to compare the medians.

Figure 2.3

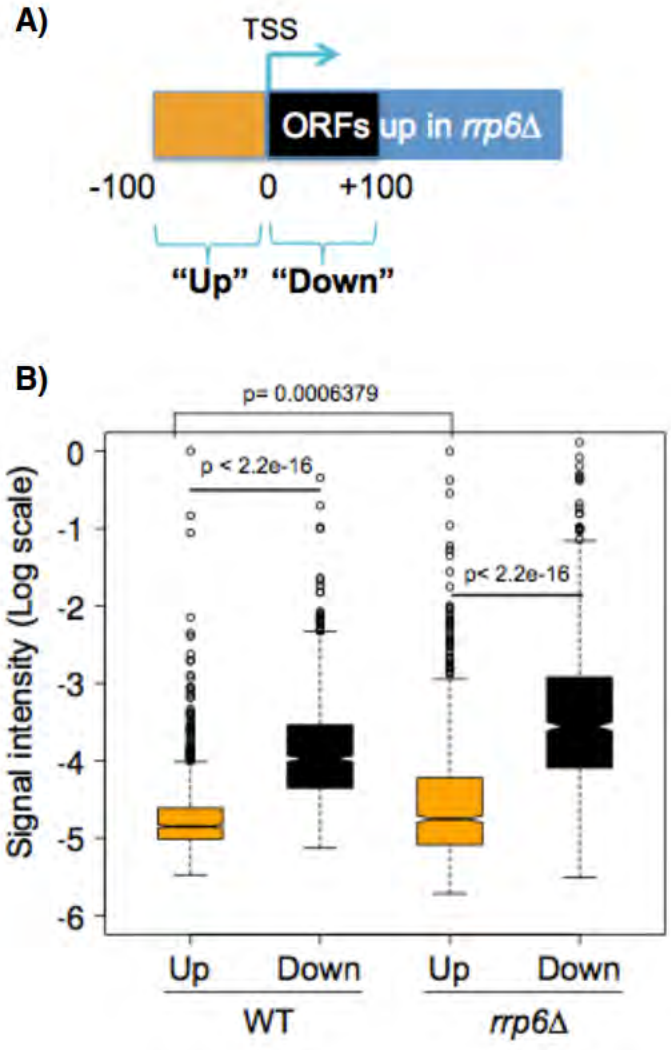
A)
TSS
ORFs up in rrp6Δ
-100
0
+100
"Up"
"Down"
B)
p= 0.0006379
p < 2.2e-16
p< 2.2e-16
Signal intensity (Log scale)
0
-1
-2
-3
-4
-5
-6
Up
Down
Up
Down
WT
rrp6Δ

Positive effect of *RTT109* on CUT and ORF transcription is uncovered in the absence of the nuclear exosome

By examining the double mutants, we found to our surprise that loss of H3-K56Ac partially suppressed many of the transcriptional changes observed in the *rrp6*Δ strain. Levels of the majority of CUTs were reduced in the *rtt109*Δ *rrp6*Δ double mutant compared to the *rrp6*Δ strain (Figure 2.4A, left and Figure 2.4B Groups C and D), with 394 CUT transcripts showing a decrease in expression of 1.5-fold or more (FDR <0.1) (Table S1 in Appendix 1). Consistent with the hypothesis that loss of *RTT109* specifically affects transcription of these ncRNAs (as opposed to RNA stability, etc.), ORF transcripts that are subject to transcriptional interference by ncRNAs were de-repressed in the *rtt109*Δ *rrp6*Δ double mutant (Figure 2.4C, Group B, Figure 3.3C).

In addition to its effects on ncRNA transcription, loss of Rtt109 also affected exosome-sensitive ORFs: those ORFs (n=985) that showed significantly increased expression in the *rrp6*Δ strain were reduced to near wild type levels in the *rtt109*Δ *rrp6*Δ double mutant (Figure 2.4A right and Figure 2.4C, Group A; defined in Materials and Methods). Only 13 of these 985 ORFs overlap with a group of growth-specific genes, indicating that these transcriptional changes are unlikely to be due to indirect effects of growth rate (Airoldi et al., 2009).

Figure 2.4: H3-K56Ac positively regulates transcription in the absence of the nuclear exosome

A) RNA abundance in the *rtt109Δ rrp6Δ* and *rrp6Δ* mutants normalized to WT. Density scatterplots show Log_2 median intensity values for *rtt109Δ rrp6Δ* plotted against the corresponding value for CUT (left) or ORF (right) transcripts from the *rrp6Δ* strain. The black line indicates x=y (no change).

B) Heatmap of normalized RNA abundance for CUTs (n= 728) in the *rtt109Δ rrp6Δ* and *swr1Δ rrp6Δ* compared to *rrp6Δ.* H3-K56Ac-dependent CUTs (Group C) as well as H2A.Z- and H3-K56Ac- dependent CUTs (Group D) are highlighted.

C) Heatmap of normalized RNA abundance for ORFs (n= 1836) in *rrp6Δ*, *swr1Δ rrp6Δ* and *rtt109Δ rrp6Δ* compared to WT. Group A and Group B ORFs are highlighted. Group B ORFs includes ORFs subject to transcriptional interference by adjacent CUTs. See Materials and Methods for Group definitions.

D) Density scatterplots of RNAP II occupancy by ChIP-seq at Group (C and D) CUTs (left) and Group A ORFs (right).

Figure 2.4

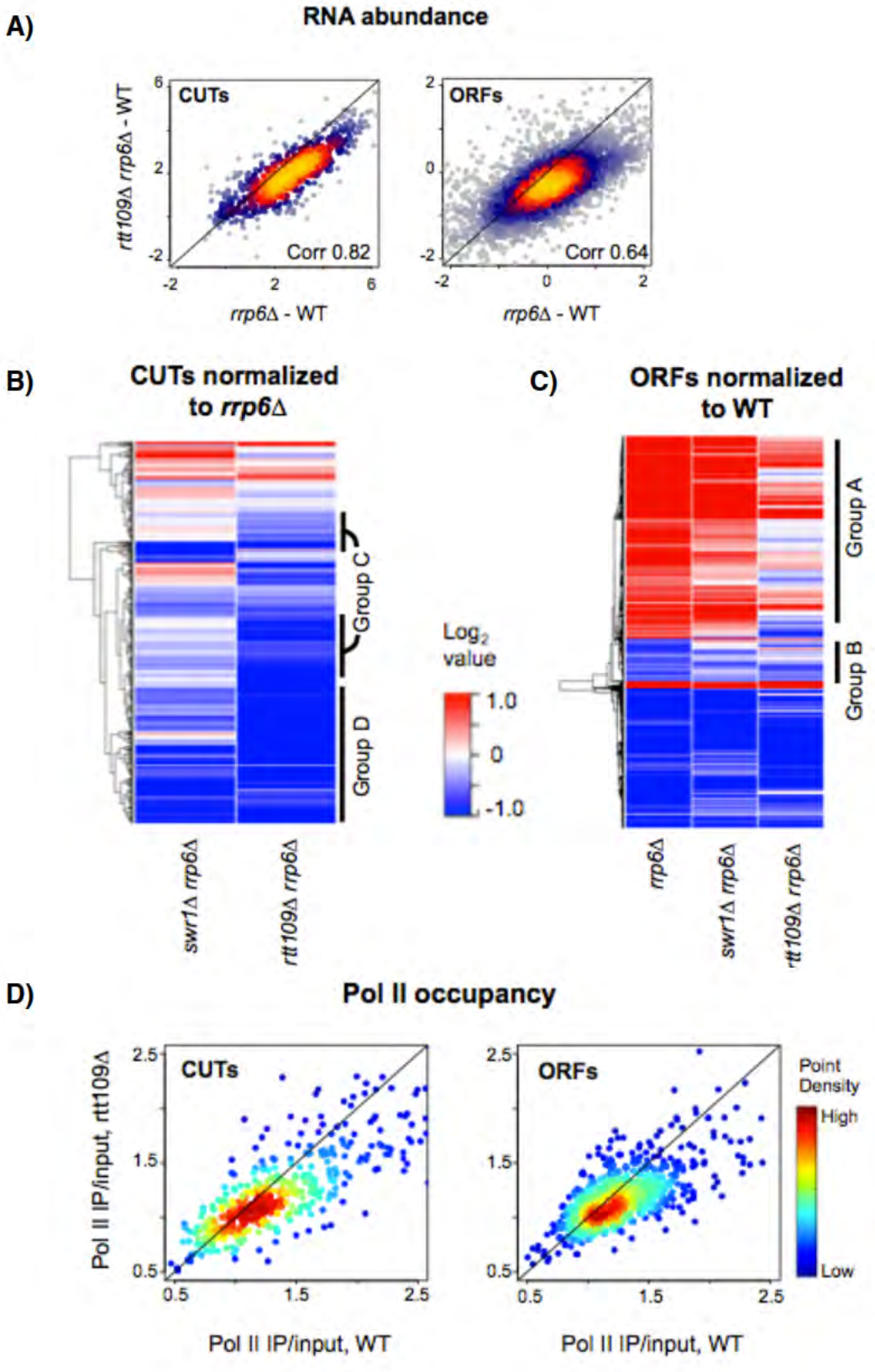
A)
RNA abundance
CUTs
Corr 0.82
rtt109Δ rrp6Δ - WT
rrp6Δ - WT
ORFs
Corr 0.64
rrp6Δ - WT
B)
CUTs normalized to rrp6Δ
Group C
Group D
swr1Δ rrp6Δ
rtt109Δ rrp6Δ
Log2 value
1.0
0
-1.0
C)
ORFs normalized to WT
Group A
Group B
rrp6Δ
swr1Δ rrp6Δ
rtt109Δ rrp6Δ
D)
Pol II occupancy
CUTs
ORFs
Pol II IP/input, rtt109Δ
Pol II IP/input, WT
Point Density
High
Low

Notably, the decreased RNA levels in the *rtt109*Δ *rrp6*Δ strain correlated well with the changes in RNAPII observed in the *rtt109*Δ single mutant, consistent with a direct role for H3-K56Ac in promoting Pol II occupancy at many CUTs and ORFs (Figure 2.4E). We do note, however, that the extensive changes in CUT RNA levels observed in the *rtt109*Δ *rrp6*Δ strain are not fully explained by decreases in RNAPII levels. This may reflect a limitation in the resolution of the ChIP-seq dataset, or indicate that Rtt109 contributes to CUT expression through additional mechanisms. The changes observed from the tiling array data were validated using qRT-PCR for a handful of loci (Figure 2.5).

Figure 2.5: qRT-PCR confirmation of yeast tiling array data

Reverse transcriptase qPCR was performed using primers listed in Table S2. Melt curve was performed to ensure primer specificity and relative abundance is plotted for CUTs and ORFs. Error bars represent standard deviations from a triplicate set of experiments and p-values are derived using a Two-sided Student's T test in comparison to the wild type.

Figure 2.5

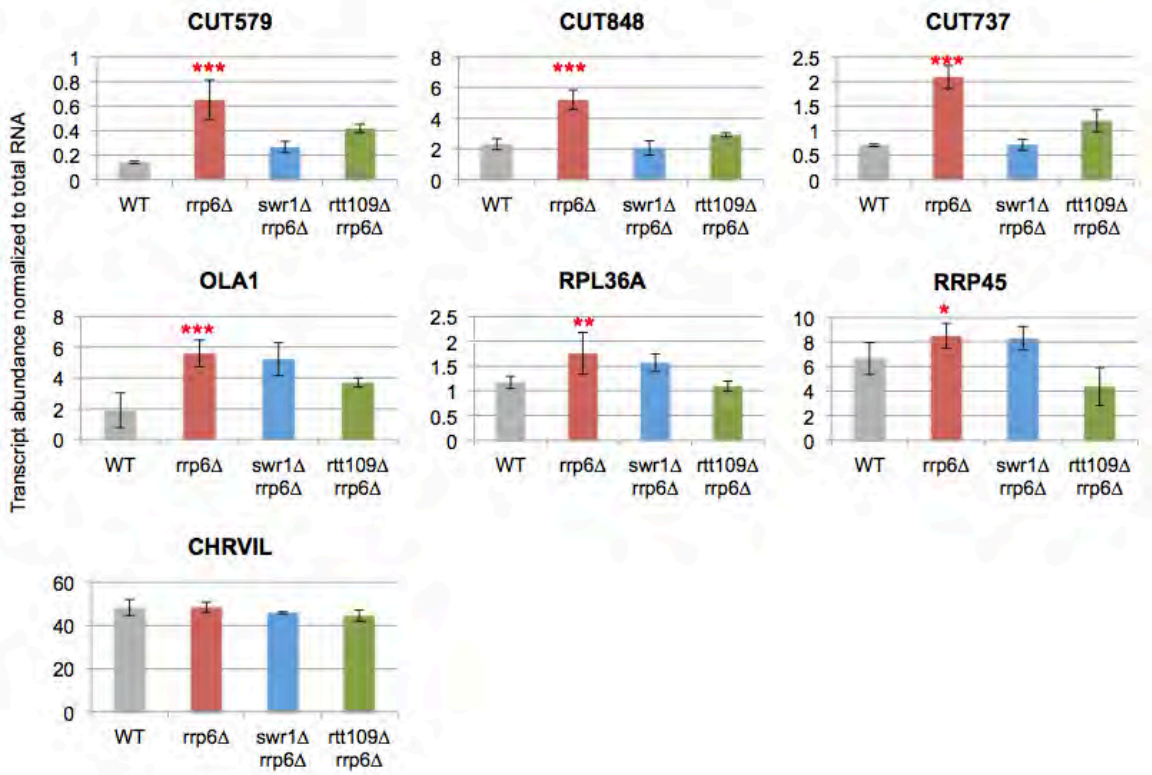
CUT579
CUT848
CUT737
OLA1
RPL36A
RRP45
CHRVIL
Transcript abundance normalized to total RNA
WT
rrp6Δ
swr1Δ rrp6Δ
rtt109Δ rrp6Δ
***
**
*

II-D. DISCUSSION

H3-K56Ac is a hallmark of dynamic nucleosomes positioned adjacent to promoters of protein-coding genes, but its impact on transcription has been enigmatic. Previous studies have shown that H3-K56Ac enhances the kinetics of transcriptional activation for some highly inducible yeast genes, but appears to play little role in the steady state expression (Williams et al., 2008; Xu et al., 2005b). Here we identify functional interactions between H3-K56Ac and the RNA exosome, revealing a general, activating role of H3-K56Ac on both ncRNA and mRNA transcription.

H3-K56Ac promotes while Rrp6 inhibits global ncRNAs levels

Many studies over the past few years have found that eukaryotic genomes are subject to pervasive transcription and produce an enormous number of ncRNA transcripts (van Dijk et al., 2011b; Neil et al., 2009; Schulz et al., 2013; Tan-Wong et al., 2012; Xu et al., 2009). The steady-state level of many such ncRNAs are held in check by machineries that target these transcripts for their rapid degradation. For instance, divergent ncRNAs that occur at many bi-directional RNAPII promoters harbor binding sites for the Nrd1/Nab3 RNA binding complex that promotes both their termination and degradation by the RNA exosome (Schulz et al., 2013). Several recent reports indicate that chromatin structure can also repress ncRNA expression (Alcid and Tsukiyama, 2014; DeGennaro et al.,

2013; Zofall et al., 2009). Buratowski and colleagues found that inactivation of the nucleosome assembly factor, CAF1, leads to increased expression of ncRNAs at many bidirectional yeast promoters (Marquardt et al., 2014). They suggested that assembly and/or stability of nucleosomes that occupy ncRNA promoters plays a key role in restricting their expression and reinforcing expression of the adjacent mRNA gene. Tsukiyama and colleagues have also reported that the yeast chromatin remodeling enzymes ISWI, RSC and INO80-C, inhibit expression of a large number of antisense ncRNAs in yeast (Alcid and Tsukiyama, 2014), and recently, we also found that INO80-C blocks ncRNA transcription within intragenic regions (Xue et al., 2015). How these enzymes prevent ncRNA expression is not yet clear, but a likely possibility is that they enforce nucleosome positions that inhibit ncRNA promoter usage.

In contrast to mechanisms that inhibit ncRNA production, our results indicate that H3- K56Ac globally stimulates expression of divergent, promoter-associated CUTs in yeast. This stimulatory role for H3-K56Ac is consistent with a previous study indicating that nucleosome turnover can promote cryptic transcription within gene transcription units (Venkatesh et al., 2012). In general, these data suggest that H3-K56Ac create a dynamic chromatin state that can facilitate expression of ncRNAs like CUTs.

H3-K56Ac promotes ORF expression while Rrp6 inhibits them

Surprisingly, our RNA analyses identified 985 ORF transcripts that increased in abundance after inactivation of the gene for nuclear exosome (*RRP6*). Rrp6 has been shown to target degradation of unspliced pre-mRNA and snRNA splicing intermediates (Schneider et al., 2012). Thus, our work suggests that Rrp6 is also involved in tempering levels of mRNAs that do not have introns. The 985 exosome targeted ORFs required H3-K56Ac for expression, as these same transcripts were reduced to wild type levels in the *rtt109*Δ *rrp6*Δ double mutant. These data suggest that H3-K56Ac and the nuclear exosome act antagonistically at these ORFs to regulate their mRNA abundance.

What is puzzling is that the steady state levels of these ORF transcripts are not decreased in the *rtt109*Δ single mutant. Why does H3-K56Ac only seem to promote expression of these mRNAs in the absence of the exosome? One possibility is that each of these ORFs expresses two populations of transcripts – one type of transcript may be aberrant and be targeted for degradation by the exosome, and a second set may be functional (Figure 2.6A). In this model, the decreased level of RNAPII, due to loss of H3-K56Ac, may favor production of functional transcripts and reduce formation of exosome-targeted transcripts (Figure 2.6A). For instance, fewer molecules of RNAPII may diminish the number of stalled, backtracking RNA polymerases that are known to be targeted for exosome action (Lemay et al., 2014). Consistent with this view, ORFs whose

transcripts increase in the absence of the exosome are enriched for both a high density of RNAPII and for high transcription rate (Figure 2.6B, C).

This type of functional interdependency between RNAPII levels and exosome degradation may also act in other cases where transcription and mRNA degradation appear to be linked (Haimovich et al., 2013; Sun et al., 2013).

Figure 2.6: Rrp6 regulates ORFs that are highly transcribed and have high Pol II density

A) Model for how the RNA exosome and nucleosome dynamics may regulate steady-state RNA levels. In WT cells, a part of the population of elongating RNAPII molecules (red) are targeted by the RNA exosome (yellow) while the remainder RNAP II (blue) produce fully functional transcripts. In the absence of H3-K56Ac (*rtt109Δ*), RNAPII density is reduced, and the remaining RNAPII produces functional (blue) transcripts. Note that the RNA exosome may be present in both cases, but its activity may only be apparent during high RNAPII density.

B) Density histogram distribution of transcriptional frequency data (from Holstege et. al, 1998) over the entire genome (Genomic) or over Group A ORFs, which are sensitive to exosome activity (red). Distributions were compared using the KS test.

C) Proportion of the entire genome (Genomic) or Group A ORFs that are members of one of four clusters defined by Venters and Pugh 2009. Statistical significance of the proportion was tested using a two-tailed Fischer's exact test. Cluster 4: no detectable Pol II; Cluster 1: Pol II primarily at promoter; Cluster 2: Pol II primarily at promoter and start of the ORF; Cluster 3: Pol II across the gene body, including 3' end.

Figure 2.6

A)

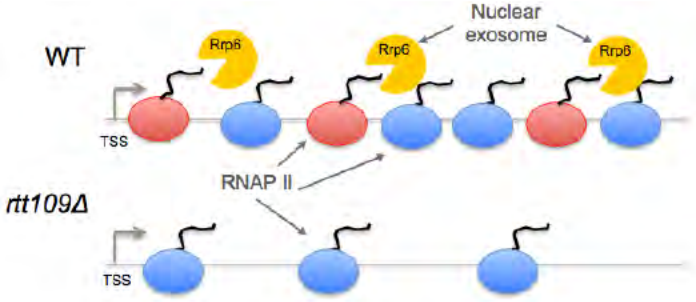

B)

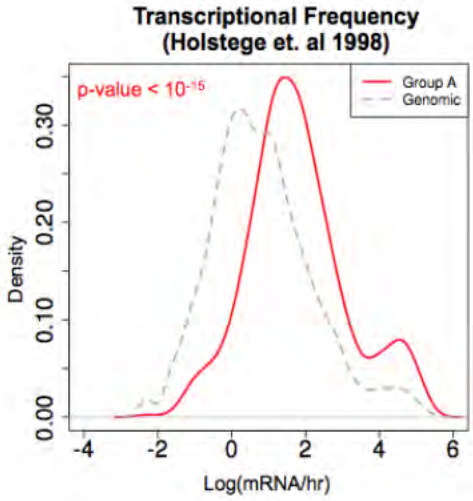

C)

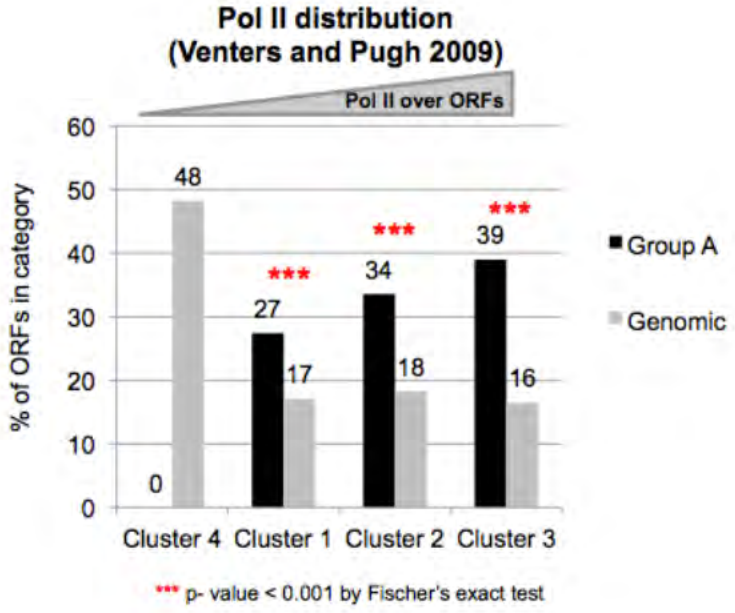

II-E. MATERIALS AND METHODS

Yeast Manipulations and Standard Molecular Biology

All yeast deletion strains were made using standard procedures (Longtine et al., 1998) by tetrad dissection of heterozygous diploids (Amberg et al., 2005) in the W303 strain background (See Appendix 3 for a list of strains).

Tiling array and RT-PCR sample preparation for RNA

Yeast were grown in Yeast Extract Peptone (YEP) media with 2% glucose at 30°C at an OD600 of 0.8 – 1.2 (log phase) and snap-frozen in liquid nitrogen until RNA was extracted. All samples in one batch were processed together for RNA extraction to minimize technical variations across mutants.

RNA extraction was done using the hot phenol method as follows. 200 µL of lysis buffer (50mM Tris pH7-7.4, 130 mM NaCl, 5mM EDTA, 5% SDS), 200 µL of Phenol (pH 4.0): Chloroform: Isoamylalcohol (PCI, 25:24:1) and 200 µl of glass beads (by volume) were added to the cell pellet on ice and vortexed in the cold room for 20min at maximum speed. Samples were spun for 15 min at 4°C at >13000 rpm to separate the organic and aqueous phases. The upper aqueous phase was transferred to a fresh precooled 1.7ml tube; an equal amount of PCI was added before shaking the tubes vigorously, followed by centrifugation at maximum speed. This step was repeated once more and then the aqueous layer

was mixed with an equal amount of Chloroform: Isoamyl alcohol (CI, 24:1) to remove any residual phenol. The tubes were shaken and spun as above. Phase Lock Heavy tubes (5 Prime) were prepared with a short pre-spin (30 sec, 3000 rpm) and the upper aqueous layer from the RNA samples added along with an equal quantity CI. The phases were mixed by inverting the tubes vigorously, taking care to avoid any vortexing, and spun at >13000 rpm for 2 min. The upper layer was transferred to fresh precooled 1.7ml tubes containing $1/20^{th}$ the volume of 3M sodium acetate (pH 4.2), 2 volumes of 100% ethanol and inverted. RNA was precipitated at -20°C for 30 mins, spun at 15 min at > 13000 rpm and supernatant discarded. The pellet was rinsed with 80% ethanol, spun for 2 min and the supernatant discarded. The pellets were allowed to air dry by inverting for ~ 30mins, resuspended in 50- 100 ul of DEPC water and quantified using a Nanodrop. Ideally, A260/280 for RNA ~2 and A260/ 230 ~2, and it is important to note that lower ratios might indicate organic contamination. Integrity of the RNA was confirmed on a 2% Agarose gel that showed a light smear with 2 bands for the high molecular weight ribosomal subunits and 3 bands for the low molecular weight RNAs. Total RNA was treated for at least one hour with TURBO DNase (TURBO DNA free kit, Ambion #1907) by incubation for 30 min in the 37°C water bath in 50 µL reactions with ≤ 25 µg of RNA in each tube. Care was taken to avoid sample agitation as DNase is extremely heat labile. 10X Inactivation reagent was added after the incubation and frequently tapped to ensure uniform

mixing. Samples were centrifuged for 2 mins at >13000 rpm and the supernatant was used for the RT-PCR or tiling array labeling reaction.

Labeling, hybridization and normalization: Total RNA was labeled and converted into cDNA by random primed retrotranscription of total RNAs as previously described (Castelnuovo et al., 2014) before being hybridized to Affymetrix tiling microarrays. At least 3 biological replicates for each genotype were analyzed from three independent array hybridizations. Each array was normalized using W303 genomic DNA as reference (Huber et al., 2006) and only transcripts scoring above a threshold background value were used for further processing, as previously published (David et al., 2006). Expression level for each transcript was estimated by the midpoint of the shorth (shortest interval that covers half the values) of the normalized probe intensities lying within the transcript boundaries as previously described (Xu et al., 2011)and differential gene expression analysis was performed using limma as described below. Microarray data can be viewed on the Steinmetz lab browser (*http://steinmetzlab.embl.de/peterssonLabArray/*).

Differential gene expression analysis for tiling array data and corresponding plots

Statistically significant transcripts between the mutants compared to either the *rrp6Δ* or WT were scored using the limma package (Smyth, 2004) in RStudio (R Core Team (2015). Appropriate model matrices were generated to apply the lmfit

model to the data, following which eBayes statistics was implemented. Varying combinations of thresholds for p_{adj} (<0.1, <0.05) and Log_2 Fold Change (LFC) (> ±0.59, > ±1.0) were tested to confirm the results were not specific to a given condition. All detectable transcripts in the tiling array data that have a p_{adj} = FDR < 0.1 and Log_2 Fold Change (LFC) > ±0.59 were defined as statistically significant for a given comparison. The number of transcripts that change in each comparison is summarized in Table S1 in Appendix 1.

Plot types: Volcano plots show the $-log_{10}$ p_{adj} value (Y-axis) obtained from limma analysis against the Log_2 Fold Change (X-axis) with transcripts with a p_{adj} =FDR < 0.1 and LFC > ±0.59 colored in blue and the rest in yellow and were made using ggplot.2 (Almada et al., 2013; Schulz et al., 2013). The scatterplots and heatmaps in Figure 2 were plotted as Log_2 ratios normalized either to wild type (WT) or the *rrp6Δ* as indicated. heatmap.2 function from the gplots package was used for hierarchical clustering and used without additional scaling of data (Warnes et al 2015). The details of the dissimilarity matrix calculation method (Euclidean) and linkage agglomeration method (complete or median) are specified in the legends of each heatmap.

Transcript annotation and categorization

Transcript annotations originally defined for CUTs, SUTs, ORFs (ORF-Ts) and other were obtained from (Xu et al., 2009) and combined with the SRT annotation

from (Tan-Wong et al., 2012) to get a comprehensive set of known annotations. The complete annotation used in this publication is available at GSE73145. This study focuses on five major groups of significantly changed (p_{adj} = FDR < 0.1 and Log2 Fold Change (LFC) > ±0.59) transcripts defined below:

Group A ORFs are i) significantly upregulated in the *rrp6Δ* compared to WT and ii) reduced by > ±0.59 LFC in *rtt109Δ rrp6Δ* compared to the *rrp6Δ*. Refer to Figure 2.4C.

Group B ORFs are i) significantly downregulated in the *rrp6Δ* compared to WT and ii) increased by > ±0.59 LFC in *rtt109Δ rrp6Δ* compared to the *rrp6Δ*. Refer to Figure 2.4C. This group includes ORFs subject to transcriptional interference by adjacent CUTs.

Group C CUTs are i) significantly upregulated in the *rrp6Δ* compared to WT and ii) reduced by > ±0.59 LFC in *rtt109Δ rrp6Δ* compared to the *rrp6Δ*. Refer to Figure 2.4B. These are also **H2A.Z independent.**

Group D CUTs are i) significantly upregulated in the *rrp6Δ* compared to WT and ii) reduced by > ±0.59 LFC in *rtt109Δ rrp6Δ* as well as *swr1Δ rrp6Δ* compared to the *rrp6Δ*. Refer to 2.4B. These are also **H2A.Z dependent.**

qRT-PCR validation of tiling arrays:

Total RNA was quantified by Nanodrop; equal amounts were taken for all the samples. Total RNA of 60ng per well was determined to amplify signal in the

linear range for most sample/ primer sets. Primers were designed to be specific using Primer3 qRT-PCR settings. The One-step RT-PCR reaction mix contained 2X Sybr Green PCR mix from Invitrogen (SyBr Green, ROX, dNTPs), Superscript RT III, primers).

Pol II ChIP-seq

Yeast were grown in Yeast Extract Peptone (YEP) media (100ml per IP) with 2% glucose at 30°C, crosslinked for 20 min with 1% formaldehyde (final concentration) at room temperature and rinsed with cold water between 2 cycles of centrifugation at 3000rpm. Pellets were resuspended in breaking buffer (20% glycerol, 100mM Tris-Cl pH 7.5 and 1x Protease Inhibitor Cocktail, EDTA free) with 600µl of silica/zirconia beads in a screw-cap microcentrifuge tube. The cells were lysed with a bead beater (Biospec) for 6 cycles of 1 min each with one minute intervals on ice and cell breakage was confirmed microscopically. After a brief spin at maximum speed, NPS buffer (0.5mM spermidine, 1mM β-mercaptoethanol, 0.075% NP-40, 50mM NaCl, 10mM Tris-Cl pH 7.4, 5mM $MgCl_2$ and 1mM $CaCl_2$) was added to the chromatin prior to MNase (Worthington, 200 units) digestion at 37°C for 20 minutes and the reaction stopped by addition of 24 mM EGTA while keeping the tubes on ice. The input fragment size distribution was confirmed to be in the range of 150-300bp by Bioanalyzer. The chromatin was immunoprecipitated with 6ul of 8WG16 Pol II antibody (Covance) or with no

antibody (input control) and the DNA was purified by phenol-chloroform extractions and ethanol precipitation. IP samples were confirmed by RT-PCR and sent to BGI, China for library preparation and single-end Illumina sequencing (Hi-seq 2000). Library preparation was done using a standard BGI protocol as follows: i) quality control by Qubit and Agilent 2100 ii) Addition of A base to 3' end and adapter ligation iii) PCR amplification and size selection for 100-300 bp and, finally iv) Library QC by Agilent 2100 and qPCR. The number of reads obtained/ uniquely mapped from each library is listed in the Table below.

Pol II ChIP-seq Library sequencing depths

Strain	Total reads	Uniquely filtered mapped reads
Wild type rep1	~7.8 Million	~7.5 Million
Wild type rep2	~11 Million	~10.0 Million
rtt109Δ rep 1	~9.8 Million	~9.3 Million
rtt109Δ rep 2	~8.7 Million	~8.2 Million
rrp6Δ rep1	~11 Million	~11.0 Million
rrp6Δ rep2	~11 Million	~10.0 Million
Input	~29 Million	~28.0 Million

ChIP-seq analysis pipeline

Fastq files were put through the FASTQC program before alignment to the sacCer3 genome using Bowtie2 to obtain SAM files (Andrews; Langmead et al., 2009; Li et al., 2009). Bowtie settings for mapping Pol II ChIP-seq reads (default preset in Galaxy) were -s 0 -u -1 -n 2 -e 70 -l 28 --nomaqround 10 -v -1 -k 1 -m -1 --maxbts 125 -o -1 --seed -1

SAMtools was used for SAM to BAM conversion with the FLAGs to discard PCR duplicates and multiple mapping reads. Each sample was normalized to total library read count (bamCoverage tool in the deepTools package) before displaying in the UCSC Genome browser. After determining strong correlation values, the replicates were summed for further analysis. The IP/input value for the corresponding transcript coordinates was calculated as described in Teytelman et al 2014 using BEDtools (Quinlan and Hall, 2010) and are available as processed data in GSE72692. Similar results were obtained if TSS- proximal regions were included in the analyses (-200 and +200 bp relative to the Transcription Start Site (TSS) and Transcription Termination Site (TTS) respectively). Additionally, the data were also analyzed by MACS2 and the peaks determined as significantly different across WT and *rtt109Δ* (*bdgDiff* module) highlighted in the genome browser views (Zhang et al., 2008).

Transcriptional Frequency of Group A ORFs

Data was downloaded from Holstege et. al, 1998 and used to plot the distribution of transcriptional frequency of Group A ORFs or the whole genome. Statistical significance of the two distributions was tested using Kolmogorov–Smirnov test (KS test) in R.

Pol II density/occupancy of Group A ORFs

Data was downloaded from (Venters and Pugh, 2009) and used to find the proportional membership of Group A ORFs or the whole genome in the clusters defined in Figure 4 of Venters and Pugh, 2009. Statistical significance of the proportion was tested using a two-tailed Fischer's exact test. The characteristics of each cluster are summarized as follows:

Cluster 4: no detectable Pol II

Cluster 1: Pol II primarily at promoter

Cluster 2: Pol II primarily at promoter and start of the ORF

Cluster 3: Pol II across the gene body, including 3' end.

For more details see Figure 4A from Venters and Pugh, 2009.

Chapter III: *SWR1* regulates ncRNAs in concert with *RRP6*

III.A. SUMMARY

Across eukaryotes, histones help fold the DNA into nucleus of a cell. Canonical histones H2A, H2B, H3 and H4 are present throughout the genome. In contrast, the histone variant H2A.Z is a hallmark of nucleosomes flanking promoters of protein-coding genes. This histone mark promotes replication-independent nucleosome turnover and has been generally associated with transcriptional activation. However, the exact mechanistic contribution of H2A.Z during steady-state transcription is unclear.

Here we find that H2A.Z alone does not have a significant impact on steady state mRNA levels in yeast. Instead, effects of H2A.Z on RNA levels are only revealed in the absence of the nuclear RNA exosome. Additionally, we show that H2A.Z facilitates formation of chromosome interaction domains (CIDs). Our study suggests that H2A.Z works in concert with the RNA exosome to control mRNA and ncRNA expression, perhaps in part by regulating higher order chromatin structures.

III.B. INTRODUCTION

Eukaryotic genomes are packaged into the nucleus using chromatin. The basic unit of chromatin is a nucleosome, which consists of 147 base pairs of DNA wrapped 1.47 times around an octamer of histone proteins: H2A, H2B, H3 and H4. While they assist in DNA folding, histones also make the sequence inaccessible. Thus, chromatin is dynamic so that cellular processes such as transcription and replication have controlled access to the DNA. Histone variants are one such strategy used by the cell to regulate access to DNA (Weber and Henikoff, 2014). Variants differ from canonical histones in the amino acid sequence and often have properties that are unique and distinguishable from the core histones.

H2A.Z is a highly conserved variant of the histone H2A and is specifically enriched in nucleosomes that flank promoter regions. Like the histone itself, this pattern of enrichment is also conserved in yeast, *Drosophila*, *Arabidopsis*, mice and humans. The chromatin remodeling enzyme SWR-C, present at TSS regions, incorporates H2A.Z into chromatin. H2A.Z promotes rapid histone turnover at promoter proximal nucleosomes (Kaplan et al., 2008). The dynamic nature of H2A.Z nucleosomes has contributed to the prevailing view that this chromatin feature may generally promote transcription. However, previous studies have implicated H2A.Z in transcriptional induction of specific loci and thus

its contribution to steady-state transcription remains unclear (Lenstra et al., 2011).

In addition to dynamic nucleosomes that characterize eukaryotic promoters, these regions are also bi-directional in nature, with divergent noncoding RNAs (ncRNAs) and mRNAs expressed from different promoters that share a common nucleosome free region (NFR) (Neil et al., 2009; Xu et al., 2009). In yeast, promoter-associated, divergent ncRNAs are called CUTs. CUTs are 5' capped, polyadenylated short RNAs that are efficiently recognized by the NNS machinery that and, in turn, targets these RNAs for degradation by the RNA exosome and TRAMP (Arigo et al., 2006; Schulz et al., 2013; Thiebaut et al., 2006). Consequently, inactivation of the nuclear exosome 3'-5' exonuclease, Rrp6, is necessary to monitor changes in CUT transcription. In addition to CUT degradation, Rrp6 also has roles in degrading unspliced pre-mRNAs (Schneider et al., 2012), facilitates maturation of sn/snoRNAs (Gudipati et al., 2012), and may broadly contribute to regulating nuclear mRNA levels (Schmid et al., 2012). Whether H2A.Z regulates expression of ncRNAs has not been thoroughly addressed.

CUTs represent but one of several classes of ncRNAs found in yeast. Another class of ncRNAs of particular interest comprises Ssu72 Restricted Transcripts (SRTs), which accumulate in the absence of the transcription termination factor Ssu72, and which also seem to be targeted by the exosome

(Tan-Wong et al., 2012). Of the 605 SRTs, 135 are promoter associated, while many are found at 3' ends of convergent gene pairs and may reflect aberrant termination events (Tan-Wong et al., 2012). Ssu72 is a subunit of the RNA 3'-end processing machinery that is associated with the RNAPII C-terminal domain (CTD) (Dichtl et al., 2002), and it functions as a CTD Ser5 phosphatase during termination (Krishnamurthy et al., 2004). Ssu72 also functionally interacts with other components of the transcription pre-initiation machinery (e.g. TFIIB) (Pappas and Hampsey, 2000), and may facilitate interactions between the 5' and 3' ends of genes, promoting gene "loops" (Tan-Wong et al., 2012). Intriguingly, the strongest genetic interactions of Ssu72 are with multiple subunits of SWR-C, an ATP-dependent chromatin remodeling complex which deposits H2A.Z at 5' and 3' ends of genes, implying that they may function together to regulate SRT expression and/or 3D genome interactions (Collins et al., 2007; Fiedler et al., 2009).

Here we present evidence that H2A.Z is a positive regulator of ncRNA expression in yeast and this function is masked by a functional nuclear exosome. Surprisingly, our study also uncovers a repressive role for H2A.Z where it may work together with the nuclear exosome to repress expression of a subset of ncRNAs. Finally, we find that H2A.Z contributes to the formation of higher order chromosome interaction domains (CIDs) that we propose may play a role in the regulation of ncRNA expression.

III.C. RESULTS

H2A.Z has little apparent impact on steady state RNA abundance

In order to monitor the effect of H2A.Z on both coding and noncoding RNA expression, total RNA was isolated from isogenic wild-type and mutant yeast strains, and samples were prepared for hybridization to strand-specific, DNA tiling arrays that provide high-density coverage of the yeast transcriptome (Castelnuovo et al., 2014; David et al., 2006; Huber et al., 2006).

Initial analyses included strains that harbor gene deletions inactivating the SWR-C chromatin remodeling enzyme that deposits H2A.Z (*swr1*Δ). Consistent with previous studies, loss of H2A.Z deposition (*swr1*Δ) had little effect on steady state transcript abundance compared to wild type (WT) (Mizuguchi et al., 2004), as no transcripts were reduced 1.5-fold or more from the 7,987 total transcripts monitored at a stringent criterion of FDR <0.1. Indeed, even at a reduced stringency (FDR <0.8) only a few transcripts were reduced 2-fold or more (Figure 3.1A, B and Table S1 in Appendix 1).

Figure 3.1: H2A.Z does not affect RNA levels alone, but positively regulates transcription in the absence of the nuclear exosome

A) RNA abundance measured by strand-specific tiling microarrays in *swr1Δ* strains. Density scatterplot shows the median signal intensity values in comparison to wild type arrays (WT). The black diagonal line indicates x=y (no change), and the horizontal and vertical lines indicate the noise threshold cut-off.

B) Volcano plot shows the transcripts that change significantly in the *swr1Δ* compared to the wild type (WT) highlighted in blue (p_{adj} = FDR < 0.1 and Log_2 Fold Change > 0.59). The Y-axis shows the p-value (no FDR correction).

C, D) RNA abundance measured by strand-specific tiling microarrays in the *swr1Δ rrp6Δ*, and *rrp6Δ* mutants normalized to WT. Density scatterplots show Log_2 median intensity values for *swr1Δ rrp6Δ* plotted against the corresponding value for **C)** CUT or **D)** ORF transcripts from the *rrp6Δ* strain. The black line indicates x=y (no change).

E) H2A.Z levels at Group A ORFs, Group C and D CUTs, Up_and unchanged ncRNAs. Two-sided KS test was used to compare medians of Group C and Group D CUTs. See Experimental procedures for definitions of each group.

F) Volcano plots as in B) for *swr1Δ rrp6Δ vs. rrp6Δ.* The Y-axis shows the p-value (after FDR correction).

For heatmaps of H2A.Z dependent transcripts, refer to Fig 2.4 (page 58).

Figure 3.1

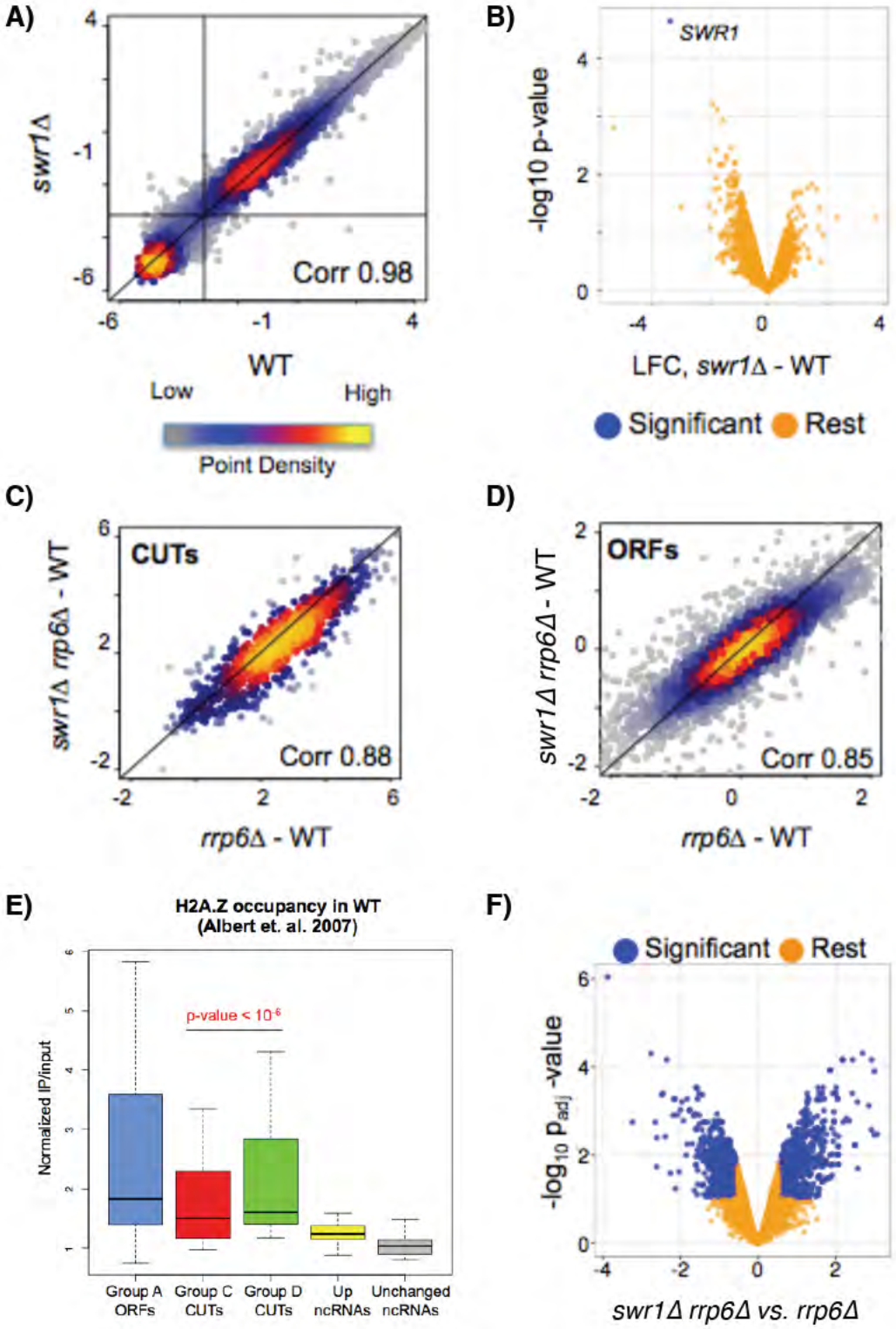
A)
swr1Δ
WT
Corr 0.98
Low
High
Point Density
B)
SWR1
-log10 p-value
LFC, swr1Δ - WT
Significant
Rest
C)
CUTs
swr1Δ rrp6Δ - WT
rrp6Δ - WT
Corr 0.88
D)
ORFs
swr1Δ rrp6Δ - WT
rrp6Δ - WT
Corr 0.85
E)
H2A.Z occupancy in WT
(Albert et. al. 2007)
Normalized IP/input
p-value < 10-6
Group A ORFs
Group C CUTs
Group D CUTs
Up ncRNAs
Unchanged ncRNAs
F)
Significant
Rest
-log10 padj -value
swr1Δ rrp6Δ vs. rrp6Δ

Positive effect of *SWR1* on CUT and ORF transcription is uncovered in the absence of the nuclear exosome

To assay effects of H2A.Z on transcription in the absence of confounding effects of exosome-mediated RNA degradation, total RNA was isolated from isogenic WT, *rrp6Δ* and *swr1Δ rrp6Δ* strains, and samples were hybridized to strand-specific DNA tiling arrays. Inactivation of the exosome revealed previously hidden roles for H2A.Z in gene regulation, as the level of a subset of CUTs (n= 202) was decreased by 1.5-fold or more (FDR <0.1) in the *swr1*Δ *rrp6*Δ strain compared to the *rrp6*Δ single mutant (Figure 3.1C, left and Figure 2.4B, Group D). This difference may be explained by the observation that CUTs that require H2A.Z for full expression are characterized by higher levels of this histone mark compared to the group of CUTs that are insensitive to H2A.Z loss (Figure 3.1E, p-value < 10^{-6}).

Additionally, loss of Swr1 activity also affected the expression of ORF transcripts that were up-regulated in *rrp6*Δ strains, although the effects of *swr1*Δ were less dramatic than those due to H3-K56Ac (Figure 3.1D, F, and Group A in Figure 2.4).

H2A.Z cooperates with the exosome to repress a subset of ncRNAs

Previous genome-wide studies uncovered strong genetic interactions among *SSU72*, *RTT109*, *HTZ1* (encoding H2A.Z), and genes encoding subunits of the

SWR-C remodeling enzyme (Collins et al., 2007; Fiedler et al., 2009). Indeed, we found that the *swr1*Δ *ssu72-2ts* double mutant exhibited a synthetic slow growth phenotype, consistent with H2A.Z deposition functioning in the same genetic pathway as *SSU72* (Figure 3.2A). Since Ssu72 represses a specific class of ncRNAs – the SRTs – we asked whether H2A.Z or H3-K56Ac might also repress these ncRNAs. Consistent with the genetic interactions, the *swr1*Δ *rrp6*Δ double mutant showed a significant up-regulation of a subset of SRTs (n= 45) by 1.5 fold or more (FDR <0.1), whereas the *rtt109Δ rrp6Δ* double mutant had less of an effect (Figure 3.2C and Figure 3.3A).

To further investigate potential repression of ncRNAs by H2A.Z, we performed automated segmentation analysis followed by manual curation (Tan-Wong et al., 2012) to identify novel transcripts that were repressed by H2A.Z and the exosome. This analysis identified 100 transcripts that were not expressed in the wild type or *swr1*Δ strain, but were significantly increased by 1.5 fold or more in the *swr1*Δ *rrp6*Δ mutant compared to the *rrp6*Δ strain (FDR <0.1) (Figure 3.2D, E). Notably, most of these transcripts were not de-repressed in the *rtt109*Δ *rrp6*Δ double mutant, although a subset was expressed at low levels in the *rrp6*Δ single mutant (Figure 3.3B). The majority of these ncRNAs (59) were located within intergenic regions, whereas the remaining 41 transcripts appear to be novel 5’ or 3’ extensions of existing transcripts (Fox et al., 2015). A subset of these unannotated ncRNAs was also derepressed in the *ssu72-2 rrp6*Δ strain,

suggesting that they may be related to SRTs (Figure 3.2 C). Thus, H2A.Z deposition promotes the expression of many CUTs and also functions to repress a distinct group of ncRNAs, including a subset of SRTs.

Figure 3.2: H2A.Z interacts with SSU72 and inhibits two classes of transcripts associated with NFR-regions

A) Ten fold dilutions of each strain grown in YEPD media at 30°C, spotted onto YEPD plates and incubated at 30°C. The *ssu72-2* allele is a temperature-sensitive lethal, but grows at the semi-permissive temperature of 30°C.

B) Volcano plots of *swr1Δ rrp6Δ* compared with *rrp6Δ* to visualize upregulated SRTs (red triangles, LFC > 0).

C) Heatmap of normalized RNA abundance for SRTs in the *swr1Δ rrp6Δ, rtt109Δ rrp6Δ*, and *ssu72-2 rrp6Δ* strains compared to their respective *rrp6Δ* after hierarchical clustering. Only SRTs that significantly upregulated in *swr1Δ rrp6Δ* compared to *rrp6Δ* (n=45) were used for the analysis.

D) RNA levels as in C) for *SWR1* repressed transcripts observed in this study. Transcripts that significantly upregulated in *swr1Δ rrp6Δ* compared to *rrp6Δ* (n=100) were used for the analysis.

E) Tiling array heatmap where the rows represent each replicate illustrate an example of genomic transcription of a previously unannotated transcript observed in *swr1Δ rrp6Δ* adjacent to a gene promoter. The green boxes shown above the gene browser view represent nucleosome positions, with dark green marking well-positioned nucleosomes. For the complete genome see: Steinmetz lab server.

Figure 3.2

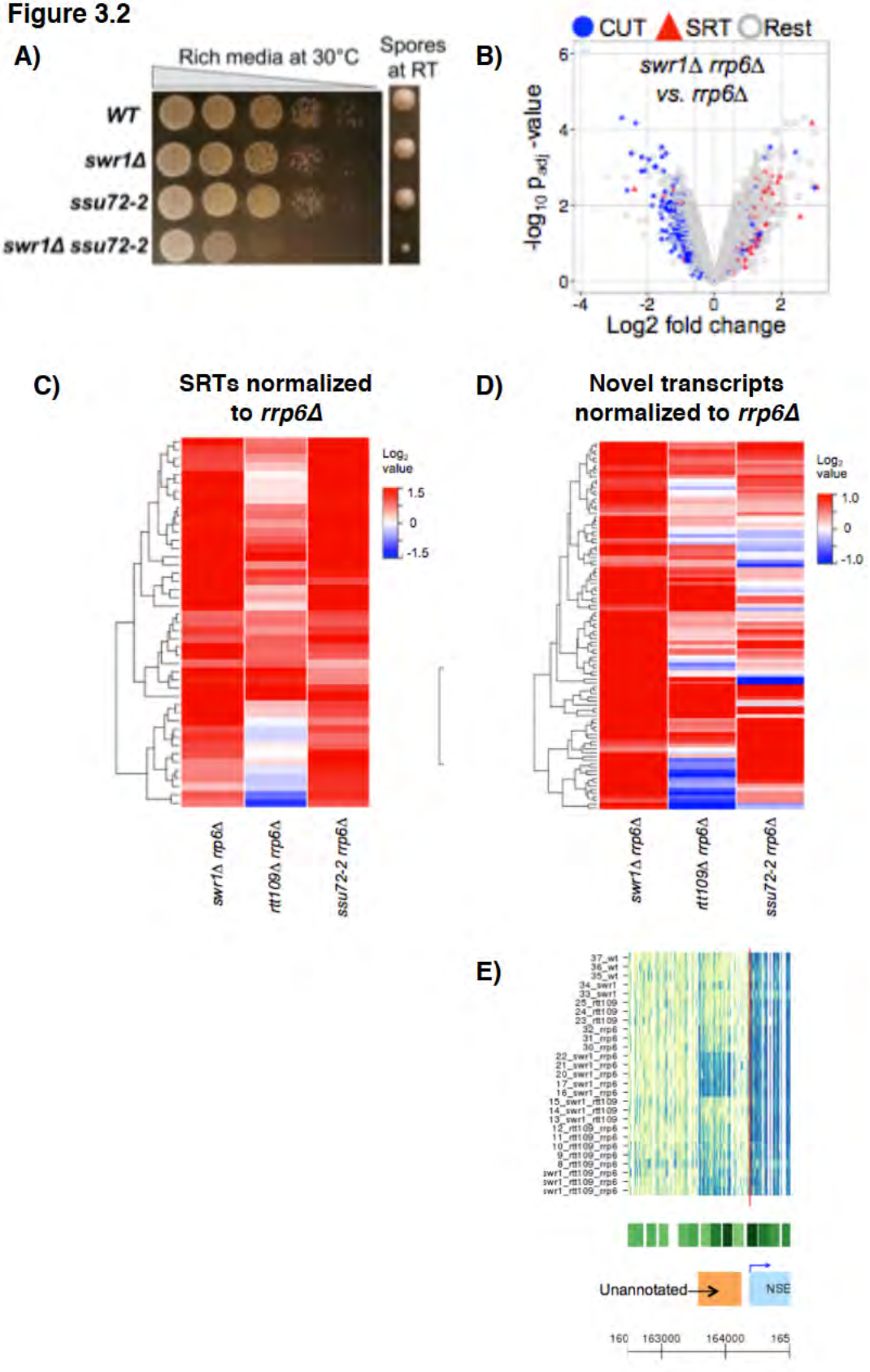
A)
Rich media at 30°C
Spores at RT
WT
swr1Δ
ssu72-2
swr1Δ ssu72-2
B)
CUT
SRT
Rest
swr1Δ rrp6Δ vs. rrp6Δ
-log10 padj -value
Log2 fold change
C)
SRTs normalized to rrp6Δ
Log2 value
1.5
0
-1.5
swr1Δ rrp6Δ
rtt109Δ rrp6Δ
ssu72-2 rrp6Δ
D)
Novel transcripts normalized to rrp6Δ
Log2 value
1.0
0
-1.0
swr1Δ rrp6Δ
rtt109Δ rrp6Δ
ssu72-2 rrp6Δ
E)
Unannotated
NSE
160
163000
164000
165

Figure 3.3: Tiling array screenshots of different types of transcripts observed

A) SRTs enriched in the *swr1Δ rrp6Δ;*

B) SWR-C repressed transcripts found in this study and

C) Transcriptional interference examples from Group B ORFs (see Figure 2.5, Chapter II).

Figure 3.3

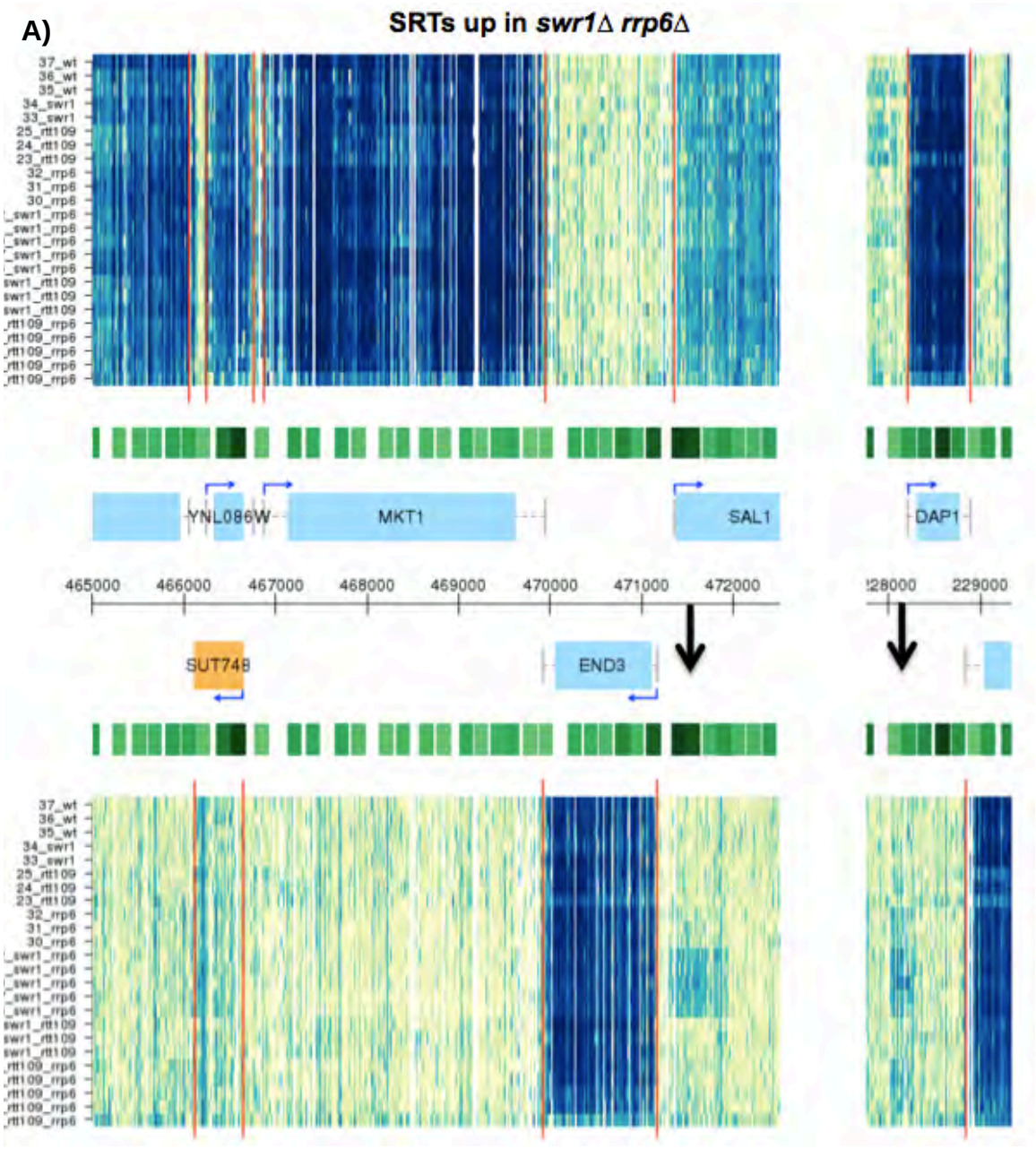

continued on next page..

Figure 3.3

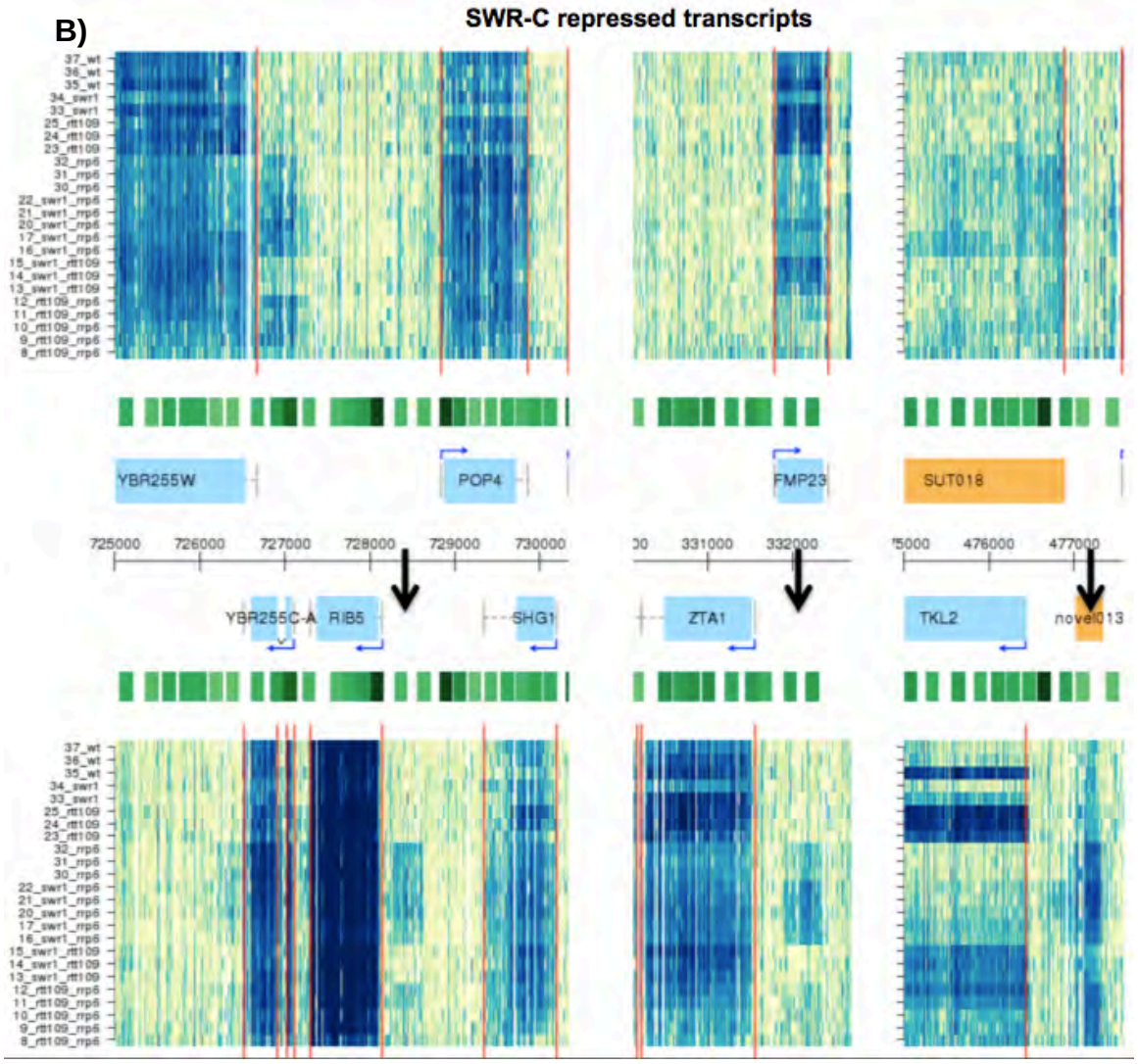

continued on next page..

Figure 3.3

C)

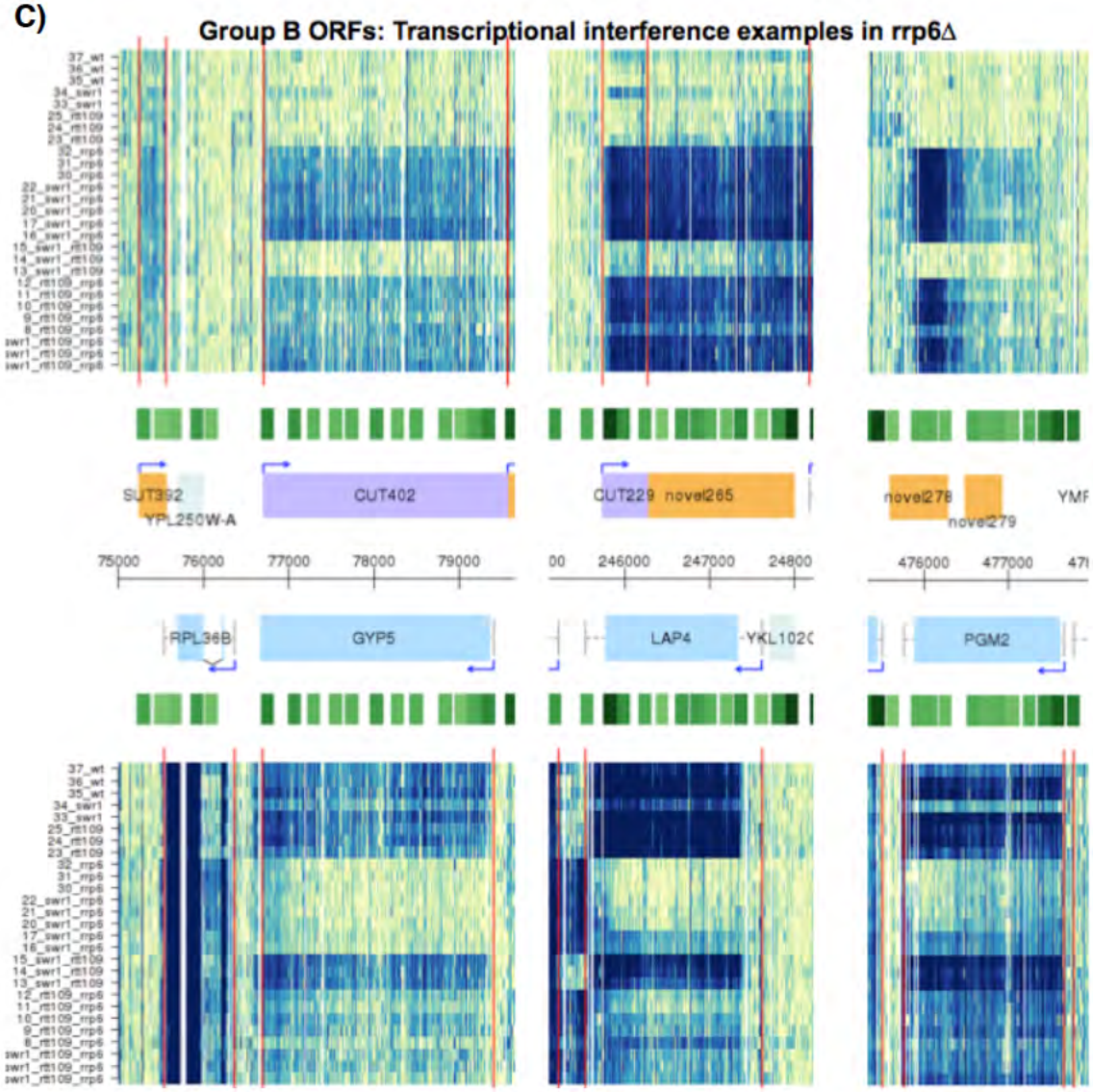
Group B ORFs: Transcriptional interference examples in rrp6Δ
37_wt
36_wt
35_wt
34_swr1
33_swr1
25_rtt109
24_rtt109
23_rtt109
32_rrp6
31_rrp6
30_rrp6
22_swr1_rrp6
21_swr1_rrp6
20_swr1_rrp6
17_swr1_rrp6
16_swr1_rrp6
15_swr1_rtt109
14_swr1_rtt109
13_swr1_rtt109
12_rtt109_rrp6
11_rtt109_rrp6
10_rtt109_rrp6
9_rtt109_rrp6
8_rtt109_rrp6
swr1_rtt109_rrp6
SUT352
YPL250W-A
CUT402
CUT229
novel265
novel278
novel279
YMF
75000
76000
77000
78000
79000
246000
247000
24800
476000
477000
RPL36B
GYP5
LAP4
YKL102C
PGM2

H2A.Z facilitates formation of Chromosome Interaction Domains (CIDs)

Previous chromosome conformation capture (3C) studies suggested that Ssu72 functions as a “gene looping” factor and that this higher order chromosome structure may be key for repressing SRT transcription (Tan-Wong et al., 2012). Given the genetic and functional interactions between *SSU72* and *SWR1*, we tested whether H2A.Z might also regulate chromosome interactions that could underlie the repression of ncRNAs. First, we used 3C to monitor chromosome interaction frequencies at the *BLM10* locus, a known target of Ssu72-dependent gene compaction (Dekker et al., 2002; Singh et al., 2009). The 5’ and 3’ ends of *BLM10* exhibited far stronger interactions with one another than with intervening regions of this gene, consistent with localized gene compaction (Figure 3.4A). These enhanced interactions were lost in *swr1*Δ, indicating that compaction of this gene requires H2A.Z deposition (Figure 3.4A).

To ask whether H2A.Z affects genome organization at a global level, we used a modified Hi-C method developed by the Rando group, called Micro-C, to generate a high-resolution chromosome folding map for budding yeast. Micro-C has lead to the identification of abundant chromosome interaction domains (CIDs) (Hsieh et al., 2015) which appear similar to mammalian Topological Associated Domains (TADs) (Dixon et al., 2012), although yeast CIDs are smaller (~5 kb) and contain an average of ~1-5 genes with strongly self-associating nucleosomes. Both transcriptionally active and repressed genes are

found within CIDs, although highly-transcribed genes are generally less compact than other genes in the genome. In a recent study, Rando and colleagues reported that loss of *SSU72 and RTT109* results in diminished gene compaction (Hsieh et al., 2015).

To test whether H2A.Z also contributes to this chromosome architecture, Micro-C analyses were performed in the *swr1*Δ strain. Interestingly, loss of H2A.Z deposition partially disrupted chromosome folding, consistent with a role for H2A.Z in CID formation (Figure 3.4B-D). In particular, the loss of H2A.Z weakened the compaction of CIDs (Figure 3.4C,D), though the strength of boundary regions between CIDs remained largely intact (Figure 3.4B). Furthermore, loss of H2A.Z decreased compaction of the CID containing the *BLM10* gene, consistent with the 3C results (Figure 3.4E). Even CIDs that lacked ncRNAs showed decreased compaction, consistent with a genome-wide defect in CID architecture that was independent of the transcriptional changes due to loss of H2A.Z (Figure 3.4F). Notably, the impact of H2A.Z on global gene compaction is less than either H3-K56Ac or Ssu72, consistent with the correspondingly weaker transcriptional defects due to loss of H2A.Z.

Figure 3.4: SWR-C promotes formation of Chromosome Interaction Domains (CIDs)

A) Chromosome conformation capture (3C) analysis of the *BLM10* locus (top: schematic) in wild type (WT) and *swr1Δ* shows the frequency of interaction of each restriction fragment with the F1 fragment. Data is normalized to a control region on chromosome VI as the baseline contact probability. See also Figure S6B.

B) Contact frequency matrix from Micro-C analyses for wild type (left) and *swr1Δ (right*) for a region on chromosome VI with the gene annotations listed at the top.

C) Micro-C analyses show the Log_2 interaction count of one nucleosome with its successive neighboring nucleosomes in wild type, *swr1Δ*, or *rtt109Δ* strains.

D) Density scatterplot for the compaction scores of chromosome interaction domains (CIDs) in the *swr1Δ* (Y-axis) compared to WT (x-axis) (KS test of the distributions yielded a p-value = 2.109e-15)**.** The black line indicates x=y (no change).

Micro-C data for **E)** the BLM10 locus and **F)** select genomic region devoid of ncRNA transcripts. The contact frequency of the individual nucleosomes in WT and *swr1Δ* is shown as a heatmap.

Figure 3.4

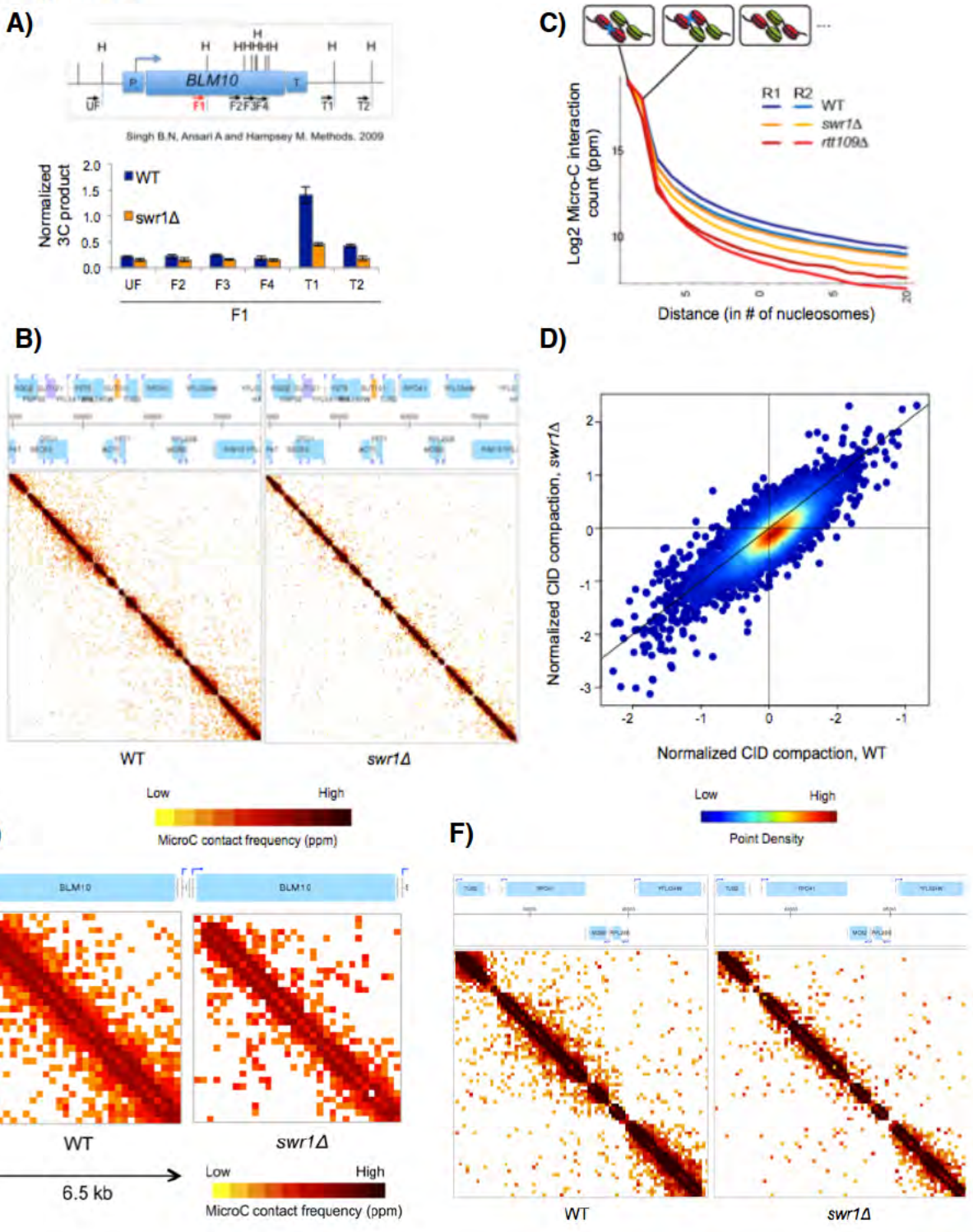
A)
H
BLM10
P
T
UF
F1
F2F3F4
T1
T2
Singh B.N, Ansari A and Hampsey M. Methods. 2009
Normalized 3C product
WT
swr1Δ
UF
F2
F3
F4
T1
T2
F1
B)
WT
swr1Δ
C)
Log2 Micro-C interaction count (ppm)
R1 R2
WT
swr1Δ
rtt109Δ
Distance (in # of nucleosomes)
D)
Normalized CID compaction, swr1Δ
Normalized CID compaction, WT
Low
High
Point Density
E)
Low
High
MicroC contact frequency (ppm)
BLM10
WT
swr1Δ
6.5 kb
Low
High
MicroC contact frequency (ppm)
F)
WT
swr1Δ

III.D. DISCUSSION

H2A.Z is a hallmark of dynamic nucleosomes positioned adjacent to promoters of protein-coding genes, but its impact on transcription has been enigmatic. Previous studies have shown that H2A.Z enhances the kinetics of transcriptional activation for highly inducible yeast genes, but appears to play little role in the steady state expression of most genes (Zhang et al., 2005). Likewise, in mouse ESCs, H2A.Z is enriched at active and repressed gene promoters but depletion of this histone variant does not affect steady state levels of active genes (Hu et al., 2013; Subramanian et al., 2013). Here we identify functional interactions between H2A.Z and the RNA exosome, revealing a role for H2A.Z in the positive and negative regulation of ncRNAs. Intriguingly, we find that H2A.Z facilitates the formation of higher order chromatin structures, called CIDs, suggesting that such structures may contribute to transcriptional control.

Chromatin dynamics regulate ncRNAs

Many studies over the past few years have found that eukaryotic genomes are subject to pervasive transcription and produce an enormous number of ncRNA transcripts (van Dijk et al., 2011a; Neil et al., 2009; Schulz et al., 2013; Tan-Wong et al., 2012; Xu et al., 2009). The steady-state level of many such ncRNAs are held in check by machineries that target these transcripts for rapid

degradation. For instance, divergent ncRNAs that occur at many bi-directional RNAPII promoters harbor binding sites for the Nrd1/Nab3 RNA binding complex that promotes both, their termination and degradation by the RNA exosome (Schulz et al., 2013). Several recent reports indicate that chromatin structure can also repress ncRNA expression (Alcid and Tsukiyama, 2014; DeGennaro et al., 2013; Zofall et al., 2009). Buratowski and colleagues found that inactivation of the nucleosome assembly factor, CAF1, leads to increased expression of ncRNAs at many bidirectional yeast promoters (Marquardt et al., 2014). They suggested that assembly and/or stability of nucleosomes that occupy ncRNA promoters plays a key role in restricting their expression and reinforcing expression of the adjacent mRNA gene. Likewise, a recent study found that the esBAF chromatin remodeling enzyme represses expression of a large set of ncRNAs in mouse ESCs by positioning nucleosomes at ncRNA promoters (Hainer et al., 2015). Tsukiyama and colleagues have also reported that two yeast chromatin remodeling enzymes, RSC and INO80-C, inhibit expression of a large number of antisense ncRNAs in yeast (Alcid and Tsukiyama, 2014), and recently, we also found that INO80-C blocks ncRNA transcription within intragenic regions (Xue et al., 2015). How these enzymes prevent ncRNA expression is not yet clear, but a likely possibility is that they also enforce nucleosome positions that inhibit ncRNA promoter usage.

In contrast to mechanisms that inhibit ncRNA production, our results

indicate that H2A.Z stimulates expression of divergent, promoter-associated CUTs in yeast. This stimulatory role for H2A.Z is consistent with a previous work where H2A.Z could promote cryptic transcription within gene transcription units (Jeronimo et al., 2015). We also found that H2A.Z functions to promote expression of a set of protein-coding genes. In general, these data suggest that H2A.Z creates a dynamic chromatin state that can facilitate expression of not only protein-coding genes, but also the adjacent ncRNA. Our study is consistent with a recent report that also identified a positive role for H2A.Z in CUT expression (Gu et al., 2015).

Genetic interactions between *SSU72* and *SWR1* led us to investigate roles for H2A.Z in repression of ncRNAs. Initially, we found that H2A.Z appears to function with the exosome and Ssu72 to repress expression of a subset of the SRT class of ncRNAs. In addition to the SRTs, we identified a group of 100 previously unannotated transcripts that were de-repressed in the *swr1Δ rrp6Δ* strain. Interestingly, these transcripts are not detected in the *ssu72-2* single mutant, but a subset show increased expression in the *ssu72-2 rrp6Δ* strain compared to the *rrp6Δ* single mutant. As with SRTs, a subset of these unannotated transcripts are 5' or 3' UTR extensions of existing ORFs (n= 41), while the rest were intergenic. Furthermore, the aberrant 3' extensions observed in the absence of *SWR1* occur primarily at convergent gene pairs, consistent with a previous report describing a role for H2A.Z in transcription termination in fission

yeast (Zofall et al., 2009). Notably, the promoter regions that flank transcripts de-repressed in the *swr1Δ rrp6Δ* strain are also depleted for H2A.Z compared to regions surrounding CUTs (Tan-Wong et al., 2012, Figure 3.1E), suggesting that the repressive role for H2A.Z in this context may be indirect, or mediated through as yet unknown factors.

Functional interactions between *SWR1* and the RNA exosome

Our RNA analyses identified 985 ORF transcripts that increased in abundance after inactivation of the nuclear exosome. A subset of these transcripts were reduced in the *swr1Δ rrp6Δ* double mutant. These data suggest that H2A.Z and the nuclear exosome act antagonistically at these ORFs to regulate their mRNA abundance. What is puzzling is that the steady state levels of these ORF transcripts are not decreased in the *swr1Δ* single mutant. Why does H2A.Z only seem to promote expression of these mRNAs in the absence of the exosome? Drawing from the observations in the *rtt109*Δ, one possibility is that each of these ORFs expresses two populations of transcripts – one type of transcript may be aberrant and be targeted for degradation by the exosome, and a second set may be functional (Figure 2.6A). In this model, the decreased level of RNAPII, due to loss of H2A.Z, may favor production of functional transcripts and reduce formation of exosome-targeted transcripts (Figure 2.6A). In support of this, work in fission yeast showed that fewer molecules of RNAPII in the *pht1Δ* (H2A.Z gene

in *S. pombe*) diminish the number of stalled, back-tracking RNA polymerases that are targeted for exosome action (Lemay et al., 2014). This type of functional interdependency between RNAPII levels and exosome degradation may also underlie the regulation of divergent transcripts by H2A.Z and the exosome in mouse ESCs (Rege et al 2015, not included in thesis), as well as other cases where transcription and mRNA degradation appear to be linked (Haimovich et al., 2013; Sun et al., 2013).

Chromosome interaction domains (CIDs) and ncRNA transcription

Genome-wide, high-resolution analysis of yeast chromosome folding identified chromosome interaction domains (CIDs) that encompass ~1-5 genes (Hsieh et al. 2015). The precise structure of these domains remains unknown, as 3C-based analyses find strong interactions between the 5' and 3' ends of genes (Figure 3.4A and (Singh and Hampsey, 2007; Tan-Wong et al., 2012)), whereas Micro-C instead recovers broader domains of interacting nucleosomes throughout gene bodies (Figure 3.4B). The technical reasons for this discrepancy remain unresolved – it seems likely that a pelleting step used in 3C may enrich for interactions between gene termini – but both CIDs and gene loops appear to unfold in *ssu72* mutants (Hsieh et al., 2015; Tan-Wong et al., 2012) and *swr1Δ* mutants (this study), suggesting that these assays provide distinct views of a common structure. Assembly of these compact domains requires subunits of the

transcription Mediator complex (Med1), Rtt109 (H3-K56Ac), Ssu72, and H2A.Z. Of this group, only H2A.Z (and subunits of the SWR-C complex) shows negative genetic interactions with all three of the other regulators, *MED1*, *RTT109*, and *SSU72*, suggesting that it may be a key nexus for CID assembly or function (Collins et al., 2007; Fiedler et al., 2009).

A key question is whether CID architecture contributes directly to transcriptional regulation. The extent of gene compaction within CIDs weakly anti-correlates with transcription, with highly active genes often localized either within or adjacent to strong boundary regions. In addition, strong boundaries are also enriched for CUTs, which are primarily divergent (Figure 3.5A). This suggests that boundaries between CIDs, which are generally associated with highly open and active promoters, may reflect chromatin domains that are generally permissive for transcription (Ulianov et al., 2015). In contrast to boundary regions, highly compact genes within CIDs are transcriptionally derepressed in mutants that disrupt CID structure, suggesting that gene compaction within the CID architecture may help to promote or reinforce transcriptional repression. An inhibitory role for CIDs may be similar to the inhibitory 'loop' mediated by H2A.Z between the promoter and the 3' enhancer of the *CCND1* oncogene in mammalian cells (Dalvai et al., 2012, 2013). Likewise, the 3D organization of genes into CIDs may help to prevent expression of ncRNAs, such as SRTs and other ncRNAs that are repressed by H2A.Z.

Figure 3.5: Micro-C analysis of different genomic regions, and transcripts of interest

A) Box plot analysis of boundary strength associated with different loci. Promoter proximal regions are associated with strong boundaries irrespective of transcript type. p-values were determined by Fischer's Exact Test **(**)**. CUT promoters are particularly enriched for strong boundaries, compared to other transcript promoters **(***)**. Null are non-promoter NFRs. p-values determined by Fischer's Exact Test are all at least $p < 0.0001$.

B) Cumulative Distribution Function (CDF) of the compaction score for Up_ncRNA (n=269) and Unchanged_ncRNA (n=713) for *swr1Δ* and WT. Up_ncRNAs are SWR1- repressed. Statistical significance of the two given distributions was tested using Kolmogorov–Smirnov test (KS test) in R.

Figure 3.5

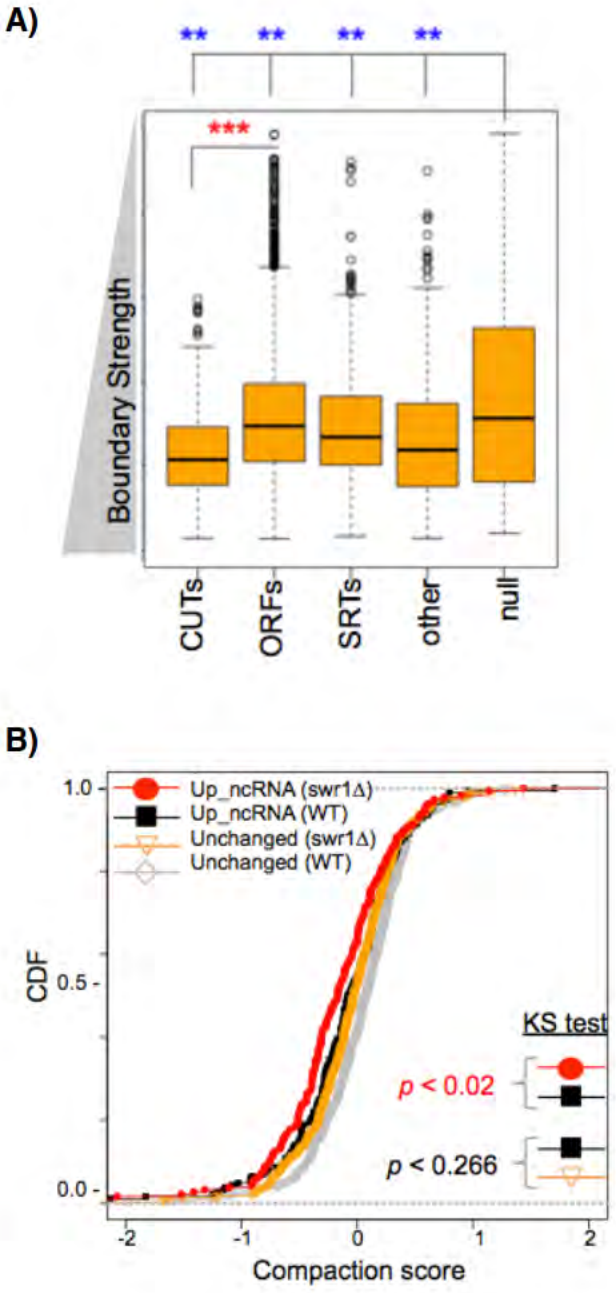
A)
**
**
**
**
***
Boundary Strength
CUTs
ORFs
SRTs
other
null
B)
Up_ncRNA (swr1Δ)
Up_ncRNA (WT)
Unchanged (swr1Δ)
Unchanged (WT)
CDF
1.0
0.5
0.0
KS test
p < 0.02
p < 0.266
-2
-1
0
1
2
Compaction score

Consistent with this view, we found that SRTs are depleted from strong CID boundary regions (Figure 3.5A), and SRTs are de-repressed when CIDs are disrupted in either the *ssu72-2* or *swr1Δ* strain. A role for CIDs in repression of SRTs provides an explanation for why a subset of SRTs is derepressed in the *swr1Δ* strain even though H2A.Z is not enriched at SRT promoters. Indeed, ncRNA transcripts that are repressed by H2A.Z are contained within CIDs that are more strongly de-condensed in the *swr1Δ* strain than CIDs harboring SRTs that are not repressed by H2A.Z (Figure 3.5B). An additional possibility that is consistent with the phenotype of *swr1Δ* and *ssu72-2* strains is that CID architecture may promote transcriptional fidelity by guiding correct sites of transcription initiation and termination, perhaps in part by localizing all of the machineries into a confined transcription domain. Thus, CIDs may generally reinforce normal transcriptional homeostasis, fine-tuning transcription of both coding and noncoding RNAs.

III.E. MATERIALS AND METHODS

Yeast growth and Tiling array sample preparation

As described in Chapter I.

Differential gene expression analysis for tiling array data and corresponding plots

As described in Chapter I.

Transcript annotation and categorization

Transcript annotations originally defined for CUTs, SUTs, ORFs (ORF-Ts) and other were obtained from (Xu et al., 2009) and combined with the SRT annotation from (Tan-Wong et al., 2012) to get a comprehensive set of known annotations. Additional segment features were further searched in the absence of *SWR1* and *RRP6* using the automatic segmentation algorithm with default parameter (Huber et al., 2006). Two criteria were used to focus on previously unannotated transcripts of interest to this study: 1) the transcript did not overlap with the known annotation set and 2) transcript abundance in the *swr1Δ rrp6Δ* was greater than that in the *rrp6Δ*. Although we cannot determine the precise origin of these transcripts from tiling arrays, we classified them as 5' or 3' UTR extensions of existing ORFs, rather than 'novel' transcripts, if the tiling array signal was obviously contiguous with and of the same intensity as the corresponding ORF.

The complete annotation used in this publication is listed on the Cell Reports website. The corresponding signal intensity values are available as processed data in the GEO subseries GSE73110.

Group D CUTs are i) significantly upregulated in the *rrp6Δ* compared to WT and ii) reduced by > 0.59 LFC in *rtt109Δ rrp6Δ* as well as *swr1Δ rrp6Δ* compared to the *rrp6Δ*. Refer to Figure 2.4B and TableS1F.

Up_ncRNAs are i) significantly upregulated in the *swr1Δ rrp6Δ* compared to *rrp6Δ* and include SRTs (n= 45), Novel (n= 100), SUTs (n= 50), CUTs (n= 29). Refer to Figure 2.4B, Figure 3.1E and Table S1E in Appendix 1.

Unchanged_ncRNAs (n=485) are SRTs that do not change statistically significantly in the *swr1Δ rrp6Δ* compared to *rrp6Δ*. Refer to Figure 3.1E and Table S1E in Appendix 1.

Chapter IV: CONCLUSIONS AND OUTLOOK

IV-A. Transcription: Then and Now

Transcription is at the heart of gene regulation. For the past 50 years, a large body of work has advanced the field by determining the structure of the RNA polymerase II and figuring out the mechanistic details of how model genes are transcribed. The overarching theme in the transcription field has been to understand how RNA polymerase II is recruited to a gene via various co-factors/ co-activators. Histone modifications, histone variants and chromatin remodeling enzymes are also examples of crucial players that have significantly advanced the transcription field.

However, after the coming-of-age of high throughput genomics technology, this paradigm has shifted remarkably. It is now clear that RNA Pol II is rather sloppy and can indiscriminately transcribe from DNA regions that are accessible to it. A majority of these hidden (cryptic) transcripts originate from a nucleosome free region (NFR) upstream of genes. Although the NFR is shared, bidirectional promoters form distinct PICs to produce cryptic transcripts, which are then degraded. This remarkable observation has fueled an understanding of the mechanisms that degrade ncRNAs and help discriminate functional from non-functional transcripts.

Although most eukaryotic genomes are transcribed in this ‘pervasive’ manner, only a handful of studies have identified a function for these cryptic transcripts. Cryptic non-coding transcripts can disrupt ORF transcription by directly transcribing through the ORF promoter, in either a sense or antisense orientation. Thus, so far, cryptic transcripts appear to ‘interfere’ with transcription of the ORF they are close to. However, the function of a majority of cryptic transcripts is currently unknown and is an open area of investigation.

To understand the function of an RNA molecule, it is helpful to figure out how it is regulated. Likewise, the cellular pathways that promote or inhibit ncRNA production may give us a clue about their function as well. Since cryptic transcripts described so far antagonize ORF expression, the field has focused on understanding factors that act to curb them (Tudek et al., 2015). Indeed, the discovery of cryptic ncRNAs and their subsequent categorization into various classes was only possible when proteins that degrade them were inactivated.

The RNA processing, termination and degradation machinery are major players that help degrade cryptic ncRNA once they are produced. So far, these include the RNA exosome (Rrp44/Dis3p, Rrp6), cytoplasmic exonuclease Xrn1, TRAMP component Trf4p, Nrd1 (part of the NNS machinery) and the termination factor Ssu72. Deletion or depletion of all of these factors leads to an increase in ncRNA abundance (van Dijk et al., 2011b; Neil et al., 2009; Schulz et al., 2013; Tan-Wong et al., 2012; Xu et al., 2009). Some of these proteins have evolved to

bind to particular sequence motifs present abundantly in cryptic transcripts, and help the degradation machinery discriminate functional and cryptic RNA products. Although the exact proteins involved are different, this general theme has been reported in yeast, as well as mammals (Almada et al., 2013; Schulz et al., 2013).

In parallel, others also reported that chromatin associated factors seem to work either alone or together with the RNA exosome to prevent cryptic ncRNA initiation. Histone chaperones that promote histone assembly, HDACs, methylated histones and chromatin remodeling factors that position nucleosomes to discourage Pol II initiation ‘in the wrong direction’ from promoters or intergenic regions are all part of the chromatin associated arsenal that limit cryptic ncRNAs (Alcid and Tsukiyama, 2014; Carrozza et al., 2005; DeGennaro et al., 2013; Jeronimo et al., 2015; Keogh et al., 2005; Marquardt et al., 2014; Whitehouse et al., 2007).

In comparison to these inhibitory mechanisms, little is known about pathways that promote ncRNA initiation. SWI/SNF, a chromatin remodeling enzyme, is the only reported factor that can promote ncRNA production (Marquardt et al., 2014). The remodeling activity of this enzyme is positively affected by histone acetylation, which is most enriched around gene promoters. It was speculated that SWI/SNF might evict nucleosomes to expose ncRNA TSS to the transcription machinery, facilitating their transcription. In contrast to this, the

SWI/SNF homolog in mESCs, esBAF, seems to broadly inhibit ncRNA production by enforcing nucleosome occupancy over ncRNA TSS (Hainer et al., 2015). These data may be reconciled by considering that observations from model genes loci likely reflect a subset of patterns observed in a genome-wide study with mESCs. Thus, whether SWI/SNF activates or represses ncRNA production may be context specific, and the outcome dependent on ncRNA promoter accessibility.

IV-B. In this work

We report the first widespread mechanism that promotes ncRNA transcription in a genome-wide manner. In budding yeast, a large number of cryptic non-coding transcripts originate from genic promoters that are bidirectional. A hallmark of a majority of nucleosomes that flank promoter regions is their rapid turnover rate. Such dynamic nucleosomes increase accessibility to DNA, and presumably increase the chance of RNA Pol II successfully initiating transcription. The histone mark H3-K56Ac and the variant H2A.Z are also highly enriched in promoter proximal nucleosomes, and they synergistically increase histone turnover (Kaplan et al., 2008; Rufiange et al., 2007). Although prevalent at a majority of genes, the contribution of these histone marks to transcription has remained elusive. We find that H3-K56Ac and H2A.Z are broadly required for CUT transcription, a type of cryptic ncRNA in budding yeast. A fraction of CUTs

require both of these histone marks in a non-redundant manner, consistent with the observation that H3-K56Ac and H2A.Z function together yet contribute in distinct ways.

SWR1 also inhibits some of the SRT class of ncRNAs, similar to Ssu72. As these *SWR1*-repressed transcripts are not enriched for the histone variant, this is likely to be an indirect effect. These loci are among the most de-compacted regions in *swr1*Δ by Micro-C*,* suggesting that the repressive effect of *SWR1* at these transcripts may be an outcome of disrupting CID compaction.

Transcripts originating from bidirectional promoters can be co-regulated at the RNA level (Scruggs et al., 2015; Xu et al., 2009). This coupling between the downstream ORF and an upstream cryptic transcript in a divergent configuration can reduce transcriptional noise, and thus has been proposed to have an evolutionary impact (Wang et al., 2011). It should be noted that such studies are particularly challenging in budding yeast due to its compact genome, such that a particular cryptic transcript can be divergent with respect to one ORF and tandem with a another neighbor. A visual inspection of our data does not show any evidence of such coordinated changes in RNA abundance and is consistent with previous work showing that transcriptional activity is set by distinct PICs for divergent transcripts (Murray et al., 2012; Rhee and Pugh, 2012; Schulz et al., 2013; Yassour et al., 2010).

What is the advantage of promoting cryptic transcription? Several possibilities exist, most of which are speculative. Similar to XUT stabilization in wild type cells after lithium exposure, ncRNA transcription could functionally assist in environmental stress responses, although exactly how this works is unknown. On an evolutionary time-scale, CUTs may eventually become novel genes, like SUTs. Conceptually, a SUT is a CUT without the NNS binding sites, such that is exported into the cytoplasm like an mRNA. Even if cryptic transcripts are themselves not functional, the act of transcribing from their promoter, albeit non-productive, could reduce the response time of regulating the adjacent locus. This could be especially important at genes that respond to changes in the environment where, transcriptional interference via a ncRNA shuts off transcription of the overlapping protein-coding gene (Kim and Buratowski, 2009). Finally, ncRNAs/ their transcription may help to create a platform and confine the RNA transcription, processing and degradation machinery within a domain, making the process streamlined.

Aside from its role in ncRNAs, we also report that H3-K56Ac promotes transcription of a subset of highly transcribed ORFs (Group A ORFs) and this effect is masked by a functional nuclear exosome. RNA levels of these ORFs increase in the absence of *RRP6*, suggesting that the nuclear exosome negatively regulates Group A ORFs. Conversely, Pol II occupancy at Group A ORFs decreases in the absence of Rtt109, suggesting that H3-K56Ac/ Rtt109

positively regulate them, although their RNA levels are unchanged in the *rtt109*Δ. Thus, *RTT109* likely promotes two opposing pathways simultaneously: Pol II occupancy that positively affects RNA levels, and the nuclear exosome that negatively affects RNA levels. As a result, in the *rtt109Δ* single mutant, both activities that normally balance each other are lost, and there is no apparent change in RNA abundance.

Why might Group A ORFs specifically targeted by the nuclear exosome? Using published data, we found that the ORFs regulated by Rrp6 tend to have high Pol II occupancy and transcriptional rates. Higher number of Pol II molecules may increase the number of stalled, backtracking RNA polymerases, which are known to be targeted for exosome action (Lemay et al., 2014). Thus, at highly transcribed ORFs, the nuclear exosome may function as a quality control mechanism. Whether this action requires the exosome to be associated with the polymerase, as observed previously in flies, is open question for future studies (Andrulis et al., 2002; Lim et al., 2013).

We complemented our RNA data with parallel investigations into the effect of these marks on chromatin structure. We report that H2A.Z is required for 3D genome organization. 3C and Micro-C analyses with *swr1Δ* suggest that H2A.Z helps in compaction of chromosomal interaction domains (CIDS). Each CIDs encompasses an average of 1- 5 genes and is characterized by the extensive intragenic nucleosomal contacts (Hsieh et al., 2015). From genome-wide ChIP

studies, we know that each gene possesses an H2A.Z nucleosome at either end of it. Thus, H2A.Z nucleosomes appear to somehow preferentially associate with each other to assist in CID formation. Likewise, H3-K56Ac is also a key player in genome organization, as *rtt109Δ* show a dramatic loss of CID decondensation. How might these promoter-proximal features facilitate compaction within a gene?

A clue comes from previously published *in vitro* experiments on chromatin fiber condensation using solution state sedimentation velocity. Tremethick and colleagues reported that saturated H2A.Z arrays facilitated dramatic intramolecular folding of nucleosomal arrays (Fan et al., 2002). Similarly, Luger and co-workers showed that sub-saturated H3-K56Q arrays (acetylation mimic) inhibited inter-array interactions, which are indicative of higher order structures (Watanabe et al., 2010). Thus, *in vitro* condensation studies suggest that both H2A.Z and H3-K56Ac create an open chromatin structure, by associating preferentially with themselves and simultaneously antagonizing higher order condensation. We speculate that, in the absence of H2A.Z, the chromatin fiber becomes less flexible and CID formation is hindered. Importantly, in this model, CID boundaries are intact, as observed in *swr1*Δ. Along the same lines, Micro-C analyses of highly transcribed genes, which are enriched for H3-K56Ac even in the gene body, display decompaction of CIDs, consistent with these arrays inhibiting higher order folding.

That said, *in vitro* chromatin condensation data are heavily affected by the extent of array saturation. Also, the above-mentioned studies were performed with an entire array of H2A.Z or H3-K56Q nucleosomes, which does not reflect physiological conditions at TSSs of genes. Thus, a lot remains to be learnt about how these histone marks influence CID formation.

Taken together, our RNA transcriptome, Pol II ChIP-seq and Micro-C analyses suggest that H2A.Z and H3-K56Ac coordinate with the nuclear exosome to regulate RNA levels of a large number of ncRNAs as well many protein-coding genes. These dynamic nucleosomes may help to establish a chromosomal interaction domain that balances activities of Rrp6 (yin, negative) and Pol II (yang, positive), and achieves transcriptional homeostasis (Figure 4.1).

Figure 4.1: Model of how chromatin factors may coordinate with the RNA exosome to maintain transcriptional homeostasis

H2A.Z and H3-K56Ac nucleosomes present at 5’ and 3’ ends of genes and make nucleosomes dynamic. These chromatin features may help recruit both, the transcriptional machinery and the nuclear exosome for transcriptional homeostasis. This may be mediated via compaction of CIDs (Chromosomal Interaction Domains).

Normally, CIDs encompass promoters of SRTs (Ssu72-Restricted Transcripts), which likely represses this class of cryptic non-coding transcripts. In contrast, CUTs (Cryptic Unstable Transcripts) are associated with CID boundaries that correlate strongly with active histone marks (Hsieh et al., 2015b) and are permissive for transcription.

Functional interplay between chromatin dynamics and the RNA exosome

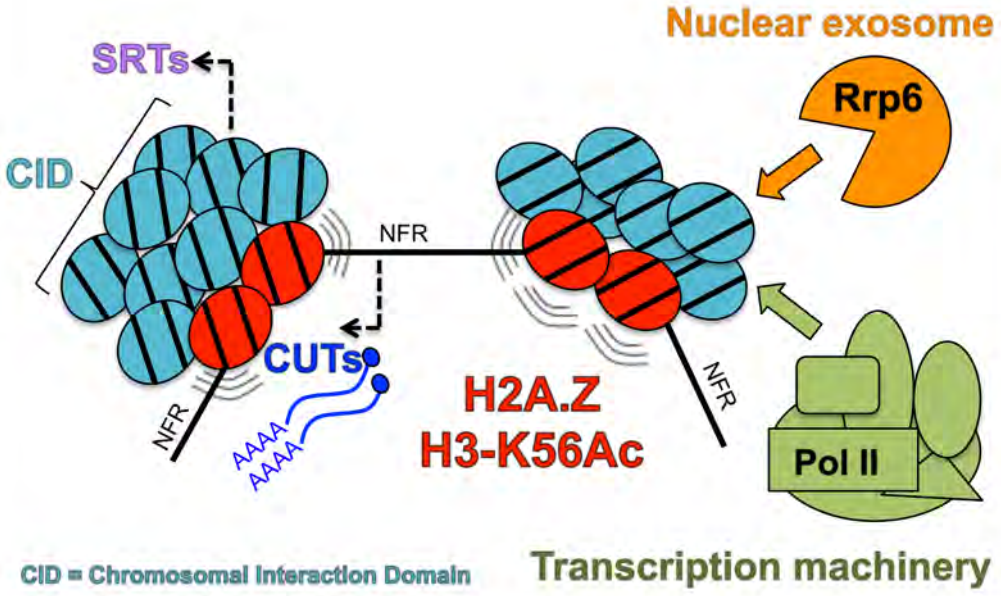

IV-C. Outstanding questions

This study has laid the groundwork for future investigations into how transcriptional homeostasis may be achieved by crosstalk between chromatin-associated factors and the RNA exosome, and whether CIDs play a direct role in this. We outline a few key experiments to help address some outstanding questions that have emerged from this work.

A major prediction of our model is that in wild-type cells, a fraction of Pol II is targeted by the exosome, leading to non-functional transcripts. Native elongating transcript, or NET-seq is a technique that specifically captures the actively elongating population in comparison to total chromatin bound Pol II observed using ChIP-seq experiments (Churchman and Weismann, 2011). An additional advantage is that NET-seq is strand specific, because it captures the RNA-bound Pol II, which will help resolve to a finer degree if the decreases in Pol II occupancy correspond to the changes in RNA abundance.

Rtt109 is a histone acetyltransferasee that can acetylate a number of residues on H3, the specificity of which is determined by the chaperone associated with it (Abshiru et al., 2013). Rtt109-Vps75 preferentially acetylates H3K9 and K23, while Rtt109-Asf1 is specific for acetylation on H3K56, the modification that promotes histone turnover (Berndsen et al., 2008; Tsubota et al., 2007). Although there is considerable evidence suggesting that the *in vivo* phenotypes of *rtt109*Δ are phenocopied by *asf1*Δ, this work could be

complemented by similar analysis of either *asf1*Δ or H3K56R mutants that block acetylation to test this more directly.

In addition to histone turnover, Rtt109p is also involved in histone assembly during S-phase, when newly replicated DNA is packaged into chromatin. Due to this dual role, studies in asynchronous populations do not accurately estimate of the contributions of this histone mark in promoting Pol II occupancy and CID compaction via histone turnover. Presumably, *RTT109* also influences CID compaction during/ soon after replication is complete in late S/ early G2. It is essential to quantify the contribution of replication dependent actions of Rtt109 (*de novo* assembly coupled to the replication fork) from replication-independent incorporation (histone turnover at TSSs) in CID formation. About 20% of the total H3-K56Ac signal is present in G1-phase, primarily in the high turnover promoter-proximal nucleosomes (Kaplan et al., 2008). Thus, Micro-C, Pol II occupancy, and transcriptome analysis of G1-arrested *rtt109*Δ will help elucidate whether replication-independent histone turnover in particular contributes to the Micro-C phenotypes we observe.

Finally, we proposed that CIDs coordinate activities of RNAP II and the nuclear exosome, by creating a platform for them to come together. Although our data are consistent with this idea, whether CIDs are the cause or the effect of reduced Pol II occupancy in *rtt109*Δ, is unclear. Since Pol II occupancy is concomitantly affected with CID compaction in this mutant, testing the model is

non-trivial. CID decompaction could lead to lower Pol II, or conversely, reduced/aberrant transcription such as transcriptional readthrough could, in turn, decompact CIDs.

A starting point would be to assess if CID decompaction causes reduced exosome activity. There is some evidence from work in budding yeast that the activity of the nuclear exosome is coupled to its chromatin localization (Camblong et al., 2007). Thus, a proxy for measuring Rrp6 activity would be to analyze ChIP-seq profiles exosome components in the absence of Rtt109 (or Swr1). If chromatin bound Rrp6 is reduced in the *rtt109*Δ, this would be consistent with the model, while no change in chromatin bound Rrp6 would negate the hypothesis.

The most direct test of the model is to ask whether CID formation is affected in *rrp6*Δ. If CIDs are disrupted, similar to what was observed when Pol II is inhibited using thiolutin (Hsieh et al., 2015), then it would appear that CID structure is made by the concomitant localization of RNA exosome and RNA Pol II. The exciting alternate possibility, given that Pol II occupancy is unchanged in the absence of Rrp6, is that CID formation is intact in *rrp6*Δ, and directly leads to increased RNA abundance of Group A ORFs.

APPENDIX 1

Table S1: Summary of differential gene expression analysis by limma (Panels A-G).

(A)

swr1 vs. wt				Lowered stringency		
	UP with adj.P.value<0.1 (FDR)			UP with adj.P.value<0.8 (FDR)		
	> 1.5 fold or	total	% 1.5 fold	> 2 fold or m	total	% 1.5 fold
CUT	0	925	0.00	0	925	0.00
ORF	0	5171	0.00	0	5171	0.00
other	0	329	0.00	0	329	0.00
SRT	0	536	0.00	0	536	0.00
SUT	0	847	0.00	0	847	0.00
total	0	7808		0	7808	

	DOWN with adj.P.value <0.1 (FDR)			DOWN with adj.P.value <0.8 (FDR)		
	> 1.5 fold or	total	% 1.5 fold	> 2 fold or m	total	% 1.5 fold
CUT	0	925	0.00	0	925	0.00
ORF	0	5171	0.00	1	5171	0.02
other	0	329	0.00	0	329	0.00
SRT	0	536	0.00	0	536	0.00
SUT	0	847	0.00	0	847	0.00
total	0	7808		1	7808	

(B)

rtt109 vs. wt			
	UP with adj.P.value<0.1 (FDR)		
	> 1.5 fold or	total	% 1.5 fold
CUT	8	925	0.86
ORF	28	5171	0.54
other	3	329	0.91
SRT	6	536	1.12
SUT	25	847	2.95
total	70	7808	0.89651639

	DOWN with adj.P.value <0.1 (FDR)		
	> 1.5 fold or	total	% 1.5 fold
CUT	0	925	0
ORF	62	5171	1.19899439
other	7	329	2.12765957
SRT	0	536	0
SUT	2	847	0.23612751
total	71	7808	0.90932377

(C)

swr1_rtt109 vs. wt			
	UP with adj.P.value<0.1 (FDR)		
	> 1.5 fold or	total	% 1.5 fold
CUT	28	925	3.03
ORF	246	5171	4.76
other	28	329	8.51
SRT	9	536	1.68
SUT	50	847	5.90
total	361	7808	

	DOWN with adj.P.value <0.1 (FDR)		
	> 1.5 fold or	total	% 1.5 fold
CUT	1	925	0.11
ORF	214	5171	4.14
other	21	329	6.38
SRT	3	536	0.56
SUT	20	847	2.36
total	259	7808	

(D)

rrp6 vs. wt					
	UP with adj.P.value<0.1 (FDR)				
	> 1.5 fold or	total	% 1.5 fold		
CUT	726	925	78.49		
ORF	985	5171	19.05	includes 90 ORFS with introns	
other	128	329	38.91	total 281 spliced genes in genome	
SRT	48	536	8.96		
SUT	317	847	37.43		
total	2204	7808			1836
	DOWN with adj.P.value <0.1 (FDR)				
	> 1.5 fold or	total	% 1.5 fold		
CUT	2	925	0.22		
ORF	851	5171	16.46		
other	32	329	9.73		
SRT	2	536	0.37		
SUT	30	847	3.54		
total	917	7808			

(E)

swr1_rrp6 vs. rrp6					
	UP with adj.P.value<0.1 (FDR)				
	> 1.5 fold or	total	% 1.5 fold	Cryptic_up_s	unchanged
CUT	29	925	3.14	yes	713
ORF	260	5171	5.03		4618
other	13	329	3.95		301
SRT	45	536	8.40	yes	485
SUT	50	847	5.90	yes	734
total	397	7808			
	DOWN with adj.P.value <0.1 (FDR)				
	> 1.5 fold or	total	% 1.5 fold		
CUT	183	925	19.78	40 CUTs unique to swr; rest in rtt10	
ORF	293	5171	5.67		
other	15	329	4.56		
SRT	6	536	1.12		
SUT	63	847	7.44		
total	560	7808			

(F)

rtt109_rrp6 vs. rrp6			
	UP with adj.P.value<0.1 (FDR)		
	> 1.5 fold or	total	% 1.5 fold
CUT	20	925	2.16
ORF	175	5171	3.38
other	5	329	1.52
SRT	13	536	2.43
SUT	20	847	2.36
total	233	7808	
	DOWN with adj.P.value <0.1 (FDR)		
	> 1.5 fold or	total	% 1.5 fold
CUT	394	925	42.59
ORF	1129	5171	21.83
other	54	329	16.41
SRT	16	536	2.99
SUT	140	847	16.53
total	1733	7808	

13 in Botstein group

(G)

swr1_rtt109_rrp6 vs. rrp6			
	UP with adj.P.value<0.1 (FDR)		
	> 1.5 fold or	total	% 1.5 fold
CUT	50	925	5.41
ORF	298	5171	5.76
other	22	329	6.69
SRT	24	536	4.48
SUT	42	847	4.96
total	436	7808	
	DOWN with adj.P.value <0.1 (FDR)		
	> 1.5 fold or	total	% 1.5 fold
CUT	471	925	50.92
ORF	1627	5171	31.46
other	85	329	25.84
SRT	17	536	3.17
SUT	207	847	24.44
total	2407	7808	

Table S2: Primer sequences for qPCR analysis

Name	Coding-Fwd	Coding-Rev
CUT579	GCCGAATATTAGCTCCTTCG	TACATAATGCCAGCGACAGC
CUT848	AAACGGAGGTTTGTCACGTC	ACTTTTGCGGTTGCTCTCTC
CUT737	GCGCAAAAAGCTCAGTCTTG	ATCTGTCCCCGAATGGTATC
OLA1	AGAAGCCCGTGTTATTGTCC	GCATTACCCAAACCTTCACC
RPL36A	AGGGGTTTACCCCAAATACG	CTCTGGCTATTTCCATTGGTC
RRP45	GCAACACCAAAGTTCACTGC	CCTTCAAATGGCCTGTCTTC
CHRVIL	CATGACCAGTCCTCATTTCCATC	ACGTTTAGCTGAGTTTAACGGTG

APPENDIX 2

Manuscript in preparation:

SWI/SNF antagonizes Sir3 to activate transcription of genes expressed at G2/M phase of the cell cycle

Mayuri Rege[1] and Craig L. Peterson[1 2]

[1] Program in Molecular Medicine

373 Plantation Street, Biotech 2, Suite 210, Worcester, MA 01605

Ph#508-856-5858

FAX#508-856-5011

[2]Corresponding author

Email: craig.peterson@umassmed.edu

ABSTRACT:

Heterochromatin and euchromatin form functionally distinct compartments, although proteins that silence heterochromatin can bind euchromatin regions. We have previously shown that the SWI/SNF chromatin remodeling enzyme can evict Sir proteins, which form heterochromatin in budding yeast. Whether this activity contributes to the role of SWI/SNF as a transcriptional activator at euchromatic loci is unknown. We characterized genetic interactions between the SIR genes (*SIR2*, *SIR3*, and *SIR4*) and *SWI2,* which encodes for the catalytic subunit of SWI/SNF. Loss of either *SIR3* or *SIR4* partially rescues growth defects of *swi2Δ* on rich media, although growth on alternative carbon sources is largely unaffected. In contrast, loss of *SIR2* has no effect on the phenotypes of *swi2Δ*; the suppression is specific to structural Sir proteins. Transcriptional profiling of *swi2Δ*, *sir3Δ* and *swi2Δ sir3Δ* showed that specific transcriptional defects of *swi2Δ* were rescued by a deletion of *SIR3*. Comparison of the null mutant datasets with those from a conditionally depleted *SWI2* strain allowed us to separate out indirect transcriptional changes due to slow growth. Genes that are activated by *SWI2* and repressed by *SIR3* tend to be expressed in the G2/M phase of the cell cycle. In addition to reporting transcriptional profiles of conditional SWI/SNF mutants, our work identifies a key set of genes that may require SWI/SNF to antagonize Sir3 and activate their gene expression.

INTRODUCTION:

Extensive condensation is necessary to fit the genome within the dimensions of the nucleus. The DNA is packaged with positively charged histone proteins to form chromatin. Chromatin can be divided into two functional categories: transcriptionally active (euchromatin) and transcriptionally silent (heterochromatin). The constitutive heterochromatic structures in the budding yeast are formed at telomeres and silent mating type loci (*HM* loci). These regions are silenced by the SIR complex, consisting of Sir2, Sir3 and Sir4 proteins (*S*ilent *i*nformation *r*egulators) (Rusche et al., 2003; Rusché et al., 2002). Sir2 is a histone deacetylase while Sir3 and Sir4 are believed to play structural roles during heterochromatin formation.

Overexpression of Sir3 causes gene-silencing defects in euchromatin (Taddei et al., 2009) and also affects boundaries between heterochromatin and euchromatin (Holmes et al., 1997). Chromatin immunoprecipitation studies of native Sir3 in wild type cells report localization to euchromatin, although the implications of this are not understood (Radman-Livaja et al., 2011). Immunofluorescence studies of Sir3 have revealed that Sir3 forms discrete puncta for most of the cell cycle, except for a diffuse staining pattern in the G2/M phase (Laroche et al., 2000). Thus, several groups have reported that Sir3 can bind outside of heterochromatin and active mechanisms that correct this re-distribution remain unknown.

ATP dependent chromatin remodeling enzymes are a major contributor to the dynamic nature of chromatin. They modify chromatin structure by mobilizing or disrupting nucleosomes in an ATP-dependent reaction (Clapier and Cairns, 2009). The SWI/SNF chromatin remodeling enzyme is the founding member of its subfamily(Smith and Peterson, 2005). The catalytic subunit Swi2 is essential for ATP binding and hydrolysis (Richmond and Peterson, 1996) and is the business end of the enzyme. *SWI2* knockout mutants (*swi2*Δ) fail to activate expression of highly inducible genes (Holstege et al., 1998; Sudarsanam et al., 2000) and show defects in exit from mitosis (Krebs et al., 2000).

Functionally, SWI/SNF is recruited to promoter sequences where it remodels nucleosomes to uncover underlying regulatory sequences. In addition to its recruitment at promoters, SWI/SNF also associates with RNA Polymerase II (Pol II) during transcriptional elongation, where it has been shown to evict H2A-H2B dimers ahead of the polymerase (Schwabish and Struhl, 2007; Wilson et al., 1996). In addition to these roles, our recent work showed that SWI/SNF can evict Sir3 from nucleosomal arrays *in vitro* and contributes to establishment of heterochromatin formation *in vivo* (Manning and Peterson, 2014; Sinha et al., 2009). Notably, RSC, a chromatin remodeler highly related to SWI/SNF, is unable to perform these functions. Thus, SWI/SNF has a distinct role in the removal of Sir3, although whether this activity is important in the process of transcription has not been thoroughly addressed.

In this work, we report that the catalytic subunit of SWI/SNF genetically interacts with *SIR3* and *SIR4*, but not with *SIR2*. Many phenotypic defects of *swi2*Δ are partially rescued by a concomitant deletion of *SIR3*. To circumvent the severe growth retardation associated with knockout *SWI2* alleles, we compared our findings to a conditionally depleted *SWI2* allele. This rigorous approach identified a common set of genes, where SWI/SNF likely antagonizes Sir3 to promote expression.

RESULTS:

Specific growth phenotypes of *swi2*Δ are partially rescued by *sir3*Δ

We made isogenic *sir3Δ, swi2Δ* and *swi2Δ sir3Δ* strains from a swi2Δ/*SWI2 sir3Δ/SIR3* heterozygous diploid in the S288C background. Swi2 is the catalytic subunit of the SWI/SNF chromatin remodeling enzyme and *swi2*Δ mutants have dramatically slowed growth rates. Deletion of *SIR3* partially suppresses thr growth defect of *swi2*Δ on rich media (Figure A2.1A, B), suggesting that these loci genetically interact. Importantly, this suppression segregates with markers for the double mutant after tetrad analysis, eliminating the possibility that a background suppressor mutation causes the growth suppression in *swi2Δ sir3Δ* (Figure A2.1A). In addition to glucose, *swi2*Δ mutants are also unable to metabolize alternative carbon sources like raffinose and galactose (Abrams et al., 1986; Carlson et al., 1981). Growth on these media requires nucleosome

remodeling at gene promoters facilitated by SWI/SNF and is expected to be decoupled from the Sir3 eviction activity of this enzyme. Consistent with this, deletion of *SIR3* does not suppress growth defects of swi2Δ on raffinose and only a marginal suppression is seen for galactose (Figure A2.1B). Growth on non-fermentable carbon sources such as glycerol and ethanol also requires Swi2. Defects of *swi2Δ* on ethanol and glycerol are partially suppressed by deletion of *SIR3*. *SWI2* is required for progression through replication stress, mimicked by the drug hydroxyurea (HU), and *swi2*Δ show a delayed growth rate in this condition (Sharma et al., 2003). Interestingly, deletion of *SIR3* partially relieves this HU sensitive phenotype when *SWI2* is knocked out (*swi2*Δ; Figure A2.1B). Thus, specific phenotypes of *swi2*Δ are partially suppressed by deleting *SIR3*.

Suppression of *swi2*Δ phenotypes is not dependent on the strain background

Many genetic interactions have been found to be specific to either the S288C or W303 background strains commonly used by the yeast community, although these strains are very similar. To test the generality of our findings, we extended our genetic analyses to mutants made in the W303 background. Indeed, we find that the growth defects of *swi2Δ* are suppressed by *sir3Δ* irrespective of the strain background (Figure A2.1C).

To eliminate the possibility that a background mutation other than the sir3Δ segregated with, and caused the growth suppression seen in the double mutant, we transformed the *swi2Δ sir3Δ* with a plasmid containing *SIR3* expressed from its endogenous promoter. As expected, complementation with a vector plasmid alone had no effect on the growth rate while the *SIR3* plasmid slowed the growth of *swi2Δ sir3Δ* noticeably (Figure A2.1D). Given that *sir3Δ* suppresses the severe growth defects of *swi2Δ* in multiple strain backgrounds and that this suppression can be reversed when *swi2Δ sir3Δ* is complemented by a *SIR3* plasmid suggest that SWI/SNF antagonizes Sir3 *in vivo*.

Absence of *SIR2* does not suppress *swi2*Δ growth defects

Given that *SIR3* showed negative genetic interactions with *SWI2*, we asked whether other components of the SIR complex (*SIR2* and *SIR4*) involved in heterochromatin formation also showed similar genetic interactions. Sir2 is a histone deacetylase (HDAC) that promotes Sir3 binding to nucleosomes by removing the acetyl group on histone H4 lysine 16. Unlike deletion of *SIR3*, *swi2Δ sir2Δ* mutants do not show suppression of the *swi2*Δ growth defect (Figure A2S.1 B, C). This indicates that the pseudo-diploid state is not sufficient to see the suppression of *swi2*Δ growth defects. Furthermore, we observe that *sir2*Δ in the SWI2AA background also does not suppress the HU sensitivity or ethanol

sensitivity phenotype of *SWI2*-FRB on rapamycin (Figure A2.2E and Figure A2S.1 D).

Sir4 is a structural protein like Sir3 that helps to establish heterochromatin formation at telomeres and mating type loci (Rusché et al., 2002; Thurtle and Rine, 2014). Loss of *SIR4* suppresses growth defects of *swi2*Δ mutants, as was seen with the deletion of *SIR3* (Figure A2S.1 E, F). Thus, SWI/SNF may antagonize Sir3 and Sir4, but does not appear to genetically interact with Sir2.

Comparison of *swi2Δ* alleles with conditional depletion of *SWI2*

As *swi2Δ* null mutants are slow growing, we wanted to establish an alternative approach to interrogate gene expression profiles in the absence of SWI2. The Anchor away system developed by the Laemmli lab was used to conditionally deplete Swi2 from the nucleus (Haruki et al., 2008). The parent wild type strain has a FK506 binding protein (FKBP12) tag fused to the C-terminus of an anchor protein, RPL13A. RPL13A is a ribosomal protein that is present in high copy numbers in the cell and transitions from the nucleus to cytoplasm during ribosome assembly, as shown in Figure A2.2A. In this parent strain, we tagged the endogenous *SWI2* locus at the C-terminus with the FKBP12-rapamycin-binding (FRB) domain. Rapamycin induces formation of a ternary complex between the FKBP12 and FRB domains, and thus, rapidly depletes *SWI2*-FRB from the nucleus (Figure A2.2A).

We first compared growth rates of *SWI2*-FRB strains with or without the *SIR3* gene using spot assays. In the presence of DMSO solvent, growth rates of all the strains are identical on rich media (Figure A2.2B, left), indicating that the *SWI2-FRB* construct itself did not impair cell growth. In the presence of rapamycin, *SWI2-FRB* strains show a decrease in growth rate compared to the WT, suggesting that the anchor away system works as expected (Figure A2.2B, right). However, the *SWI2-FRB* strains have a milder growth defect compared to the *swi2Δ* (null) mutant, perhaps due to some residual Swi2 present in the nucleus. As the growth rates of *SWI2-FRB* and *SWI2-FRB sir3Δ* strains are comparable, we can use this system to dissect out indirect changes due to slow growth observed in genomic studies (see below).

Similar to *swi2*Δ, depletion of *SWI2* also causes HU sensitivity and this phenotype is partially suppressed by deletion of *SIR3*, suggesting an important link between *SWI2* and *SIR3* in HU stress (Figure A2.2C, right). Previous work has shown that *SWI2* induces transcription of the ribonucleotide reductase (RNR) genes in the presence of HU (Sharma et al., 2003). Consistent with this, we see a large reduction of these transcripts in *swi2*Δ (Figure A2S.1A). However, unlike the rescue of growth, the transcription of RNR transcripts was not restored in the *SWI2*-FRB *sir3*Δ. This observation suggests that in HU stress, SWI/SNF remodels Sir3 independent of transcription; possibly by assisting DNA repair in SIR heterochromatin.

A subset of SWI-dependent genes are restored to wild type levels in the absence of *SIR3*

Our genetic studies indicate that SWI/SNF antagonizes Sir3. To identify transcriptional targets that depend on this activity, we analyzed RNA profiles of isogenic wild type, *swi2Δ*, *sir3Δ* and *swi2Δ sir3Δ* from 5716 ORFs using microarrays. Consistent with published data, we observed that deletion of *sir3Δ* alone misregulates genes in the mating type cascade, with almost no other changes (Figure A2.3A, middle) (Lenstra et al., 2011). In contrast, *SWI2* regulates 203 genes positively (FDR < 0.1 and LFC < -0.58) and 488 genes negatively (FDR < 0.1 and LFC > 0.58). Many genes classically discovered to be dependent on SWI/SNF such as SER3, YOR222W and the acid phosphatase genes, changed as predicted by previous studies (Figure A2.3B) (Sudarsanam et al., 2000). These genes were unaffected by a deletion of *SIR3* (Figure A2.3B, third column).

To identify genes that are regulated both by *SWI2* and *SIR3*, we first selected genes that changed significantly in the *swi2Δ* compared to wild type by limma (Figure A2.3B), performed hierarchical clustering and classified various sub-groups of interest. Genes that *decrease* significantly (LFC < -0.58 and FDR < 0.1) in *swi2*Δ and are restored to wild type levels in the *swi2*Δ *sir3*Δ are defined as Group 1_KO. The top GO term category enriched in Group 1_KO is ribosome

biogenesis/ ribosomal protein coding genes. This suggests that these genes require SWI/SNF to remodel Sir3 to promote their transcription. Indeed, prior studies have reported Sir3 binding to many ribosomal protein genes using a Gal inducible strain (Radman-Livaja et al., 2011). However, genes involved in ribosome biogenesis/ ribosomal proteins strongly anti-correlate with growth rate and can confound our results (Airoldi et al., 2009). Thus, we compared our findings from the null mutants to those from the anchor-away strains.

In the anchor away background, we again selected genes that changed by 1.5 fold or more after depletion of *SWI2-FRB* and performed hierarchical clustering to identify subsets that are co-regulated by *sir3Δ*. Genes that *decrease* (LFC < -0.58) in *SWI2*-FRB and were restored to wild type levels in the *SWI2*-FRB *sir3*Δ were defined as Group 1_AA. The top GO term category enriched in Group 1_AA is ion/ carbohydrate transport and primarily reflects the metabolic defects of *SWI2* mutants in carbon source utilization.

Overlap between RNA profiles of *swi2*Δ and *SWI2*-FRB alleles

A comparison of findings from the knockout allele with the anchor-away allele of SWI2 revealed many interesting similarities and differences that we describe in detail below. Many classically SWI/SNF dependent genes identified from previous studies change as predicted also when *SWI2* is anchored away (Figure

A2.3C). This validates the anchor-away system for genomic studies of SWI/SNF mutants.

We first compared genes that are activated by SWI/SNF in a Sir3 dependent manner in the anchor away strains and the knockout alleles. These correspond to Group 1_AA (n= 263) and Group 1_KO (n= 192), respectively (Figure A2.4A, B). The overlap between the Group1_AA and Group1_KO sets revealed a very select set of 28 genes, with a p-value of 8.7×10^{-9} (Figure A2.4C). This common subset of genes, consolidated as Group 1, corresponds to GO term categories of ‘cell cycle’, ‘cytokinesis’ and ‘lipid metabolism’. Our lab has previously reported that SWI/SNF is required for expression of genes expressed at the G2/M phase boundary of the cell cycle, although the mechanism of transcriptional activation was not completely understood (Krebs et al., 2000). Our findings now suggest that SWI/SNF may alleviate Sir3 binding at these genes to promote their transcription. As might be expected from the slow growth, genes involved in ribosome biogenesis and gene expression were affected only in the null mutant dataset, and therefore were not included in further analysis.

We also observed a second group of genes that seem to be inhibited by SWI/SNF in a Sir3 dependent manner, in both the anchor away strains and the knockout. Although this has been reported previously, in our approach we focused on genes that were common to the null mutant and the anchor away

datasets (Sudarsanam et al., 2000). Genes that are upregulated in the *swi2*Δ and reduced to wild type in the *swi2*Δ *sir3*Δ are designated as Group 2_KO (n= 482) (LFC < -0.58 and FDR < 0.1) (Figure A2S.2, B). Corresponding to this, genes identified with these criteria from the anchor away dataset were called Group 2_AA (n= 192). However, an overlap of Group 2_KO and Group 2_AA sets revealed very few commonalities (Figure A2S.2, C). This suggests that SWI/SNF does not directly inhibit Group 2 genes and the changes, including those published previously, are likely due to indirect effects (Holstege et al., 1998; Sudarsanam et al., 2000). As there were very few Group 2 genes in common from the knockout data and the anchor away data, we did not analyze this group further.

Analysis of Sir3 binding at Group 1 target genes

The genetic and transcriptome analyses suggest that SWI/SNF antagonizes Sir3 to promote expression of specific genes. One prediction of the model is that Sir3 accumulates in the absence of *SWI2* at target genes, the ones are transcribed mainly at the G2/M boundary. To test the model, we analyzed Sir3 recruitment by chromatin immunoprecipitation (ChIP) in WT and *swi2*Δ mutants arrested in nocodazole. Nocodazole is a microtubule depolymerizing agent that blocks entry into mitosis and thus, cells accumulate at the G2/M border (Jacobs et al., 1988). Sir3 binding was measured using a native antibody to Sir3, as well as an anti-

FLAG antibody in a strain expressing *SIR3*-FLAG tagged gene from its endogenous locus. In both cases, the wild type strain was enriched for Sir3 at heterochromatic loci like HMR and TELVI-R, used as positive controls. However, we observe no detectable difference in Sir3 enrichment in *swi2*Δ compared to WT at the promoters of target genes tested (Figure A2S.3). This could be due to transient binding of Sir3 that is not captured by the ChIP assay. Nonetheless, we report a decrease in Sir3 occupancy in *swi2*Δ at telomeres, consistent with redistribution of Sir3 to ectopic loci (Figure A2S.3).

DISCUSSION:

Establishing the separation between euchromatin and heterochromatin is crucial for the functioning of a cell. The mechanisms that actively exclude heterochromatin proteins from euchromatin remain poorly understood. We identified that the SWI/SNF chromatin remodeling enzyme participates in this process. We report that a subset of genes expressed in the G2/M transition of the cell cycle require the Sir3 remodeling activity of SWI/SNF.

Growth defects *swi2*Δ are suppressed by *SIR3, SIR4 but not SIR2*

Our *in vitro* studies indicated that the SWI/SNF chromatin remodeling enzyme was uniquely able to evict the heterochromatin protein Sir3 from arrays (Manning and Peterson, 2014; Sinha et al., 2009). To investigate the physiological

significance of this finding, we characterized the genetic interactions between *SWI2*, the catalytic subunit of SWI/SNF, and the *SIR2, SIR3, SIR4* genes, which encode for heterochromatin proteins in yeast. Deletion of *SWI2* causes retardation in growth in multiple carbon sources, and *sir3*Δ and *sir4*Δ were able to partially suppress this slow growth in glucose, ethanol and glycerol rich media. This was consistently observed across different strain backgrounds. In contrast, *sir3*Δ and *sir4*Δ do not significantly rescue the severe growth defects of *swi2*Δ on alternative carbon sources like raffinose and galactose. This suggests that the ability of SWI/SNF to mobilize nucleosomes at promoter regions is decoupled from its Sir3 remodeling activity. Consistent with this hypothesis, our lab has recently characterized a separation of function allele (*swi2Δ10R*) that can remodel nucleosomes, yet is unable to evict Sir3 *in vitro* (Manning and Peterson, 2014). In this manner, many classically studied SWI/SNF dependent genes are not sensitive to removal of heterochromatin proteins Sir3 and Sir4.

Genes expressed at the G2/M boundary are dependent on SWI/SNF to antagonize Sir3

Our microarray analysis of *swi2*Δ and *swi2*Δ *sir3*Δ strains revealed two categories of genes that required *SWI2* for activation and were also repressed by *SIR3*. The first category were ribosomal biogenesis and ribosomal protein coding genes that are very sensitive to growth rate and likely indirect effects (Airoldi et al., 2009).

The second category were genes involved in ‘cytokinesis’, ‘cell division’ and expressed at the G2/M boundary in the cell cycle. To circumvent the issues related with slow growth of null mutants, we compared our knockout (*swi2*Δ) microarray data to similar data from the conditionally depleted *SWI2*-Anchor Away set. The only genes that were common to both data were the G2/M expressed genes, suggesting that they were likely direct targets where SWI/SNF antagonizes Sir3. This is consistent with previous findings from our lab that SWI/SNF mutants are defective in exiting mitosis (Krebs et al., 2000).

Genes expressed at the G2/M boundary are dependent on SWI/SNF to antagonize Sir3

Sir3 may dynamically associate with genes expressed in the G2/M phase. If SWI/SNF antagonizes Sir3 at specific targets genes, we expect that in the *swi2*Δ, there would be an accumulation of Sir3 at these loci. ChIP analysis at promoters of some target loci did not show an increase in Sir3 occupancy in nocodazole or asynchronous cells, although we do observe a significant decrease of Sir3 binding from telomeric loci, which has been reported before (Dror and Winston, 2004; Manning and Peterson, 2014). This suggests that Sir3 may delocalize from telomeres in the absence of SWI/SNF and bind euchromatic loci in a manner that is incompatible with chromatin immunoprecipitation analysis. Alternatively, ChIP-seq analysis of Sir3 in *swi2*Δ could determine

whether this heterochromatin protein accumulates within coding regions of targets genes, which are highly deacetylated and may act as Sir binding sites in euchromatin (Carmen et al., 2002; Carrozza et al., 2005; Keogh et al., 2005).

Cytological studies from the Gasser lab support our model. Sir proteins bound to heterochromatin are localized in discrete foci during a majority of the cell cycle (Laroche et al., 2000). In contrast, at the G2/M boundary, Sir proteins show a distinctly diffused staining pattern, possibly providing a window for them to bind ectopic euchromatin sites and impact gene expression. Our *in vitro* studies implicated that the SWI/SNF chromatin remodeling enzyme was uniquely able to evict the heterochromatin protein Sir3. In this work, we find that SWI/SNF functionally antagonizes Sir3 to positively facilitate gene expression. This role is fundamentally different from the classically studied function of SWI/SNF in transcriptional activation by promoter nucleosome remodeling.

FIGURE LEGENDS:

Figure A2.1: *SWI2* growth defects are partially rescued by deletion of *SIR3*

A) Tetrad dissection plates of the *swi2*Δ *sir3*Δ heterozygous diploid on YEPD plates with the corressponding genotypes marked with symbols listed on the left. A single dissected spore yields an isogenic colony, imaged after 10 days. Relative size of each colony is representative of the growth rate.

B) Equal cell numbers of the strains listed were spotted in consecutive ten-fold dilutions on agar plates with different carbon sources and imaged after 3 days. Raffinose and Galactose plates also contain 2% antimycin to prevent respiratory growth.

C) Spot assay was performed as described in B) on null mutants dissected from the W303 background.

D) *swi2Δ sir3Δ* mutants transformed with a plasmid containing either the vector backbone (left) or with a construct expressing Sir3 from its endogenous promoter (right) and spot assays performed on individual isolates as described in B).

Figure A2.1

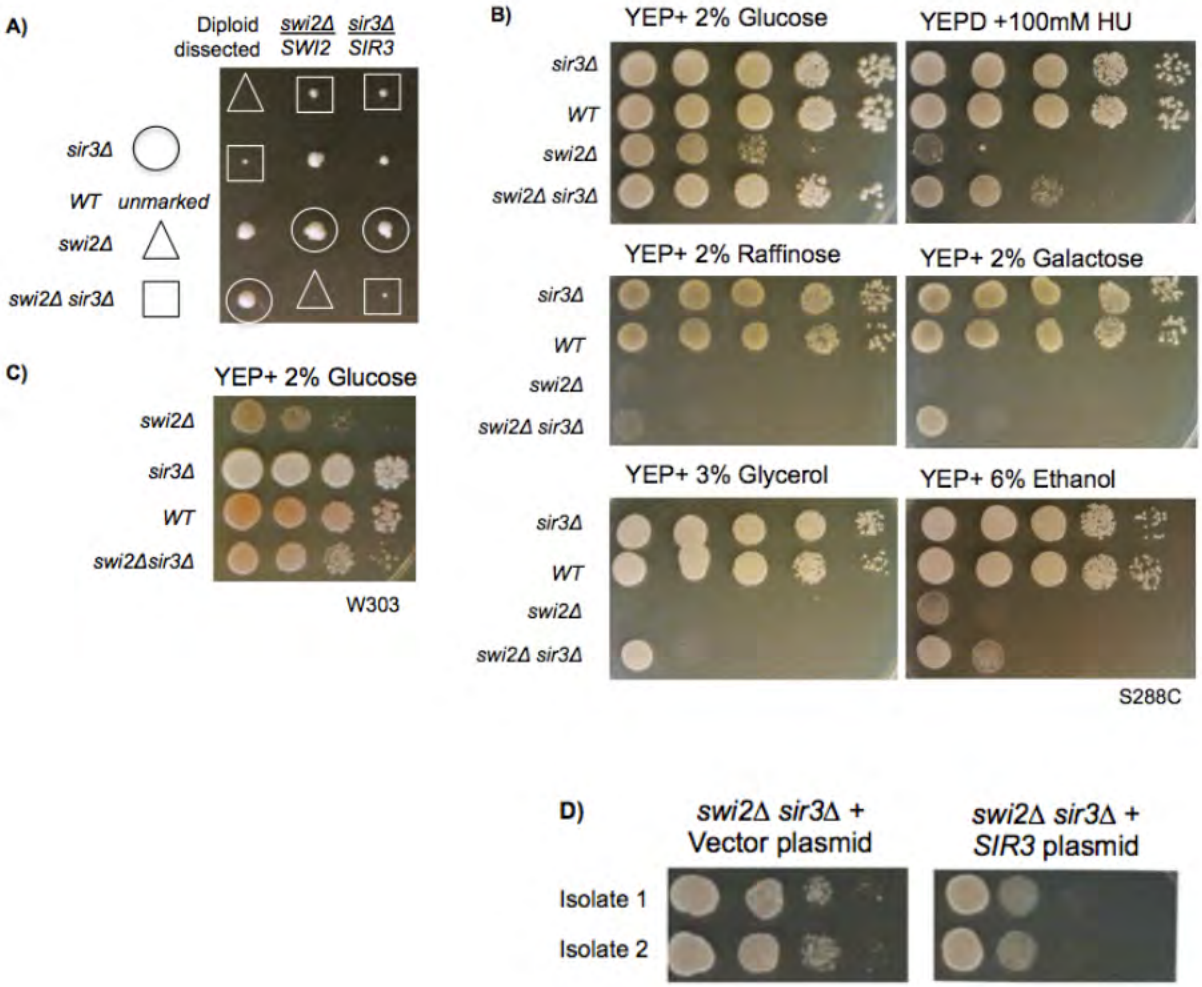
A)
Diploid dissected
swi2Δ SWI2
sir3Δ SIR3
sir3Δ
WT unmarked
swi2Δ
swi2Δ sir3Δ
B)
YEP+ 2% Glucose
YEPD +100mM HU
sir3Δ
WT
swi2Δ
swi2Δ sir3Δ
YEP+ 2% Raffinose
YEP+ 2% Galactose
YEP+ 3% Glycerol
YEP+ 6% Ethanol
S288C
C)
YEP+ 2% Glucose
swi2Δ
sir3Δ
WT
swi2Δsir3Δ
W303
D)
swi2Δ sir3Δ + Vector plasmid
swi2Δ sir3Δ + SIR3 plasmid
Isolate 1
Isolate 2

Figure A2.2: Absence of *SIR2* does not rescue *swi2Δ* growth

A) Schematic of the Anchor-away system to induce conditional depletion of nuclear proteins. C-terminally tagged versions of the nucleo-cytoplasmic shuttling protein (*RPL13A-FKBP12*) and the *SWI2* gene locus (*SWI2-FRB*) do not affect localization of the tagged protein in DMSO solvent (left). Addition of Rapamycin (red dot) facilitates formation of a ternary complex between FKBP12 and FRB, rapidly depleting *SWI2-FRB* from the nucleus (right).

B) Spot assays of wild type or *sir3*Δ with/ without the *SWI2*-FRB tag on DMSO solvent (left) and 8µg/ml rapamycin (RAP) on 2% glucose after 2 days at 30˚C. The same cultures and dilutions were used for a pair of DMSO and RAP plates.

C) Spot assays as in B) in the presence of 100mM hydroxyurea (HU).

D) Spot assays of wild type or *sir2*Δ with/ without the *SWI2*-FRB tag as in B).

E) Spot assays as in D) in the presence of 100mM hydroxyurea (HU).

Figure A2.2

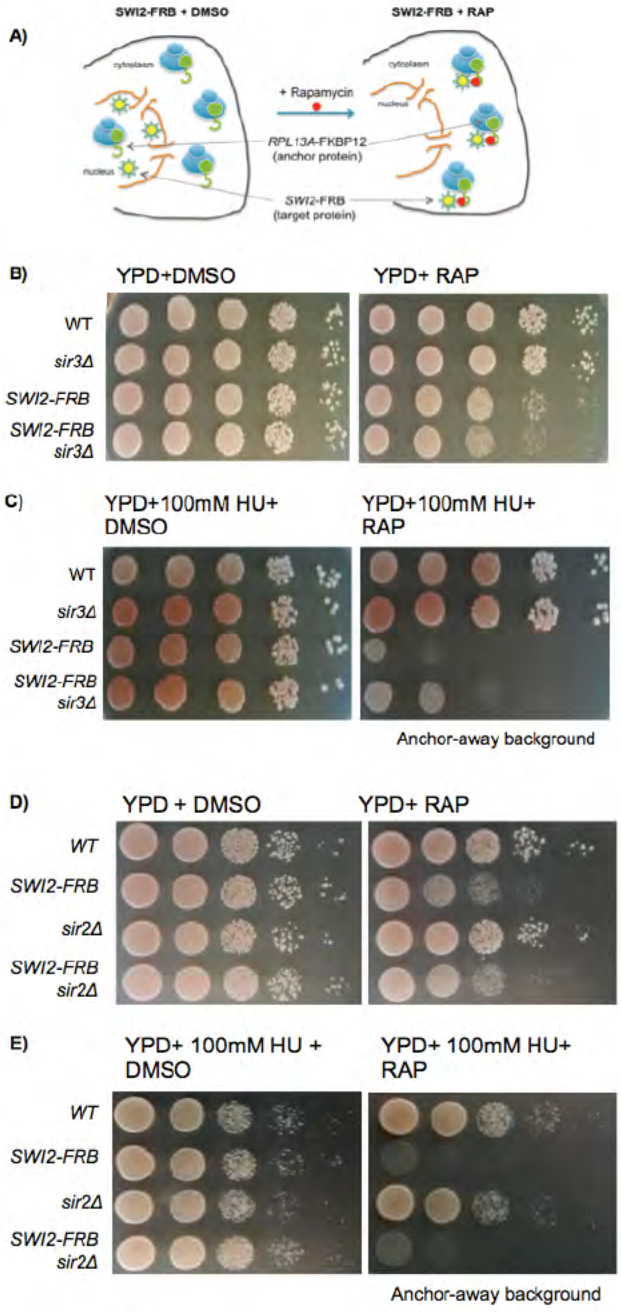
A)
SWI2-FRB + DMSO
SWI2-FRB + RAP
cytoplasm
nucleus
+ Rapamycin
RPL13A-FKBP12
(anchor protein)
SWI2-FRB
(target protein)
B)
YPD+DMSO
YPD+ RAP
WT
sir3Δ
SWI2-FRB
SWI2-FRB sir3Δ
C)
YPD+100mM HU+ DMSO
YPD+100mM HU+ RAP
WT
sir3Δ
SWI2-FRB
SWI2-FRB sir3Δ
Anchor-away background
D)
YPD + DMSO
YPD+ RAP
WT
SWI2-FRB
sir2Δ
SWI2-FRB sir2Δ
E)
YPD+ 100mM HU + DMSO
YPD+ 100mM HU+ RAP
WT
SWI2-FRB
sir2Δ
SWI2-FRB sir2Δ
Anchor-away background

Figure A2.3: Whole-genome microarray analysis of null mutants and anchor-away strains

A) Volcano plots show the transcripts that change significantly in the mutant compared to the wild type (WT) highlighted in blue (p.adj = FDR < 0.1 and Log2 Fold Change > 0.59).

B) Heatmap of normalized RNA abundance for ORFs that are significantly down-regulated (n= 167) and up-regulated (n=488) in the *swi2Δ* arrays compared to WT. Corresponding values for these genes from *swi2Δ sir3Δ* and *sir3Δ* arrays compared to WT are also shown. Group 1_KO are defined as significantly down-regulated in the *swi2Δ* and comparatively de-repressed in *swi2Δ sir3Δ*, while Group 2_KO are defined as significantly up-regulated in the *swi2Δ* and comparatively de-activated in *swi2Δ sir3Δ*. Examples of ORFs identified in previous studies that do not change in *swi2Δ sir3Δ* compared to *swi2Δ* (> ± 1.5 fold are listed along the right.

C) Heatmap of normalized RNA abundance for genes that are down-regulated (n=264) and up-regulated (n=193) in the *SWI2*-FRB compared to WT in the presence of 8µg/ ml of rapamycin (RAP). Corresponding values for these genes from *SWI2-FRB sir3Δ* and *sir3Δ* arrays compared to WT are also shown. 'Group 1_AA' and 'Group 2_AA' are defined essentially as described in B). Examples of ORFs identified in previous studies that do not change in *swi2Δ sir3Δ* compared to *swi2Δ* (> ± 1.5 fold are listed along the right.

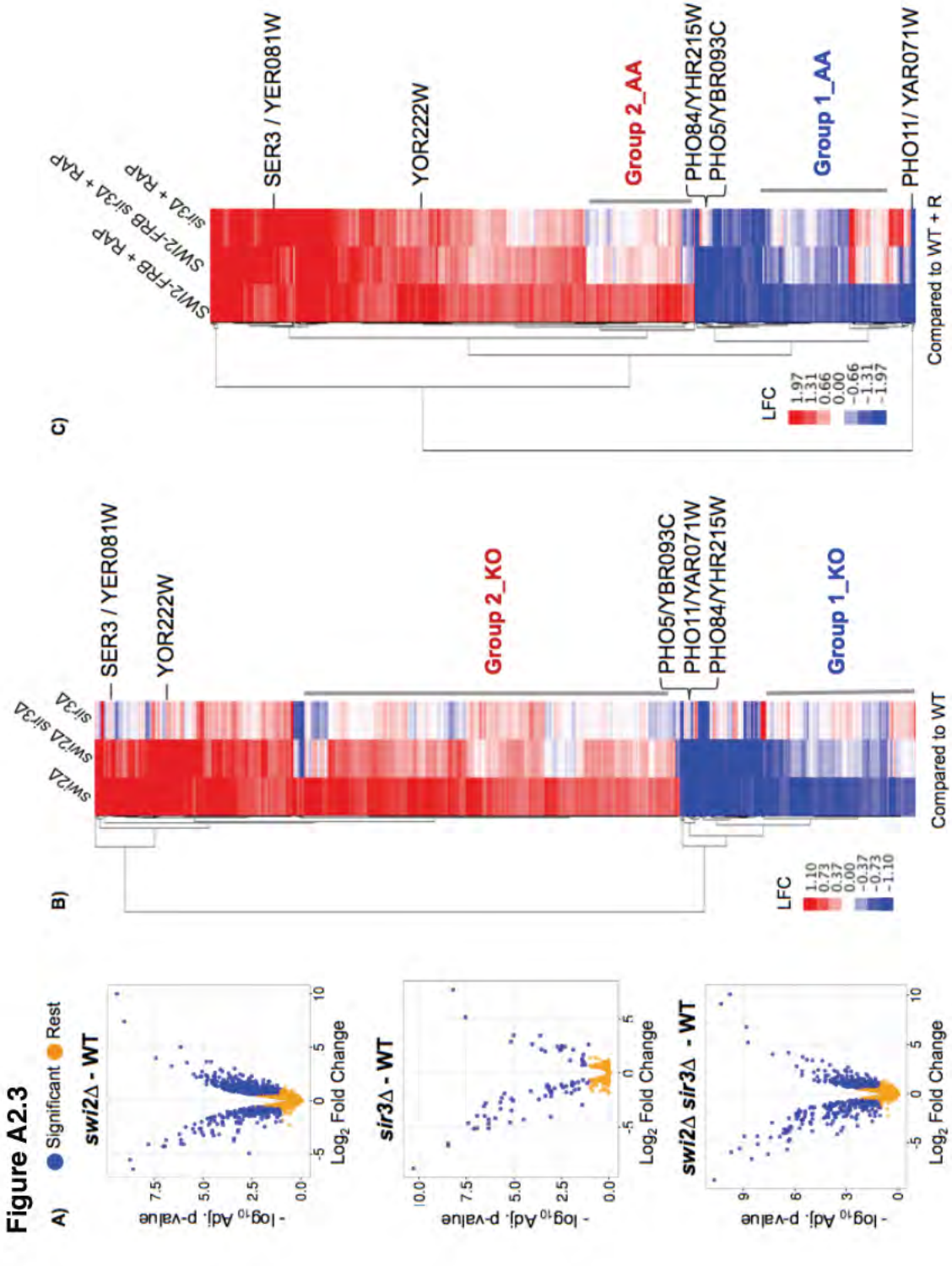
Figure A2.3
A)
Significant
Rest
swi2Δ - WT
sir3Δ - WT
swi2Δ sir3Δ - WT
- log10 Adj. p-value
Log2 Fold Change
B)
swi2Δ
swi2Δ sir3Δ
sir3Δ
SER3 / YER081W
YOR222W
Group 2_KO
PHO5/YBR093C
PHO11/YAR071W
PHO84/YHR215W
Group 1_KO
LFC
Compared to WT
C)
SWI2-FRB + RAP
SWI2-FRB sir3Δ + RAP
sir3Δ + RAP
SER3 / YER081W
YOR222W
Group 2_AA
PHO84/YHR215W
PHO5/YBR093C
Group 1_AA
PHO11/ YAR071W
LFC
Compared to WT + R

Figure A2.4: G2/M expressed genes are regulated by SWI/SNF in a Sir3 dependent manner in both the *SWI2* anchor-away and knockout strains

A) Heatmap of normalized RNA abundance for Group1_AA ORFs (n= XX) in the *SWI2-FRB*, *SWI2-FRB sir3Δ* and *sir3Δ* arrays compared to WT in the presence of 8µg/ ml of rapamycin (RAP) after hierarchical clustering.

B) Heatmap of normalized RNA abundance for Group1_KO ORFs (n= XX) in the *swi2Δ*, *swi2Δ sir3Δ* and *sir3Δ* arrays compared to WT after hierarchical clustering.

C) Venn diagram depicting the overlap of genes from Group 1_AA and Group 1_KO. GO terms specific and common to the knockout (KO) and anchor-away (AA) datasets are shown.

D) qRT-PCR analysis of some Group 1 genes commonly identified from both the knockout and anchor-away datasets sets.

Figure A2.4

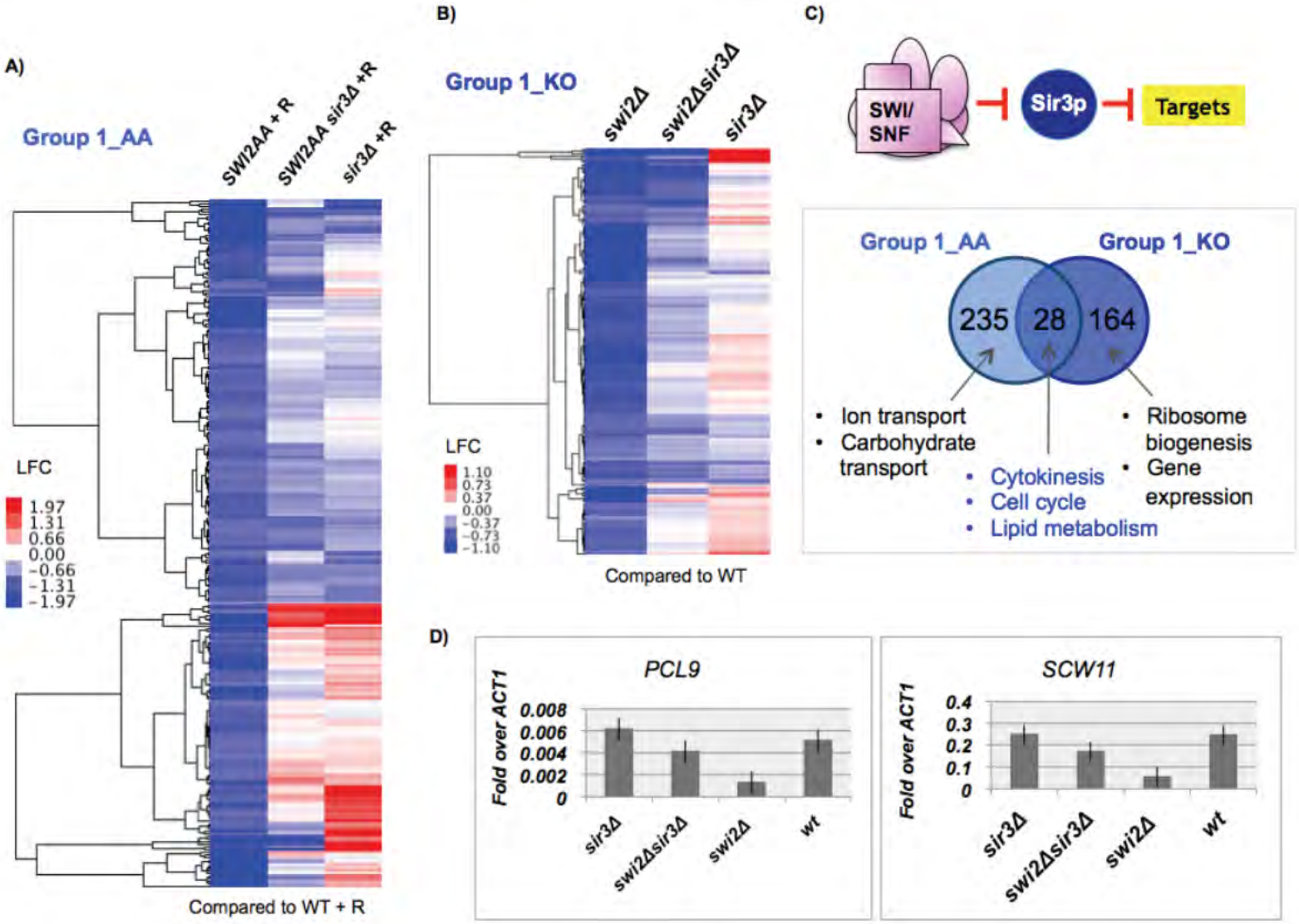
A)
Group 1_AA
SWI2AA + R
SWI2AA sir3Δ +R
sir3Δ +R
LFC
1.97
1.31
0.66
0.00
-0.66
-1.31
-1.97
Compared to WT + R
B)
Group 1_KO
swi2Δ
swi2Δsir3Δ
sir3Δ
LFC
1.10
0.73
0.37
0.00
-0.37
-0.73
-1.10
Compared to WT
C)
SWI/ SNF
Sir3p
Targets
Group 1_AA
Group 1_KO
235
28
164
• Ion transport
• Carbohydrate transport
• Cytokinesis
• Cell cycle
• Lipid metabolism
• Ribosome biogenesis
• Gene expression
D)
PCL9
Fold over ACT1
0.008
0.006
0.004
0.002
0
sir3Δ
swi2Δsir3Δ
swi2Δ
wt
SCW11
Fold over ACT1
0.4
0.3
0.2
0.1
0
sir3Δ
swi2Δsir3Δ
swi2Δ
wt

Figure A2S.1: Gene expression and genetic interactions of *SIR3*, *SIR2* and *SIR4* with *SWI2*.

A) Absence of *SIR3* does not impact RNR gene expression and genetic interactions.

B, C, and D) Absence of *SIR2* does not suppress growth defects of *swi2Δ*.

E, F) Absence of *SIR4* suppresses the growth defects of *swi2Δ*.

Figure A2S.1

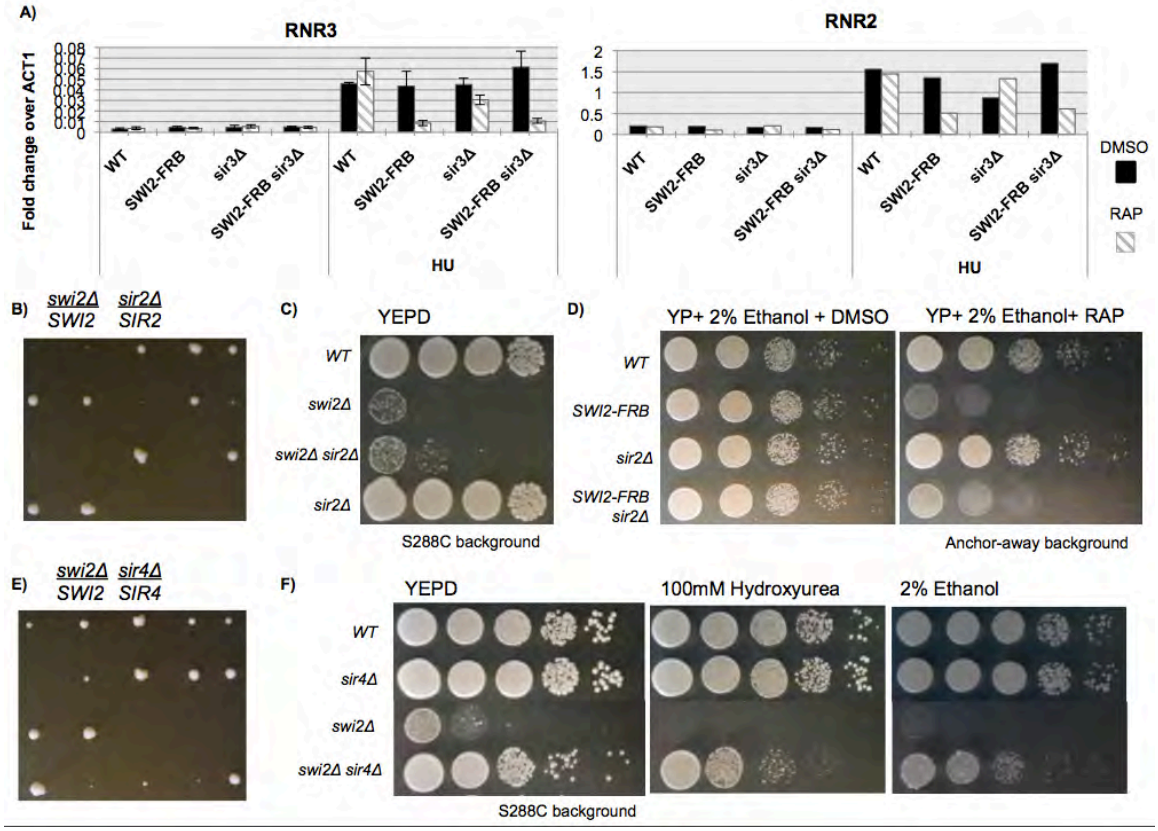
A)
RNR3
RNR2
Fold change over ACT1
WT
SWI2-FRB
sir3Δ
SWI2-FRB sir3Δ
HU
DMSO
RAP
B)
swi2Δ SWI2
sir2Δ SIR2
C)
YEPD
WT
swi2Δ
swi2Δ sir2Δ
sir2Δ
S288C background
D)
YP+ 2% Ethanol + DMSO
YP+ 2% Ethanol+ RAP
WT
SWI2-FRB
sir2Δ
SWI2-FRB sir2Δ
Anchor-away background
E)
swi2Δ SWI2
sir4Δ SIR4
F)
YEPD
100mM Hydroxyurea
2% Ethanol
WT
sir4Δ
swi2Δ
swi2Δ sir4Δ
S288C background

Figure A2S.2: Overlap of Group 2 genes (those repressed by *SWI2*) from null mutants and anchor-away strains

A) Group 2_AA heatmap with strains compared to WT anchor away strain.

B) Group 2_KO heatmap with null mutants compared to WT.

C) Overlap of the number of genes from Group 2_AA and Group 2_KO and the corresponding GO term categories.

Figure A2S.2

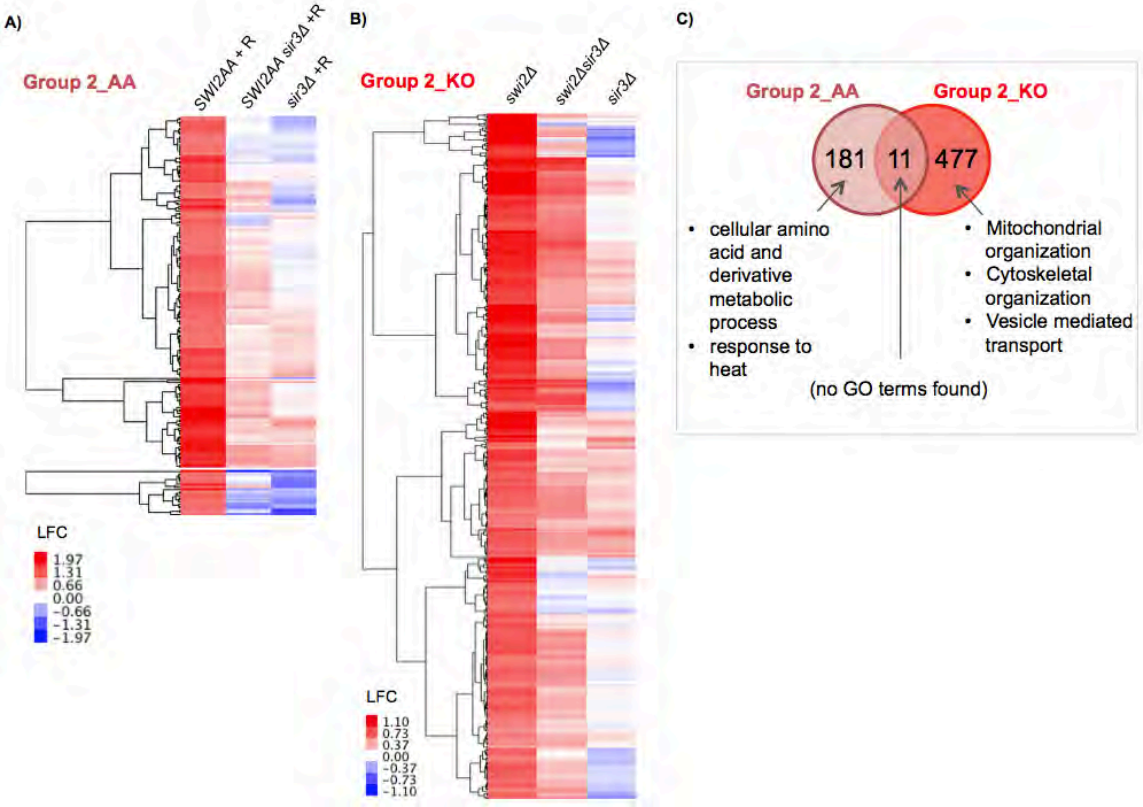
A)
Group 2_AA
SWI2AA + R
SWI2AA sir3Δ +R
sir3Δ +R
LFC
1.97
1.31
0.66
0.00
-0.66
-1.31
-1.97
B)
Group 2_KO
swi2Δ
swi2Δsir3Δ
sir3Δ
LFC
1.10
0.73
0.37
0.00
-0.37
-0.73
-1.10
C)
Group 2_AA
Group 2_KO
181
11
477
• cellular amino acid and derivative metabolic process
• response to heat
• Mitochondrial organization
• Cytoskeletal organization
• Vesicle mediated transport
(no GO terms found)

Figure A2S.3: No detectable change in Sir3 occupancy in euchromatin in *sir3*Δ

A) Chromatin immunoprecipitation (ChIP) for native Sir3 in nocodazole-arrested (G2/M boundary) cells at two heterochromatic loci in WT, *sir3*Δ and *swi2*Δ cells.

B) ChIP for *SIR3*-FLAG in nocodazole-arrested (G2/M boundary) cells at promoters of *SWI2* dependent genes in WT and *swi2*Δ cells.

Figure A2S.3

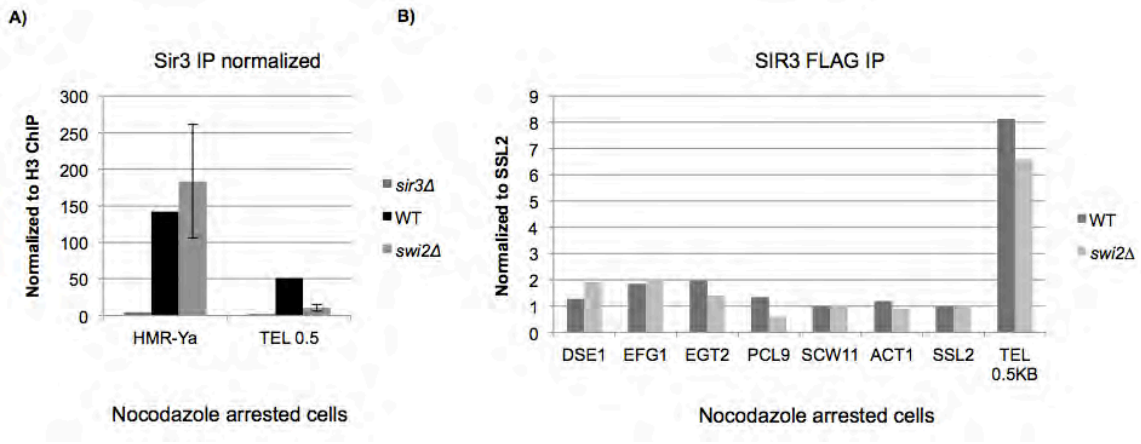
A)
Sir3 IP normalized
Normalized to H3 ChIP
300
250
200
150
100
50
0
HMR-Ya
TEL 0.5
sir3Δ
WT
swi2Δ
Nocodazole arrested cells
B)
SIR3 FLAG IP
Normalized to SSL2
9
8
7
6
5
4
3
2
1
0
DSE1
EFG1
EGT2
PCL9
SCW11
ACT1
SSL2
TEL 0.5KB
WT
swi2Δ
Nocodazole arrested cells

MATERIALS AND METHODS:

Yeast growth media and genetic methods

Yeast were cultured for spot assays as described in Chapter II, Materials and Methods section. For tetrad analysis, at least 30 tetrads were dissected for segregation analysis and growth rates noted.

Chromatin Immunoprecipitation (ChIP)

Yeast strains were grown in rich media with 2% glucose at 30°C and either DMSO or Rapamycin (8µg/ml final concentration) was added for 60 minutes before fixation with 1.2% formaldehyde. Cells were quenched with 2.5M glycine, centrifuged, rinsed with cold water and stored at -80°C until chromatin preparation. Chromatin preparation, immunoprecipitation and DNA extraction were performed as described in (Bennett et al., 2013). The anti-Sir3 antibody (1 µL for 100µL chromatin) was used to immunoprecipitate native Sir3. The anti-H3 antibody, ab1791 from Abcam (1 µL for 100µL chromatin) was used to immunoprecipitate histone H3. The *SIR3* gene was C-terminally tagged with a FLAG tag and an anti-FLAG antibody used for immunoprecipitation.

Microarray analysis:

Yeast strains were grown in rich media with 2% glucose at 30°C in 50 ml cultures and collected at OD = 0.8. Four replicates of *swi2*Δ and *swi2*Δ *sir3*Δ strains were

analyzed by limma analysis in R (Bioconductor package). Yeast strains were grown in rich media with 2% glucose at 30°C to OD = 0.6. and either DMSO or Rapamycin (8µg/ml final concentration) was added for 60 minutes and pelleted for RNA preparation. One replicate each of the *SWI2-FRB*, *SWI2-FRB sir3Δ* and *sir3Δ* arrays and corresponding WT arrays was used. Total RNA was hybridized on Affymetrix Yeast 2.0 arrays and analyzed using a log2 fold change cut-off.

REFERENCES:

Abrams, E., Neigeborn, L., and Carlson, M. (1986). Molecular analysis of SNF2 and SNF5, genes required for expression of glucose-repressible genes in Saccharomyces cerevisiae. Mol. Cell. Biol. *6*, 3643–3651.

Airoldi, E.M., Huttenhower, C., Gresham, D., Lu, C., Caudy, A.A., Dunham, M.J., Broach, J.R., Botstein, D., and Troyanskaya, O.G. (2009). Predicting cellular growth from gene expression signatures. PLoS Comput. Biol. *5*, e1000257.

Bennett, G., Papamichos-Chronakis, M., and Peterson, C.L. (2013). DNA repair choice defines a common pathway for recruitment of chromatin regulators. Nat. Commun. *4*, 2084.

Carlson, M., Osmond, B.C., and Botstein, D. (1981). Mutants of yeast defective in sucrose utilization. Genetics 98:25-40.

Carmen, A.A., Milne, L., and Grunstein, M. (2002). Acetylation of the yeast histone H4 N terminus regulates its binding to heterochromatin protein SIR3. J Biol Chem *277*, 4778–4781.

Carrozza, M.J., Li, B., Florens, L., Suganuma, T., Swanson, S.K., Lee, K.K., Shia, W.-J., Anderson, S., Yates, J., Washburn, M.P., et al. (2005). Histone H3 methylation by Set2 directs deacetylation of coding regions by Rpd3S to suppress spurious intragenic transcription. Cell *123*, 581–592.

Clapier, C.R., and Cairns, B.R. (2009). The biology of chromatin remodeling complexes. Annu. Rev. Biochem. *78*, 273–304.

Dror, V., and Winston, F. (2004). The Swi / Snf Chromatin Remodeling Complex Is Required for Ribosomal DNA and Telomeric Silencing in Saccharomyces cerevisiae. Mol Cell Biol *24*: 8227–8235.

Haruki, H., Nishikawa, J., and Laemmli, U.K. (2008). The anchor-away technique: rapid, conditional establishment of yeast mutant phenotypes. Mol. Cell *31*, 925–932.

Holmes, S.G., Rose, A.B., Steuerle, K., Saez, E., Sayegh, S., Lee, Y.M., and Broach, J.R. (1997). Hyperactivation of the silencing proteins, Sir2 and Sir3, causes chromosome loss. Genetics *145*, 605–614.

Holstege, F.C., Jennings, E.G., Wyrick, J.J., Lee, T.I., Hengartner, C.J., Green, M.R., Golub, T.R., Lander, E.S., and Young, R.A. (1998). Dissecting the regulatory circuitry of a eukaryotic genome. Cell *95*, 717–728.

Jacobs, C.W., Adams, A.E., Szaniszlo, P.J., and Pringle, J.R. (1988). Functions of microtubules in the Saccharomyces cerevisiae cell cycle. J. Cell Biol. *107*, 1409–1426.

Keogh, M.-C., Kurdistani, S.K., Morris, S. a, Ahn, S.H., Podolny, V., Collins, S.R., Schuldiner, M., Chin, K., Punna, T., Thompson, N.J., et al. (2005). Cotranscriptional set2 methylation of histone H3 lysine 36 recruits a repressive Rpd3 complex. Cell *123*, 593–605.

Krebs, J.E., Fry, C.J., Samuels, M.L., and Peterson, C.L. (2000). Global role for chromatin remodeling enzymes in mitotic gene expression. Cell *102*, 587–598.

Laroche, T., Martin, S.G., Tsai-Pflugfelder, M., and Gasser, S.M. (2000). The dynamics of yeast telomeres and silencing proteins through the cell cycle. J. Struct. Biol. *129*, 159–174.

Lenstra, T.L., Benschop, J.J., Kim, T., Schulze, J.M., Brabers, N. a C.H., Margaritis, T., van de Pasch, L. a L., van Heesch, S. a a C., Brok, M.O., Groot Koerkamp, M.J. a, et al. (2011). The Specificity and Topology of Chromatin Interaction Pathways in Yeast. Mol. Cell *42*, 536–549.

Manning, B.J., and Peterson, C.L. (2014). Direct interactions promote eviction of the Sir3 heterochromatin protein by the SWI/SNF chromatin remodeling enzyme. Proc. Natl. Acad. Sci. U. S. A. *111*, 17827–17832.

Radman-Livaja, M., Ruben, G., Weiner, A., Friedman, N., Kamakaka, R., and Rando, O.J. (2011). Dynamics of Sir3 spreading in budding yeast: secondary recruitment sites and euchromatic localization. EMBO J. *30*, 1012–1026.

Richmond, E., and Peterson, C.L. (1996). Functional analysis of the DNA-stimulated ATPase domain of yeast SWI2/SNF2. Nucleic Acids Res *24*, 3685–3692.

Rusche, L.N., Kirchmaier, A.L., and Rine, J. (2003). The establishment, inheritance, and function of silenced chromatin in Saccharomyces cerevisiae. Annu Rev Biochem *72*, 481–516.

Rusché, L.N., Kirchmaier, A.L., and Rine, J. (2002). Ordered nucleation and spreading of silenced chromatin in Saccharomyces cerevisiae. Mol Biol Cell *13*, 2207–2222.

Schwabish, M.A., and Struhl, K. (2007). The Swi/Snf complex is important for histone eviction during transcriptional activation and RNA polymerase II elongation in vivo. Mol Cell Biol *27*, 6987–6995.

Sharma, V.M., Li, B., and Reese, J.C. (2003). SWI/SNF-dependent chromatin remodeling of RNR3 requires TAF(II)s and the general transcription machinery. Genes Dev. *17*, 502–515.

Sinha, M., Watanabe, S., Johnson, A., Moazed, D., and Peterson, C.L. (2009). Recombinational repair within heterochromatin requires ATP-dependent chromatin remodeling. Cell *138*, 1109–1121.

Smith, C.L., and Peterson, C.L. (2005). ATP-dependent chromatin remodeling. Curr Top Dev Biol *65*, 115–148.

Sudarsanam, P., Iyer, V.R., Brown, P.O., and Winston, F. (2000). Whole-genome expression analysis of snf/swi mutants of Saccharomyces cerevisiae. Proc Natl Acad Sci U S A *97*, 3364–3369.

Taddei, A., Van Houwe, G., Nagai, S., Erb, I., van Nimwegen, E., and Gasser, S.M. (2009). The functional importance of telomere clustering: global changes in gene expression result from SIR factor dispersion. Genome Res *19*, 611–625.

Thurtle, D.M., and Rine, J. (2014). The molecular topography of silenced chromatin in Saccharomyces cerevisiae. Genes Dev. *28*, 245–258.

Wilson, C.J., Chao, D.M., Imbalzano, A.N., Schnitzler, G.R., Kingston, R.E., and Young, R.A. (1996). RNA polymerase II holoenzyme contains SWI/SNF regulators involved in chromatin remodeling. Cell *84*, 235–244.

APPENDIX 3

List of strains

Name	***Genotype***
CY1089	*HKY 579-10A Mata leu2-3, 112 his3-11, 15 ade2-1 ura3-1 trp1-1 can1-100 Rad5+ (W303)*
CY1983	*swr1Δ::HpH from CY1089*
CY2071	*rrp6Δ::NAT^{R} MATa, dissected from CY2052; spore 3B*
CY2076	*swr1Δ::G418^{R} rrp6Δ::NAT^{R}, MATa, dissected from CY2052, spore 9C*
CY2210	*rtt109Δ::HPH^{R}, clone 23D segregant from CY2170*
CY2211	*swr1Δ::G418^{R} rtt109Δ::HPH^{R} MATa clone 16D, segregant from CY2170*
CY2212	*rtt109::HPH^{R} rrp6Δ::NAT^{R} MATa clone 29c, segregant from CY2170*
CY2213	*swr1Δ::G418^{R} rrp6Δ::NAT^{R} rtt109Δ::HPH^{R} MATa clone 29A, segregant from CY2170*
CY2052	*MAT a/α rrp6Δ::NAT in CY2031 clone 1*
CY2031	*MAT a/α CY1983 X CY927 swr1Δ/SWR1 in W303, Clone 1*
CY927	*W303-1B Mat a ade2-1 can1-100 his3-11,15 leu2-3,112 trp1-1 ura3-1*
CY2301	*MATa ura3-52 leu2-3,112 his3Δ200 ssu72-2^{ts} (Buratowski Lab)*
CY1653	*BY4743; MATa/a ;his3Δ1/his3Δ1; leu2Δ0/leu2Δ0; lys2Δ0/LYS2; MET15/met15Δ0; ura3Δ0/ura3Δ0; swi2::KanMX4/SWI2 sir3Δ::HPH^{R}/SIR3*
CY1618	*MAT (a) segregant from CY1653, clone 15A, sir3Δ::HPH*

CY1619	*MAT (a) segregant from CY1653, clone 15B, swi2Δ::KANMX and sir3Δ::HPH*
CY1620	*MAT a segregant from CY1653, clone 15C (wild type)*
CY1621	*MAT a segregant from CY1653, clone 15D, swi2::KANMX*
CY1809	*Y40345 MATa tor1-1 fpr1::loxP-LEU2-loxP RPL13A-2x FKBP12:loxP (HHY221)*
CY1810	*Y40362 MATα tor1-1 fpr1::NAT RPL 13A-2x FKB12::TRP1 SNF2-FRB:kanMX6*
CY1853	*MAT a sir3Δ::HYGRO^R in CY1809, clone 1*
CY1854	*MAT α, sir3Δ::HYGRO^R in CY1810, clone 16*
CY1953	*MATα sir2Δ::HIS in CY1885, clone 12*
CY1954	*MATα sir2Δ::HIS in CY1810, clone 10*
CY1907	*MATa/a ;his3Δ1/his3Δ1; leu2Δ0/leu2Δ0; lys2Δ0/LYS2; MET15/met15Δ0; ura3Δ0/ura3Δ0; swi2::KanMX4/SWI2 sir2Δ::HPH^R/SIR2*
CY1908	*MATa/a ;his3Δ1/his3Δ1; leu2Δ0/leu2Δ0; lys2Δ0/LYS2; MET15/met15Δ0; ura3Δ0/ura3Δ0; swi2::KanMX4/SWI2 sir4Δ::HPH^R/SIR4*
CY1752	*MATa/α CY927 X CY971; sir3Δ::HYGRO^R, diploid 2*
CY2041	*swi2Δ in W303, spore 21A dissected from CY1752*
CY2042	*sir3Δ in W303, spore 21B dissected from CY1752*
CY2043	*WT in W303, spore 21C dissected from CY1752*
CY2044	*swi2Δ sir3Δ in W303, spore 21D dissected from CY1752*

Plasmid	
CP1212	pAG25; CEN/ARS w/ NAT cassette. Plasmid #35121 (Addgene)
CP1234	CEN/ARS SIR3 w/ NAT cassette

BIBLIOGRAPHY

Abshiru, N., Ippersiel, K., Tang, Y., Yuan, H., Marmorstein, R., Verreault, A., and Thibault, P. (2013). Chaperone-mediated acetylation of histones by Rtt109 identified by quantitative proteomics. J. Proteomics *81*, 80–90.

Adam, M., Robert, F., Larochelle, M., and Gaudreau, L. (2001). H2A.Z is required for global chromatin integrity and for recruitment of RNA polymerase II under specific conditions. Mol. Cell. Biol. *21*, 6270–6279.

Adkins, M.W., Howar, S.R., and Tyler, J.K. (2004). Chromatin disassembly mediated by the histone chaperone Asf1 is essential for transcriptional activation of the yeast PHO5 and PHO8 genes. Mol. Cell *14*, 657–666.

Airoldi, E.M., Huttenhower, C., Gresham, D., Lu, C., Caudy, A.A., Dunham, M.J., Broach, J.R., Botstein, D., and Troyanskaya, O.G. (2009). Predicting cellular growth from gene expression signatures. PLoS Comput. Biol. *5*, e1000257.

Albert, I., Mavrich, T.N., Tomsho, L.P., Qi, J., Zanton, S.J., Schuster, S.C., and Pugh, B.F. (2007). Translational and rotational settings of H2A.Z nucleosomes across the Saccharomyces cerevisiae genome. Nature *446*, 572–576.

Alcid, E. a, and Tsukiyama, T. (2014). ATP-dependent chromatin remodeling shapes the long noncoding RNA landscape. 2348–2360.

Almada, A.E., Wu, X., Kriz, A.J., Burge, C.B., and Sharp, P. a (2013). Promoter directionality is controlled by U1 snRNP and polyadenylation signals. Nature *499*, 360–363.

Amaral, P.P., Dinger, M.E., Mercer, T.R., and Mattick, J.S. (2008). The eukaryotic genome as an RNA machine. Science *319*, 1787–1789.

Amberg, D.C., Burke, D.J., and Strathern, J.N. (2005). Methods in Yeast Genetics: A Cold Spring Harbor Laboratory Course Manual, 2005 Edition.

Andrews, S. FastQC A Quality Control tool for High Throughput Sequence Data. Http://www.bioinformatics.babraham.ac.uk/projects/fastqc/.

Andrulis, E.D., Werner, J., Nazarian, A., Erdjument-Bromage, H., Tempst, P., and Lis, J.T. (2002). The RNA processing exosome is linked to elongating RNA polymerase II in Drosophila. Nature *420*, 837–841.

Arigo, J.T., Eyler, D.E., Carroll, K.L., and Corden, J.L. (2006). Termination of Cryptic Unstable Transcripts Is Directed by Yeast RNA-Binding Proteins Nrd1 and Nab3. Mol. Cell *23*, 841–851.

Armache, K.-J., Mitterweger, S., Meinhart, A., and Cramer, P. (2005). Structures of complete RNA polymerase II and its subcomplex, Rpb4/7. J. Biol. Chem. *280*, 7131–7134.

Armstrong, J.A., Papoulas, O., Daubresse, G., Sperling, A.S., Lis, J.T., Scott, M.P., and Tamkun, J.W. (2002). The Drosophila BRM complex facilitates global transcription by RNA polymerase II. *21*, 5245–5254.

van Attikum, H., Fritsch, O., Hohn, B., and Gasser, S.M. (2004). Recruitment of the INO80 complex by H2A phosphorylation links ATP-dependent chromatin remodeling with DNA double-strand break repair. Cell *119*, 777–788.

Avvakumov, N., Nourani, A., and Côté, J. (2011). Histone chaperones: modulators of chromatin marks. Mol. Cell *41*, 502–514.

Bao, Y., and Shen, X. (2011). Chromatin Remodeling: INO80 and SWR1. Cell *144*, 158–158.e2.

Bartkowiak, B., Liu, P., Phatnani, H.P., Fuda, N.J., Cooper, J.J., Price, D.H., Adelman, K., Lis, J.T., and Greenleaf, A.L. (2010). CDK12 is a transcription elongation-associated CTD kinase, the metazoan ortholog of yeast Ctk1. Genes Dev. *24*, 2303–2316.

Bataille, A.R., Jeronimo, C., Jacques, P.-É., Laramée, L., Fortin, M.-È., Forest, A., Bergeron, M., Hanes, S.D., and Robert, F. (2012). A universal RNA polymerase II CTD cycle is orchestrated by complex interplays between kinase, phosphatase, and isomerase enzymes along genes. Mol. Cell *45*, 158–170.

Bennett, G., Papamichos-Chronakis, M., and Peterson, C.L. (2013). DNA repair choice defines a common pathway for recruitment of chromatin regulators. Nat. Commun. *4*, 2084.

Berndsen, C.E., Tsubota, T., Lindner, S.E., Lee, S., Holton, J.M., Kaufman, P.D., Keck, J.L., and Denu, J.M. (2008). Molecular functions of the histone acetyltransferase chaperone complex Rtt109-Vps75. Nat. Struct. Mol. Biol. *15*, 948–956.

Birney, E., Stamatoyannopoulos, J.A., Dutta, A., Guigó, R., Gingeras, T.R., Margulies, E.H., Weng, Z., Snyder, M., Dermitzakis, E.T., Thurman, R.E., et al.

(2007). Identification and analysis of functional elements in 1% of the human genome by the ENCODE pilot project. Nature *447*, 799–816.

Bönisch, C., and Hake, S.B. (2012). Histone H2A variants in nucleosomes and chromatin: more or less stable? Nucleic Acids Res. *40*, 10719–10741.

Braberg, H., Jin, H., Moehle, E.A., Chan, Y.A., Wang, S., Shales, M., Benschop, J.J., Morris, J.H., Qiu, C., Hu, F., et al. (2013). From structure to systems: high-resolution, quantitative genetic analysis of RNA polymerase II. Cell *154*, 775–788.

Buratowski, S. (2009). Progression through the RNA polymerase II CTD cycle. Mol. Cell *36*, 541–546.

Buratowski, S., Hahn, S., Guarente, L., and Sharp, P.A. (1989). Five intermediate complexes in transcription initiation by RNA polymerase II. Cell *56*, 549–561.

Cairns, B.R., Erdjument-Bromage, H., Tempst, P., Winston, F., and Kornberg, R.D. (1998). Two actin-related proteins are shared functional components of the chromatin-remodeling complexes RSC and SWI/SNF. Mol. Cell *2*, 639–651.

Camblong, J., Iglesias, N., Fickentscher, C., Dieppois, G., and Stutz, F. (2007). Antisense RNA Stabilization Induces Transcriptional Gene Silencing via Histone Deacetylation in S. cerevisiae. Cell *131*, 706–717.

Carninci, P., Kasukawa, T., Katayama, S., Gough, J., Frith, M.C., Maeda, N., Oyama, R., Ravasi, T., Lenhard, B., Wells, C., et al. (2005). The transcriptional landscape of the mammalian genome. Science *309*, 1559–1563.

Carroll, K.L., Ghirlando, R., Ames, J.M., and Corden, J.L. (2007). Interaction of yeast RNA-binding proteins Nrd1 and Nab3 with RNA polymerase II terminator elements. RNA *13*, 361–373.

Carrozza, M.J., Li, B., Florens, L., Suganuma, T., Swanson, S.K., Lee, K.K., Shia, W.-J., Anderson, S., Yates, J., Washburn, M.P., et al. (2005). Histone H3 methylation by Set2 directs deacetylation of coding regions by Rpd3S to suppress spurious intragenic transcription. Cell *123*, 581–592.

Castelnuovo, M., Zaugg, J.B., Guffanti, E., Maffioletti, A., Camblong, J., Xu, Z., Clauder-Münster, S., Steinmetz, L.M., Luscombe, N.M., and Stutz, F. (2014a). Role of histone modifications and early termination in pervasive transcription and antisense-mediated gene silencing in yeast. Nucleic Acids Res. *42*, 4348–4362.

Castelnuovo, M., Zaugg, J.B., Guffanti, E., Maffioletti, A., Camblong, J., Xu, Z., Clauder-Münster, S., Steinmetz, L.M., Luscombe, N.M., and Stutz, F. (2014b). Role of histone modifications and early termination in pervasive transcription and antisense-mediated gene silencing in yeast. Nucleic Acids Res. *42*, 4348–4362.

Chen, C.C., Carson, J.J., Feser, J., Tamburini, B., Zabaronick, S., Linger, J., and Tyler, J.K. (2008). Acetylated Lysine 56 on Histone H3 Drives Chromatin Assembly after Repair and Signals for the Completion of Repair. Cell *134*, 231–243.

Cheung, V., Chua, G., Batada, N.N., Landry, C.R., Michnick, S.W., Hughes, T.R., and Winston, F. (2008). Chromatin- and transcription-related factors repress transcription from within coding regions throughout the Saccharomyces cerevisiae genome. PLoS Biol. *6*, e277.

Cho, E.-J., Kobor, M.S., Kim, M., Greenblatt, J., and Buratowski, S. (2001). Opposing effects of Ctk1 kinase and Fcp1 phosphatase at Ser 2 of the RNA polymerase II C-terminal domain. Genes Dev. *15*, 3319–3329.

Christie, K.R., Awrey, D.E., Edwards, A.M., and Kane, C.M. (1994). Purified yeast RNA polymerase II reads through intrinsic blocks to elongation in response to the yeast TFIIS analogue, P37. J. Biol. Chem. *269*, 936–943.

Churchman LS, Weissman JS. Nascent transcript sequencing visualizes transcription at nucleotide resolution. Nature. 2011;469: 368–373.

Clapier, C.R., and Cairns, B.R. (2009). The biology of chromatin remodeling complexes. Annu. Rev. Biochem. *78*, 273–304.

Clarkson, M.J., Wells, J.R., Gibson, F., Saint, R., and Tremethick, D.J. (1999). Regions of variant histone His2AvD required for Drosophila development. Nature *399*, 694–697.

Collins, S.R., Miller, K.M., Maas, N.L., Roguev, A., Fillingham, J., Chu, C.S., Schuldiner, M., Gebbia, M., Recht, J., Shales, M., et al. (2007). Functional dissection of protein complexes involved in yeast chromosome biology using a genetic interaction map. Nature *446*, 806–810.

Conaway, R.C., and Conaway, J.W. (1993). General initiation factors for RNA polymerase II. Annu. Rev. Biochem. *62*, 161–190.

Core, L.J., Waterfall, J.J., and Lis, J.T. (2008). Nascent RNA sequencing reveals widespread pausing and divergent initiation at human promoters. Science *322*, 1845–1848.

Cormack, B.P., and Struhl, K. (1992). The TATA-binding protein is required for transcription by all three nuclear RNA polymerases in yeast cells. Cell *69*, 685–696.

Corona, D.F.V., and Tamkun, J.W. (2004). Multiple roles for ISWI in transcription, chromosome organization and DNA replication. Biochim. Biophys. Acta *1677*, 113–119.

Cosma, M.P., Tanaka, T., and Nasmyth, K. (1999). Ordered recruitment of transcription and chromatin remodeling factors to a cell cycle- and developmentally regulated promoter. Cell *97*, 299–311.

Coy, S., Volanakis, A., Shah, S., and Vasiljeva, L. (2013). The Sm Complex Is Required for the Processing of Non-Coding RNAs by the Exosome. PLoS ONE *8*, e65606.

Cramer, P. (2002). Multisubunit RNA polymerases. Curr. Opin. Struct. Biol. *12*, 89–97.

Creyghton, M.P., Markoulaki, S., Levine, S.S., Hanna, J., Lodato, M. a., Sha, K., Young, R. a., Jaenisch, R., and Boyer, L. a. (2008). H2AZ Is Enriched at Polycomb Complex Target Genes in ES Cells and Is Necessary for Lineage Commitment. Cell *135*, 649–661.

van Daal, A., and Elgin, S.C. (1992). A histone variant, H2AvD, is essential in Drosophila melanogaster. Mol. Biol. Cell *3*, 593–602.

Dalvai, M., Bellucci, L., Fleury, L., Lavigne, a-C., Moutahir, F., and Bystricky, K. (2012). H2A.Z-dependent crosstalk between enhancer and promoter regulates Cyclin D1 expression. Oncogene 1–9.

Dalvai, M., Fleury, L., Bellucci, L., Kocanova, S., and Bystricky, K. (2013). TIP48/Reptin and H2A.Z Requirement for Initiating Chromatin Remodeling in Estrogen-Activated Transcription. PLoS Genet. *9*, 1–12.

David, L., Huber, W., Granovskaia, M., Toedling, J., Palm, C.J., Bofkin, L., Jones, T., Davis, R.W., and Steinmetz, L.M. (2006). A high-resolution map of transcription in the yeast genome. Proc. Natl. Acad. Sci. U. S. A. *103*, 5320–5325.

Davis, C.A., and Ares, M. (2006). Accumulation of unstable promoter-associated transcripts upon loss of the nuclear exosome subunit Rrp6p in Saccharomyces cerevisiae. Proc. Natl. Acad. Sci. U. S. A. *103*, 3262–3267.

DeGennaro, C.M., Alver, B.H., Marguerat, S., Stepanova, E., Davis, C.P., Bahler, J., Park, P.J., and Winston, F. (2013). Spt6 Regulates Intragenic and Antisense Transcription, Nucleosome Positioning, and Histone Modifications Genome-Wide in Fission Yeast. Mol. Cell. Biol. *33*, 4779–4792.

Dekker, J., Rippe, K., Dekker, M., and Kleckner, N. (2002). Capturing chromosome conformation. Science *295*, 1306–1311.

Dekker, J., Marti-Renom, M.A., and Mirny, L.A. (2013). Exploring the three-dimensional organization of genomes: interpreting chromatin interaction data. Nat. Rev. Genet. *14*, 390–403.

Deng, W., Rupon, J.W., Krivega, I., Breda, L., Motta, I., Jahn, K.S., Reik, A., Gregory, P.D., Rivella, S., Dean, A., et al. (2014). Reactivation of developmentally silenced globin genes by forced chromatin looping. Cell *158*, 849–860.

Deutscher, M.P. (2006). Degradation of RNA in bacteria: comparison of mRNA and stable RNA. Nucleic Acids Res. *34*, 659–666.

Dichtl, B., Blank, D., Ohnacker, M., Friedlein, A., Roeder, D., Langen, H., and Keller, W. (2002). A role for SSU72 in balancing RNA polymerase II transcription elongation and termination. Mol. Cell *10*, 1139–1150.

van Dijk, E.L., Chen, C.L., d'Aubenton-Carafa, Y., Gourvennec, S., Kwapisz, M., Roche, V., Bertrand, C., Silvain, M., Legoix-Né, P., Loeillet, S., et al. (2011a). XUTs are a class of Xrn1-sensitive antisense regulatory non-coding RNA in yeast. Nature *475*, 114–117.

van Dijk, E.L., Chen, C.L., D'Aubenton-Carafa, Y., Gourvennec, S., Kwapisz, M., Roche, V., Bertrand, C., Silvain, M., Legoix-Né, P., Loeillet, S., et al. (2011b). XUTs are a class of Xrn1-sensitive antisense regulatory non-coding RNA in yeast. Nature *475*, 114–117.

Dion, M.F., Kaplan, T., Kim, M., Buratowski, S., Friedman, N., and Rando, O.J. (2007). Dynamics of replication-independent histone turnover in budding yeast. Science *315*, 1405–1408.

Dixon, J.R., Selvaraj, S., Yue, F., Kim, A., Li, Y., Shen, Y., Hu, M., Liu, J.S., and Ren, B. (2012). Topological domains in mammalian genomes identified by analysis of chromatin interactions. Nature *485*, 376–380.

Djebali, S., Davis, C.A., Merkel, A., Dobin, A., Lassmann, T., Mortazavi, A., Tanzer, A., Lagarde, J., Lin, W., Schlesinger, F., et al. (2012). Landscape of transcription in human cells. Nature *489*, 101–108.

Driscoll, R., Hudson, A., and Jackson, S.P. (2007). Yeast Rtt109 promotes genome stability by acetylating histone H3 on lysine 56. Science *315*, 649–652.

Drouin, S., Laramée, L., Jacques, P.-É., Forest, A., Bergeron, M., and Robert, F. (2010). DSIF and RNA polymerase II CTD phosphorylation coordinate the recruitment of Rpd3S to actively transcribed genes. PLoS Genet. *6*, e1001173.

Dziembowski, A., Lorentzen, E., Conti, E., and Séraphin, B. (2007). A single subunit, Dis3, is essentially responsible for yeast exosome core activity. Nat. Struct. Mol. Biol. *14*, 15–22.

Edwards, A.M., Kane, C.M., Young, R.A., and Kornberg, R.D. (1991). Two dissociable subunits of yeast RNA polymerase II stimulate the initiation of transcription at a promoter in vitro. J. Biol. Chem. *266*, 71–75.

Elfring, L.K., Deuring, R., McCallum, C.M., Peterson, C.L., and Tamkun, J.W. (1994). Identification and characterization of Drosophila relatives of the yeast transcriptional activator SNF2/SWI2. Mol. Cell. Biol. *14*, 2225–2234.

Faast, R., Thonglairoam, V., Schulz, T.C., Beall, J., Wells, J.R., Taylor, H., Matthaei, K., Rathjen, P.D., Tremethick, D.J., and Lyons, I. (2001). Histone variant H2A.Z is required for early mammalian development. Curr. Biol. CB *11*, 1183–1187.

Fan, J.Y., Gordon, F., Luger, K., Hansen, J.C., and Tremethick, D.J. (2002). The essential histone variant H2A.Z regulates the equilibrium between different chromatin conformational states. Nat. Struct. Biol. *9*, 172–176

Fan, X., Shi, H., and Lis, J.T. (2005). Distinct transcriptional responses of RNA polymerases I, II and III to aptamers that bind TBP. Nucleic Acids Res. *33*, 838–845.

Farris, S.D., Rubio, E.D., Moon, J.J., Gombert, W.M., Nelson, B.H., and Krumm, A. (2005). Transcription-induced chromatin remodeling at the c-myc gene involves the local exchange of histone H2A.Z. J. Biol. Chem. *280*, 25298–25303.

Fazzio, T.G., Kooperberg, C., Goldmark, J.P., Neal, C., Basom, R., Delrow, J., and Tsukiyama, T. (2001). Widespread collaboration of Isw2 and Sin3-Rpd3 chromatin remodeling complexes in transcriptional repression. Mol. Cell. Biol. *21*, 6450–6460.

Fiedler, D., Braberg, H., Mehta, M., Chechik, G., Cagney, G., Mukherjee, P., Silva, A.C., Shales, M., Collins, S.R., van Wageningen, S., et al. (2009). Functional Organization of the S. cerevisiae Phosphorylation Network. Cell *136*, 952–963.

Flemming, W. (1882). Zellsubstanz, kern und zelltheilung.

Fox, M.J., Gao, H., Smith-Kinnaman, W.R., Liu, Y., and Mosley, A.L. (2015). The Exosome Component Rrp6 Is Required for RNA Polymerase II Termination at Specific Targets of the Nrd1-Nab3 Pathway. PLOS Genet. *10*, e1004999.

Ghazal, G., Gagnon, J., Jacques, P.-E., Landry, J.-R., Robert, F., and Elela, S.A. (2009). Yeast RNase III triggers polyadenylation-independent transcription termination. Mol. Cell *36*, 99–109.

Ghaemmaghami S, Huh WK, Bower K, Howson RW, Belle A, Dephoure N, et al. Global analysis of protein expression in yeast. Nature. 2003. October 16;425(6959):737–41.

Goldman, J.A., Garlick, J.D., and Kingston, R.E. (2010). Chromatin remodeling by imitation switch (ISWI) class ATP-dependent remodelers is stimulated by histone variant H2A.Z. J. Biol. Chem. *285*, 4645–4651.

Goldmark, J.P., Fazzio, T.G., Estep, P.W., Church, G.M., and Tsukiyama, T. (2000). The Isw2 chromatin remodeling complex represses early meiotic genes upon recruitment by Ume6p. Cell *103*, 423–433.

Gómez-Díaz, E., and Corces, V.G. (2014). Architectural proteins: regulators of 3D genome organization in cell fate. Trends Cell Biol. *24*, 703–711.

Govind, C.K., Qiu, H., Ginsburg, D.S., Ruan, C., Hofmeyer, K., Hu, C., Swaminathan, V., Workman, J.L., Li, B., and Hinnebusch, A.G. (2010). Phosphorylated Pol II CTD recruits multiple HDACs, including Rpd3C(S), for methylation-dependent deacetylation of ORF nucleosomes. Mol. Cell *39*, 234–246.

Grünberg, S., and Hahn, S. (2013). Structural insights into transcription initiation by RNA polymerase II. Trends Biochem. Sci. *38*, 603–611.

Grzechnik, P., and Kufel, J. (2008). Polyadenylation Linked to Transcription Termination Directs the Processing of snoRNA Precursors in Yeast. Mol. Cell *32*, 247–258.

Gu, M., Naiyachit, Y., Wood, T.J., and Millar, C.B. (2015). H2A.Z marks antisense promoters and has positive effects on antisense transcript levels in budding yeast. BMC Genomics *16*, 1–11.

Gudipati, R.K., Xu, Z., Lebreton, A., Séraphin, B., Steinmetz, L.M., Jacquier, A., and Libri, D. (2012a). Extensive Degradation of RNA Precursors by the Exosome in Wild-Type Cells. Mol. Cell *48*, 409–421.

Gudipati, R.K., Xu, Z., Lebreton, A., Séraphin, B., Steinmetz, L.M., Jacquier, A., and Libri, D. (2012b). Extensive Degradation of RNA Precursors by the Exosome in Wild-Type Cells. Mol. Cell *48*, 409–421.

Guillemette, B., Bataille, A.R., Gévry, N., Adam, M., Blanchette, M., Robert, F., and Gaudreau, L. (2005). Variant histone H2A.z is globally localized to the promoters of inactive yeast genes and regulates nucleosome positioning. PLoS Biol. *3*, 1–11.

Guo, Y., Xu, Q., Canzio, D., Shou, J., Li, J., Gorkin, D.U., Jung, I., Wu, H., Zhai, Y., Tang, Y., et al. (2015). CRISPR Inversion of CTCF Sites Alters Genome Topology and Enhancer/Promoter Function. Cell *162*, 900–910.

Haimovich, G., Medina, D. a., Causse, S.Z., Garber, M., Millán-Zambrano, G., Barkai, O., Chávez, S., Pérez-Ortín, J.E., Darzacq, X., and Choder, M. (2013). Gene expression is circular: Factors for mRNA degradation also foster mRNA synthesis. Cell *153*.

Hainer, S.J., Gu, W., Carone, B.R., Landry, B.D., Rando, O.J., Mello, C.C., and Fazzio, T.G. (2015). Suppression of pervasive noncoding transcription in embryonic stem cells by esBAF. Genes Dev. *29*, 362–378.

Hampsey, M. (1998). Molecular genetics of the RNA polymerase II general transcriptional machinery. Microbiol. Mol. Biol. Rev. MMBR *62*, 465–503.

Hampsey, M., Singh, B.N., Ansari, A., Lainé, J.-P., and Krishnamurthy, S. (2011). Control of eukaryotic gene expression: gene loops and transcriptional memory. Adv. Enzyme Regul. *51*, 118–125.

Han, J., Zhou, H., Li, Z., Xu, R.M., and Zhang, Z. (2007). Acetylation of lysine 56 of histone H3 catalyzed by RTT109 and regulated by ASF1 is required for replisome integrity. J. Biol. Chem. *282*, 28587–28596.

Hazelbaker, D.Z., Marquardt, S., Wlotzka, W., and Buratowski, S. (2013). Kinetic Competition between RNA Polymerase II and Sen1-Dependent Transcription Termination. Mol. Cell *49*, 55–66.

He, Y., Vogelstein, B., Velculescu, V.E., Papadopoulos, N., and Kinzler, K.W. (2008). The antisense transcriptomes of human cells. Science *322*, 1855–1857.

Holstege, F.C.., Jennings, E.G., Wyrick, J.J., Lee, T.I., Hengartner, C.J., Green, M.R., Golub, T.R., Lander, E.S., and Young, R.A. (1998). Dissecting the Regulatory Circuitry of a Eukaryotic Genome. Cell *95*, 717–728.

Houseley, J., and Tollervey, D. (2009). The Many Pathways of RNA Degradation. Cell *136*, 763–776.

Houseley, J., LaCava, J., and Tollervey, D. (2006). RNA-quality control by the exosome. Nat. Rev. Mol. Cell Biol. *7*, 529–539.

Hsieh, T.S., Weiner, A., Lajoie, B., Dekker, J., and Friedman, N. (2015a). Micro-C : Nucleosome resolution chromosome folding in budding yeast. Cell.

Hu, G., Cui, K., Northrup, D., Liu, C., Wang, C., Tang, Q., Ge, K., Levens, D., Crane-Robinson, C., and Zhao, K. (2013). H2A.Z facilitates access of active and repressive complexes to chromatin in embryonic stem cell self-renewal and differentiation. Cell Stem Cell *12*, 180–192.

Huber, W., Toedling, J., and Steinmetz, L.M. (2006). Transcript mapping with high-density oligonucleotide tiling arrays. Bioinformatics *22*, 1963–1970.

Hyland, E.M., Cosgrove, M.S., Molina, H., Wang, D., Pandey, A., Cottee, R.J., and Boeke, J.D. (2005). Insights into the role of histone H3 and histone H4 core modifiable residues in Saccharomyces cerevisiae. Mol. Cell. Biol. *25*, 10060–10070.

Iouzalen, N., Moreau, J., and Méchali, M. (1996). H2A.ZI, a new variant histone expressed during Xenopus early development exhibits several distinct features from the core histone H2A. Nucleic Acids Res. *24*, 3947–3952.

Ito, T., Bulger, M., Pazin, M.J., Kobayashi, R., and Kadonaga, J.T. (1997). ACF, an ISWI-containing and ATP-utilizing chromatin assembly and remodeling factor. Cell *90*, 145–155.

Jeronimo C, Watanabe S, Kaplan CD, Peterson CL et al. The Histone Chaperones FACT and Spt6 Restrict H2A.Z from Intragenic Locations. *Mol Cell*2015 Jun 18;58(6):1113-23.

Jónsson, Z.O., Jha, S., Wohlschlegel, J.A., and Dutta, A. (2004). Rvb1p/Rvb2p recruit Arp5p and assemble a functional Ino80 chromatin remodeling complex. Mol. Cell *16*, 465–477.

Joshi, A.A., and Struhl, K. (2005). Eaf3 chromodomain interaction with methylated H3-K36 links histone deacetylation to Pol II elongation. Mol. Cell *20*, 971–978.

Kaplan, C.D., Laprade, L., and Winston, F. (2003). Transcription elongation factors repress transcription initiation from cryptic sites. Science *301*, 1096–1099.

Kaplan, T., Liu, C.L., Erkmann, J. a., Holik, J., Grunstein, M., Kaufman, P.D., Friedman, N., and Rando, O.J. (2008). Cell cycle- and chaperone-mediated regulation of H3K56ac incorporation in yeast. PLoS Genet. *4*.

Kapranov, P., Cheng, J., Dike, S., Nix, D.A., Duttagupta, R., Willingham, A.T., Stadler, P.F., Hertel, J., Hackermüller, J., Hofacker, I.L., et al. (2007). RNA Maps Reveal New RNA Classes and a Possible Function for Pervasive Transcription. Science *316*, 1484–1488.

Katayama, S., Tomaru, Y., Kasukawa, T., Waki, K., Nakanishi, M., Nakamura, M., Nishida, H., Yap, C.C., Suzuki, M., Kawai, J., et al. (2005). Antisense transcription in the mammalian transcriptome. Science *309*, 1564–1566.

Keogh, M.-C., Podolny, V., and Buratowski, S. (2003). Bur1 kinase is required for efficient transcription elongation by RNA polymerase II. Mol. Cell. Biol. *23*, 7005–7018.

Keogh, M.-C., Kurdistani, S.K., Morris, S. a, Ahn, S.H., Podolny, V., Collins, S.R., Schuldiner, M., Chin, K., Punna, T., Thompson, N.J., et al. (2005). Cotranscriptional set2 methylation of histone H3 lysine 36 recruits a repressive Rpd3 complex. Cell *123*, 593–605.

Kim, T., and Buratowski, S. (2009). Dimethylation of H3K4 by Set1 recruits the Set3 histone deacetylase complex to 5’ transcribed regions. Cell *137*, 259–272.

Kim, H., Erickson, B., Luo, W., Seward, D., Graber, J.H., Pollock, D.D., Megee, P.C., and Bentley, D.L. (2010). Gene-specific RNA polymerase II phosphorylation and the CTD code. Nat. Struct. Mol. Biol. *17*, 1279–1286.

Kim, M., Krogan, N.J., Vasiljeva, L., Rando, O.J., Nedea, E., Greenblatt, J.F., and Buratowski, S. (2004). The yeast Rat1 exonuclease promotes transcription termination by RNA polymerase II. Nature *432*, 517–522.

Kim, M., Vasiljeva, L., Rando, O.J., Zhelkovsky, A., Moore, C., and Buratowski, S. (2006). Distinct pathways for snoRNA and mRNA termination. Mol. Cell *24*, 723–734.

Komarnitsky, P., Cho, E.J., and Buratowski, S. (2000). Different phosphorylated forms of RNA polymerase II and associated mRNA processing factors during transcription. Genes Dev. *14*, 2452–2460.

Korber, P., Barbaric, S., Luckenbach, T., Schmid, A., Schermer, U.J., Blaschke, D., and Hörz, W. (2006). The histone chaperone Asf1 increases the rate of histone eviction at the yeast PHO5 and PHO8 promoters. J. Biol. Chem. *281*, 5539–5545.

Kornberg, R.D. (1998). Mechanism and regulation of yeast RNA polymerase II transcription. Cold Spring Harb. Symp. Quant. Biol. *63*, 229–232.

Krishnamurthy, S., He, X., Reyes-Reyes, M., Moore, C., and Hampsey, M. (2004). Ssu72 is an RNA polymerase II CTD phosphatase. Mol. Cell *14*, 387–394.

Langmead, B., Trapnell, C., Pop, M., and Salzberg, S.L. (2009). Ultrafast and memory-efficient alignment of short DNA sequences to the human genome. Genome Biol. *10*: R25.

Larochelle, M., and Gaudreau, L. (2003). H2A.Z has a function reminiscent of an activator required for preferential binding to intergenic DNA. EMBO J. *22*, 4512–4522.

Lebreton, A., Tomecki, R., Dziembowski, A., and Séraphin, B. (2008). Endonucleolytic RNA cleavage by a eukaryotic exosome. Nature *456*, 993–996.

Lemay, J.-F., Larochelle, M., Marguerat, S., Atkinson, S., Bähler, J., and Bachand, F. (2014). The RNA exosome promotes transcription termination of backtracked RNA polymerase II. Nat. Struct. Mol. Biol. *21*, 919–926.

Lenstra, T.L., Benschop, J.J., Kim, T., Schulze, J.M., Brabers, N. a C.H., Margaritis, T., van de Pasch, L. a L., van Heesch, S. a a C., Brok, M.O., Groot Koerkamp, M.J. a, et al. (2011). The Specificity and Topology of Chromatin Interaction Pathways in Yeast. Mol. Cell *42*, 536–549.

Li, B., Pattenden, S.G., Lee, D., Gutiérrez, J., Chen, J., Seidel, C., Gerton, J., and Workman, J.L. (2005). Preferential occupancy of histone variant H2AZ at inactive promoters influences local histone modifications and chromatin remodeling. Proc. Natl. Acad. Sci. U. S. A. *102*, 18385–18390.

Li, H., Handsaker, B., Wysoker, A., Fennell, T., Ruan, J., Homer, N., Marth, G., Abecasis, G., and Durbin, R. (2009). The Sequence Alignment/Map format and SAMtools. Bioinforma. Oxf. Engl. *25*, 2078–2079.

Li, Q., Zhou, H., Wurtele, H., Davies, B., Horazdovsky, B., Verreault, A., and Zhang, Z. (2008). Acetylation of Histone H3 Lysine 56 Regulates Replication-Coupled Nucleosome Assembly. Cell *134*, 244–255.

Lim, S.J., Boyle, P.J., Chinen, M., Dale, R.K., and Lei, E.P. (2013). Genome-wide localization of exosome components to active promoters and chromatin insulators in Drosophila. Nucleic Acids Res. *41*, 2963–2980.

Liu, Q., Greimann, J.C., and Lima, C.D. (2006). Reconstitution, Activities, and Structure of the Eukaryotic RNA Exosome. Cell *127*, 1223–1237.

Liu, X., Li, B., and GorovskyMA, null (1996). Essential and nonessential histone H2A variants in Tetrahymena thermophila. Mol. Cell. Biol. *16*, 4305–4311.

Longtine, M.S., McKenzie, A., Demarini, D.J., Shah, N.G., Wach, A., Brachat, A., Philippsen, P., and Pringle, J.R. (1998). Additional modules for versatile and economical PCR-based gene deletion and modification in Saccharomyces cerevisiae. Yeast *14*, 953–961.

Lorentzen, E., Walter, P., Fribourg, S., Evguenieva-Hackenberg, E., Klug, G., and Conti, E. (2005). The archaeal exosome core is a hexameric ring structure with three catalytic subunits. Nat. Struct. Mol. Biol. *12*, 575–581.

Luger, K., Mäder, a W., Richmond, R.K., Sargent, D.F., and Richmond, T.J. (1997). Crystal structure of the nucleosome core particle at 2.8 A resolution. Nature *389*, 251–260.

Manning, B.J., and Peterson, C.L. (2014). Direct interactions promote eviction of the Sir3 heterochromatin protein by the SWI/SNF chromatin remodeling enzyme. Proc. Natl. Acad. Sci. U. S. A. *111*, 17827–17832.

Marfella, C.G.A., and Imbalzano, A.N. (2007). The Chd family of chromatin remodelers. Mutat. Res. *618*, 30–40.

Marquardt, S., Hazelbaker, D.Z., and Buratowski, S. (2011). Distinct RNA degradation pathways and 3’ extensions of yeast non-coding RNA species. Transcription *2*, 145–154.

Marquardt, S., Escalante-Chong, R., Pho, N., Wang, J., Churchman, L.S., Springer, M., and Buratowski, S. (2014). A chromatin-based mechanism for limiting divergent noncoding transcription. Cell *157*, 1712–1723.

Masumoto, H., Hawke, D., Kobayashi, R., and Verreault, A. (2005). A role for cell-cycle-regulated histone H3 lysine 56 acetylation in the DNA damage response. Nature *436*, 294–298.

Mavrich, T.N., Ioshikhes, I.P., Venters, B.J., Jiang, C., Tomsho, L.P., Qi, J., Schuster, S.C., Albert, I., and Pugh, B.F. (2008). A barrier nucleosome model for statistical positioning of nucleosomes throughout the yeast genome. Genome Res. *18*, 1073–1083.

Meinhart, A., Kamenski, T., Hoeppner, S., Baumli, S., and Cramer, P. (2005). A structural perspective of CTD function. Genes Dev. *19*, 1401–1415.

Meyer, P.A., Ye, P., Suh, M.-H., Zhang, M., and Fu, J. (2009). Structure of the 12-subunit RNA polymerase II refined with the aid of anomalous diffraction data. J. Biol. Chem. *284*, 12933–12939.

Millar, C.B., Xu, F., Zhang, K., and Grunstein, M. (2006). Acetylation of H2AZ Lys 14 is associated with genome-wide gene activity in yeast. Genes Dev. *20*, 711–722.

Mischo, H.E., and Proudfoot, N.J. (2013). Disengaging polymerase: terminating RNA polymerase II transcription in budding yeast. Biochim. Biophys. Acta *1829*, 174–185.

Mizuguchi, G., Shen, X., Landry, J., Wu, W.-H., Sen, S., and Wu, C. (2004). ATP-driven exchange of histone H2AZ variant catalyzed by SWR1 chromatin remodeling complex. Science *303*, 343–348.

Mohrmann, L., and Verrijzer, C.P. (2005). Composition and functional specificity of SWI2/SNF2 class chromatin remodeling complexes. Biochim. Biophys. Acta *1681*, 59–73.

Morillo-Huesca, M., Clemente-Ruiz, M., Andújar, E., and Prado, F. (2010). The SWR1 histone replacement complex causes genetic instability and genome-wide transcription misregulation in the absence of H2A.Z. PloS One *5*, e12143.

Murray, S.C., Serra Barros, A., Brown, D.A., Dudek, P., Ayling, J., and Mellor, J. (2012). A pre-initiation complex at the 3’-end of genes drives antisense transcription independent of divergent sense transcription. Nucleic Acids Res. *40*, 2432–2444.

Neigeborn, L., and Carlson, M. (1984). Genes affecting the regulation of SUC2 gene expression by glucose repression in Saccharomyces cerevisiae. Genetics *108*, 845–858.

Neil, H., Malabat, C., d'Aubenton-Carafa, Y., Xu, Z., Steinmetz, L.M., and Jacquier, A. (2009). Widespread bidirectional promoters are the major source of cryptic transcripts in yeast. Nature *457*, 1038–1042.

Neumann, H., Hancock, S.M., Buning, R., Routh, A., Chapman, L., Somers, J., Owen-Hughes, T., van Noort, J., Rhodes, D., and Chin, J.W. (2009). A method for genetically installing site-specific acetylation in recombinant histones defines the effects of H3 K56 acetylation. Mol. Cell *36*, 153–163.

Ng, H.H., Robert, F., Young, R.A., and Struhl, K. (2003). Targeted recruitment of Set1 histone methylase by elongating Pol II provides a localized mark and memory of recent transcriptional activity. Mol. Cell *11*, 709–719.

Nora, E.P., Lajoie, B.R., Schulz, E.G., Giorgetti, L., Okamoto, I., Servant, N., Piolot, T., van Berkum, N.L., Meisig, J., Sedat, J., et al. (2012). Spatial partitioning of the regulatory landscape of the X-inactivation centre. Nature *485*, 381–385.

O'Sullivan, J.M., Tan-Wong, S.M., Morillon, A., Lee, B., Coles, J., Mellor, J., and Proudfoot, N.J. (2004). Gene loops juxtapose promoters and terminators in yeast. Nat. Genet. *36*, 1014–1018.

Ozdemir, A., Spicuglia, S., Lasonder, E., Vermeulen, M., Campsteijn, C., Stunnenberg, H.G., and Logie, C. (2005). Characterization of Lysine 56 of Histone H3 as an Acetylation Site in Saccharomyces cerevisiae. J. Biol. Chem. *280*, 25949–25952.

Papamichos-Chronakis, M., and Peterson, C.L. (2008). The Ino80 chromatin-remodeling enzyme regulates replisome function and stability. Nat. Struct. Mol. Biol. *15*, 338–345.

Papamichos-Chronakis, M., Watanabe, S., Rando, O.J., and Peterson, C.L. (2011). Global regulation of H2A.Z localization by the INO80 chromatin-remodeling enzyme is essential for genome integrity. Cell *144*, 200–213.

Pappas, D.L., and Hampsey, M. (2000). Functional interaction between Ssu72 and the Rpb2 subunit of RNA polymerase II in Saccharomyces cerevisiae. Mol. Cell. Biol. *20*, 8343–8351.

Parnell, T.J., Huff, J.T., and Cairns, B.R. (2008). RSC regulates nucleosome positioning at Pol II genes and density at Pol III genes. EMBO J. *27*, 100–110.

Perales, R., and Bentley, D. (2009). “Cotranscriptionality”: the transcription elongation complex as a nexus for nuclear transactions. Mol. Cell *36*, 178–191.

Phatnani, H.P., and Greenleaf, A.L. (2006). Phosphorylation and functions of the RNA polymerase II CTD. Genes Dev. *20*, 2922–2936.

Pope, B.D., Ryba, T., Dileep, V., Yue, F., Wu, W., Denas, O., Vera, D.L., Wang, Y., Hansen, R.S., Canfield, T.K., et al. (2014). Topologically associating domains are stable units of replication-timing regulation. Nature *515*, 402–405.

Preker, P., Nielsen, J., Kammler, S., Lykke-Andersen, S., Christensen, M.S., Mapendano, C.K., Schierup, M.H., and Jensen, T.H. (2008). RNA exosome depletion reveals transcription upstream of active human promoters. Science *322*, 1851–1854.

Quinlan, A.R., and Hall, I.M. (2010). BEDTools: A flexible suite of utilities for comparing genomic features. Bioinformatics *26*, 841–842.

Raisner, R.M., Hartley, P.D., Meneghini, M.D., Bao, M.Z., Liu, C.L., Schreiber, S.L., Rando, O.J., and Madhani, H.D. (2005). Histone variant H2A.Z Marks the 5’ ends of both active and inactive genes in euchromatin. Cell *123*, 233–248.

Rando, O.J. (2012). Combinatorial complexity in chromatin structure and function: revisiting the histone code. Curr. Opin. Genet. Dev. *22*, 148–155.

Ranjan, A., Mizuguchi, G., Fitzgerald, P.C., Wei, D., Wang, F., Huang, Y., Luk, E., Woodcock, C.L., and Wu, C. (2013). Nucleosome-free region dominates histone acetylation in targeting SWR1 to promoters for H2A.Z replacement. Cell *154*, 1232–1245.

Rhee, H.S., and Pugh, B.F. (2012). Genome-wide structure and organization of eukaryotic pre-initiation complexes. Nature *483*, 295–301.

Ridgway, P., Brown, K.D., Rangasamy, D., Svensson, U., and Tremethick, D.J. (2004). Unique residues on the H2A.Z containing nucleosome surface are important for Xenopus laevis development. J. Biol. Chem. *279*, 43815–43820.

Roeder, R.G. (1996). The role of general initiation factors in transcription by RNA polymerase II. Trends Biochem. Sci. *21*, 327–335.

Rondón, A.G., Mischo, H.E., Kawauchi, J., and Proudfoot, N.J. (2009). Fail-safe transcriptional termination for protein-coding genes in S. cerevisiae. Mol. Cell *36*, 88–98.

Rufiange, A., Jacques, P.É., Bhat, W., Robert, F., and Nourani, A. (2007). Genome-Wide Replication-Independent Histone H3 Exchange Occurs Predominantly at Promoters and Implicates H3 K56 Acetylation and Asf1. Mol. Cell *27*, 393–405.

Santisteban, M.S., Kalashnikova, T., and Smith, M.M. (2000). Histone H2A.Z regulats transcription and is partially redundant with nucleosome remodeling complexes. Cell *103*, 411–422.

Schaeffer, D., and van Hoof, A. (2011). Different nuclease requirements for exosome-mediated degradation of normal and nonstop mRNAs. Proc. Natl. Acad. Sci. U. S. A. *108*, 2366–2371.

Schaeffer, D., Tsanova, B., Barbas, A., Reis, F.P., Dastidar, E.G., Sanchez-Rotunno, M., Arraiano, C.M., and van Hoof, A. (2009). The exosome contains domains with specific endoribonuclease, exoribonuclease and cytoplasmic mRNA decay activities. Nat. Struct. Mol. Biol. *16*, 56–62.

Schmid, M., Poulsen, M.B., Olszewski, P., Pelechano, V., Saguez, C., Gupta, I., Steinmetz, L.M., Moore, C., and Jensen, T.H. (2012). Rrp6p Controls mRNA Poly(A) Tail Length and Its Decoration with Poly(A) Binding Proteins. Mol. Cell *47*, 267–280.

Schneider, C., Anderson, J.T., and Tollervey, D. (2007). The Exosome Subunit Rrp44 Plays a Direct Role in RNA Substrate Recognition. Mol. Cell *27*, 324–331.

Schneider, C., Leung, E., Brown, J., and Tollervey, D. (2008). The N-terminal PIN domain of the exosome subunit Rrp44 harbors endonuclease activity and tethers Rrp44 to the yeast core exosome. Nucleic Acids Res. *37*, 1127–1140.

Schneider, C., Kudla, G., Wlotzka, W., Tuck, A., and Tollervey, D. (2012). Transcriptome-wide Analysis of Exosome Targets. Mol. Cell *48*, 422–433.

Schulz, D., Schwalb, B., Kiesel, A., Baejen, C., Torkler, P., Gagneur, J., Soeding, J., and Cramer, P. (2013). Transcriptome surveillance by selective termination of noncoding RNA synthesis. Cell *155*, 1075–1087.

Schwabish, M.A., and Struhl, K. (2007). The Swi/Snf complex is important for histone eviction during transcriptional activation and RNA polymerase II elongation in vivo. Mol. Cell. Biol. *27*, 6987–6995.

Scruggs, B.S., Gilchrist, D.A., Nechaev, S., Muse, G.W., Burkholder, A., Fargo, D.C., and Adelman, K. (2015). Bidirectional Transcription Arises from Two Distinct Hubs of Transcription Factor Binding and Active Chromatin. Mol. Cell *58*, 1101–1112.

Seila, A.C., Calabrese, J.M., Levine, S.S., Yeo, G.W., Rahl, P.B., Flynn, R. a, Young, R. a, and Sharp, P. a (2008). Divergent transcription from active promoters. Science *322*, 1849–1851.

Shen, X., Mizuguchi, G., Hamiche, A., and Wu, C. (2000). A chromatin remodelling complex involved in transcription and DNA processing. Nature *406*, 541–544.

Shimada, K., Oma, Y., Schleker, T., Kugou, K., Ohta, K., Harata, M., and Gasser, S.M. (2008). Ino80 chromatin remodeling complex promotes recovery of stalled replication forks. Curr. Biol. CB *18*, 566–575.

Singh, B.N., and Hampsey, M. (2007). A Transcription-Independent Role for TFIIB in Gene Looping. Mol. Cell *27*, 806–816.

Sinha, M., Watanabe, S., Johnson, A., Moazed, D., and Peterson, C.L. (2009). Recombinational repair within heterochromatin requires ATP-dependent chromatin remodeling. Cell *138*, 1109–1121.

Smolle, M., and Workman, J.L. (2013). Transcription-associated histone modifications and cryptic transcription. Biochim. Biophys. Acta *1829*, 84–97.

Smyth, G.K. (2004). Linear models and empirical bayes methods for assessing differential expression in microarray experiments. Stat. Appl. Genet. Mol. Biol. *3*, Article3.

Søgaard, T.M.M., and Svejstrup, J.Q. (2007). Hyperphosphorylation of the C-terminal repeat domain of RNA polymerase II facilitates dissociation of its complex with mediator. J. Biol. Chem. *282*, 14113–14120.

Steinmetz, E.J., Conrad, N.K., Brow, D.A., and Corden, J.L. (2001). RNA-binding protein Nrd1 directs poly(A)-independent 3’-end formation of RNA polymerase II transcripts. Nature *413*, 327–331.

Stern, M., Jensen, R., and Herskowitz, I. (1984). Five SWI genes are required for expression of the HO gene in yeast. J. Mol. Biol. *178*, 853–868.

Strahl, B.D., and Allis, C.D. (2000). The language of covalent histone modifications. Nature *403*, 41–45.

Struhl, K. (2007). Transcriptional noise and the fidelity of initiation by RNA polymerase II. Nat. Struct. Mol. Biol. *14*, 103–105.

Subramanian, V., Mazumder, A., Surface, L.E., Butty, V.L., Fields, P. a., Alwan, A., Torrey, L., Thai, K.K., Levine, S.S., Bathe, M., et al. (2013). H2A.Z Acidic Patch Couples Chromatin Dynamics to Regulation of Gene Expression Programs during ESC Differentiation. PLoS Genet. *9*.

Sudarsanam, P., Cao, Y., Wu, L., Laurent, B.C., and Winston, F. (1999). The nucleosome remodeling complex , Snf / Swi , is required for the maintenance of transcription in vivo and is partially redundant with the histone acetyltransferase , Gcn5. *18*, 3101–3106.

Sun, M., Schwalb, B., Pirkl, N., Maier, K.C., Schenk, A., Failmezger, H., Tresch, A., and Cramer, P. (2013). Global analysis of Eukaryotic mRNA degradation reveals Xrn1-dependent buffering of transcript levels. Mol. Cell *52*, 52–62.

Suto, R.K., Clarkson, M.J., Tremethick, D.J., and Luger, K. (2000). Crystal structure of a nucleosome core particle containing the variant histone H2A.Z. Nat. Struct. Biol. *7*, 1121–1124.

Symmons, M.F., Williams, M.G., Luisi, B.F., Jones, G.H., and Carpousis, A.J. (2002). Running rings around RNA: a superfamily of phosphate-dependent RNases. Trends Biochem. Sci. *27*, 11–18.

Tan, Y., Xue, Y., Song, C., and Grunstein, M. (2013). Acetylated histone H3K56 interacts with Oct4 to promote mouse embryonic stem cell pluripotency. Proc. Natl. Acad. Sci. U. S. A. *110*, 11493–11498.

Tan-Wong, S.M., Wijayatilake, H.D., and Proudfoot, N.J. (2009). Gene loops function to maintain transcriptional memory through interaction with the nuclear pore complex. Genes Dev. *23*, 2610–2624.

Tan-Wong, S.M., Zaugg, J.B., Camblong, J., Xu, Z., Zhang, D.W., Mischo, H.E., Ansari, a. Z., Luscombe, N.M., Steinmetz, L.M., and Proudfoot, N.J. (2012). Gene Loops Enhance Transcriptional Directionality. Science *338*, 671–675.

Teytelman, L., Thurtle, D.M., Rine, J., and van Oudenaarden, A. (2013). Highly expressed loci are vulnerable to misleading ChIP localization of multiple unrelated proteins. Proc. Natl. Acad. Sci. U. S. A. *110*, 18602–18607.

Thiebaut, M., Kisseleva-Romanova, E., Rougemaille, M., Boulay, J., and Libri, D. (2006). Transcription Termination and Nuclear Degradation of Cryptic Unstable

Transcripts: A Role for the Nrd1-Nab3 Pathway in Genome Surveillance. Mol. Cell *23*, 853–864.

Tsubota, T., Berndsen, C.E., Erkmann, J. a., Smith, C.L., Yang, L., Freitas, M. a., Denu, J.M., and Kaufman, P.D. (2007). Histone H3-K56 Acetylation Is Catalyzed by Histone Chaperone-Dependent Complexes. Mol. Cell *25*, 703–712.

Tsukiyama, T., Daniel, C., Tamkun, J., and Wu, C. (1995). ISWI, a member of the SWI2/SNF2 ATPase family, encodes the 140 kDa subunit of the nucleosome remodeling factor. Cell *83*, 1021–1026.

Tsukiyama, T., Palmer, J., Landel, C.C., Shiloach, J., and Wu, C. (1999). Characterization of the imitation switch subfamily of ATP-dependent chromatin-remodeling factors in Saccharomyces cerevisiae. Genes Dev. *13*, 686–697.

Tudek, A., Candelli, T., and Libri, D. (2015). Non-coding transcription by RNA polymerase II in yeast: Hasard or nécessité? Biochimie *117*, 28–36.

Ulianov, S.V., Khrameeva, E.E., Gavrilov, A.A., Flyamer, I.M., Kos, P., Mikhaleva, E.A., Penin, A.A., Logacheva, M.D., Imakaev, M.V., Chertovich, A., et al. (2015). Active chromatin and transcription play a key role in chromosome partitioning into topologically associating domains. Genome Res.

Varga-Weisz, P.D., Wilm, M., Bonte, E., Dumas, K., Mann, M., and Becker, P.B. (1997). Chromatin-remodelling factor CHRAC contains the ATPases ISWI and topoisomerase II. Nature *388*, 598–602.

Vasiljeva, L., and Buratowski, S. (2006). Nrd1 interacts with the nuclear exosome for 3’ processing of RNA polymerase II transcripts. Mol. Cell *21*, 239–248.

Vasiljeva, L., Kim, M., Mutschler, H., Buratowski, S., and Meinhart, A. (2008). The Nrd1-Nab3-Sen1 termination complex interacts with the Ser5-phosphorylated RNA polymerase II C-terminal domain. Nat. Struct. Mol. Biol. *15*, 795–804.

Venkatesh, S., Smolle, M., Li, H., Gogol, M.M., Saint, M., Kumar, S., Natarajan, K., and Workman, J.L. (2012). Set2 methylation of histone H3 lysine 36 suppresses histone exchange on transcribed genes. Nature *489*, 452–455.

Venters, B.J., and Pugh, B.F. (2009). A canonical promoter organization of the transcription machinery and its regulators in the Saccharomyces genome. 360–371.

Wang, G.-Z., Lercher, M.J., and Hurst, L.D. (2011). Transcriptional coupling of neighboring genes and gene expression noise: evidence that gene orientation and noncoding transcripts are modulators of noise. Genome Biol. Evol. *3*, 320–331.

Watanabe, S., Resch, M., Lilyestrom, W., Clark, N., Hansen, J.C., Peterson, C., and Luger, K. (2010). Structural characterization of H3K56Q nucleosomes and nucleosomal arrays. Biochim. Biophys. Acta *1799*, 480–486.

Watanabe, S., Radman-Livaja, M., Rando, O.J., and Peterson, C.L. (2013). A histone acetylation switch regulates H2A.Z deposition by the SWR-C remodeling enzyme. Science *340*, 195–199.

Weber, C.M., and Henikoff, S. (2014). Histone variants: dynamic punctuation in transcription. Genes Dev. *28*, 672–682.

Weiner, A., Chen, H.V., Liu, C.L., Rahat, A., Klien, A., Soares, L., Gudipati, M., Pfeffner, J., Regev, A., Buratowski, S., et al. (2012). Systematic dissection of roles for chromatin regulators in a yeast stress response. PLoS Biol. *10*, e1001369.

Weiner, A., Hsieh, T.-H.S., Appleboim, A., Chen, H.V., Rahat, A., Amit, I., Rando, O.J., and Friedman, N. (2015). High-Resolution Chromatin Dynamics during a Yeast Stress Response. Mol. Cell *58*, 371–386.

West, S., Gromak, N., Norbury, C.J., and Proudfoot, N.J. (2006). Adenylation and Exosome-Mediated Degradation of Cotranscriptionally Cleaved Pre-Messenger RNA in Human Cells. Mol. Cell *21*, 437–443.

West, S., Proudfoot, N.J., and Dye, M.J. (2008). Molecular dissection of mammalian RNA polymerase II transcriptional termination. Mol. Cell *29*, 600–610.

Whitehouse, I., Rando, O.J., Delrow, J., and Tsukiyama, T. (2007). Chromatin remodelling at promoters suppresses antisense transcription. Nature *450*, 1031–1035.

Williams, S.K., Truong, D., and Tyler, J.K. (2008). Acetylation in the globular core of histone H3 on lysine-56 promotes chromatin disassembly during transcriptional activation. Proc. Natl. Acad. Sci. U. S. A. *105*, 9000–9005.

Wilson, C.J., Chao, D.M., Imbalzano, A.N., Schnitzler, G.R., Kingston, R.E., and Young, R.A. (1996). RNA polymerase II holoenzyme contains SWI/SNF regulators involved in chromatin remodeling. Cell *84*, 235–244.

Wong, K.H., Jin, Y., and Struhl, K. (2014). TFIIH phosphorylation of the Pol II CTD stimulates mediator dissociation from the preinitiation complex and promoter escape. Mol. Cell *54*, 601–612.

Wyers, F., Rougemaille, M., Badis, G., Rousselle, J.C., Dufour, M.E., Boulay, J., Régnault, B., Devaux, F., Namane, A., Séraphin, B., et al. (2005). Cryptic Pol II transcripts are degraded by a nuclear quality control pathway involving a new poly(A) polymerase. Cell *121*, 725–737.

Xie, W., Song, C., Young, N.L., Sperling, A.S., Xu, F., Sridharan, R., Conway, A.E., Garcia, B.A., Plath, K., Clark, A.T., et al. (2009). Histone H3 Lysine 56 Acetylation Is Linked to the Core Transcriptional Network in Human Embryonic Stem Cells. Mol. Cell *33*, 417–427.

Xu, F., Zhang, K., and Grunstein, M. (2005a). Acetylation in histone H3 globular domain regulates gene expression in yeast. Cell *121*, 375–385.

Xu, F., Zhang, K., and Grunstein, M. (2005b). Acetylation in histone H3 globular domain regulates gene expression in yeast. Cell *121*, 375–385.

Xu, Z., Wei, W., Gagneur, J., Perocchi, F., Clauder-Münster, S., Camblong, J., Guffanti, E., Stutz, F., Huber, W., and Steinmetz, L.M. (2009). Bidirectional promoters generate pervasive transcription in yeast. Nature *457*, 1033–1037.

Xu, Z., Wei, W., Gagneur, J., Clauder-Münster, S., Smolik, M., Huber, W., and Steinmetz, L.M. (2011). Antisense expression increases gene expression variability and locus interdependency. Mol. Syst. Biol. *7*, 468.

Xue, Y., Van, C., Pradhan, S.K., Su, T., Gehrke, J., Kuryan, B.G., Kitada, T., Vashisht, A., Tran, N., Wohlschlegel, J., et al. (2015). The Ino80 complex prevents invasion of euchromatin into silent chromatin. Genes Dev. *29*, 350–355.

Yassour, M., Pfiffner, J., Levin, J.Z., Adiconis, X., Gnirke, A., Nusbaum, C., Thompson, D.-A., Friedman, N., and Regev, A. (2010). Strand-specific RNA sequencing reveals extensive regulated long antisense transcripts that are conserved across yeast species. Genome Biol. *11*, R87.

Yen, K., Vinayachandran, V., and Pugh, B.F. (2013). SWR-C and INO80 chromatin remodelers recognize nucleosome-free regions near +1 nucleosomes. Cell *154*, 1246–1256.

Yudkovsky, N., Logie, C., Hahn, S., and Peterson, C.L. (1999). Recruitment of the SWI/SNF chromatin remodeling complex by transcriptional activators. Genes Dev. *13*, 2369–2374.

Zhang, H., Roberts, D.N., and Cairns, B.R. (2005). Genome-wide dynamics of Htz1, a histone H2A variant that poises repressed/basal promoters for activation through histone loss. Cell *123*, 219–231.

Zhang, Y., Liu, T., Meyer, C. a, Eeckhoute, J., Johnson, D.S., Bernstein, B.E., Nusbaum, C., Myers, R.M., Brown, M., Li, W., et al. (2008). Model-based analysis of ChIP-Seq (MACS). Genome Biol. *9*, R137.

Zhou, J., Fan, J.Y., Rangasamy, D., and Tremethick, D.J. (2007). The nucleosome surface regulates chromatin compaction and couples it with transcriptional repression. *14*, 1070–1076.

Zlatanova, J., and Thakar, A. (2008). H2A.Z: View from the Top. Structure *16*, 166–179.

Zofall, M., Fischer, T., Zhang, K., Zhou, M., Cui, B., Veenstra, T.D., and Grewal, S.I.S. (2009). Histone H2A.Z cooperates with RNAi and heterochromatin factors to suppress antisense RNAs. Nature *461*, 419–422.